Ph. D. Thesis

UNDERWATER TARGET LOCALIZATION, TRACKING AND CLASSIFICATION

Submitted to

COCHIN UNIVERSITY OF SCIENCE AND TECHNOLOGY

in partial fulfilment of the requirement for the award of the degree of

Doctor of Philosophy

by

PRABHA C.

Under the guidance of

Prof. (Dr.) P. R. S. Pillai

DEPARTMENT OF ELECTRONICS
COCHIN UNIVERSITY OF SCIENCE AND TECHNOLOGY
COCHIN – 682 022, INDIA

July 2013

UNDERWATER TARGET LOCALIZATION, TRACKING AND CLASSIFICATION

Ph.D. Thesis in the field of Ocean Electronics

Author

Prabha C.
Research Scholar
Department of Electronics
Cochin University of Science And Technology
Cochin– 682 022, India
e-mail : prabhasuma@cusat.ac.in,
prabhasuma@gmail.com

Research Advisor

Dr. P. R. S. Pillai
Professor
Department of Electronics
Cochin University of Science And Technology
Cochin– 682 022, India
e-mail : prspillai@cusat.ac.in

July 2013

Dedicated to……

THE ALMIGHTY

COCHIN UNIVERSITY OF SCIENCE AND TECHNOLOGY
DEPARTMENT OF ELECTRONICS
Thrikkakara, Cochin – 682 022

CERTIFICATE

This is to certify that this thesis entitled, ***Underwater Target Localization, Tracking and Classification*** is a bonafide record of the research work carried out by Ms. Prabha C. under my supervision in the Department of Electronics, Cochin University of Science and Technology. The result presented in this thesis or parts of it have not been presented for any other degree(s).

Prof. (Dr.) P. R. S. Pillai
Supervising Guide

Cochin - 22
24th July 2013

DECLARATION

I hereby declare that the work presented in this thesis entitled ***Underwater Target Localization, Tracking and Classification*** is a bonafide record of the research work carried out by me under the supervision of Dr. P. R. S. Pillai, Professor, in the Department of Electronics, Cochin University of Science and Technology. The result presented in this thesis or parts of it have not been presented for any other degree(s).

Prabha C.

Cochin – 22
24th July 2013

COCHIN UNIVERSITY OF SCIENCE AND TECHNOLOGY
DEPARTMENT OF ELECTRONICS
Thrikkakara, Cochin – 682 022

CERTIFICATE

This is to certify that this thesis entitled, ***Underwater Target Localization, Tracking and Classification*** has been modified to effect all the relevant corrections suggested by the Doctoral Committee and the audience during the Pre-synopsis Seminar.

Prof. (Dr.) P. R. S. Pillai
Supervising Guide

Cochin - 22
24th July 2013

Acknowledgements

It is with a deep sense of gratitude that I wish to place on record my indebtedness to my supervising guide, **Prof.** (**Dr.) P. R. S. Pillai**, Department of Electronics, Cochin University of Science and Technology, whose invaluable teaching, timely guidance and constant encouragement were the cornerstones in the progress and completion of this thesis. It has been a great personal honour and humble privilege to have worked under his professional care and direction. Also, I would like to express my sincere thanks to **Dr. Supriya M. H**., Department of Electronics, Cochin University of Science and Technology, for her wholehearted support.

I am much grateful to **Dr. C. K. Aanandan**, Head, Department of Electronics, **Prof.** (**Dr.) K. Vasudevan**, **Prof. (Dr.) P. Mohanan, Dr. Tessamma Thomas & Dr. James Kurian,** Department of Electronics, Cochin University of Science and Technology, for providing timely help and fruitful suggestions.

I gratefully acknowledge the **Department of Information Technology, Government of India**, for their financial assistance.

I would like to mention a special word of thanks to all my research colleagues in the ***Centre for Ocean Electronics (CUCENTOL)***, Mr. Adrin Antony Correya, Mr. Mohan Kumar K., Mr. Prajas John, Mr. Ananthakrishnan V., Mr. Binesh, Mr. Suraj Kamal, Mr. Sajil C. K., Mr. Prasanth P. P., Mr. Sujith Kumar S. Pai, Ms. Rithu, Ms. Sherin and Ms. Sabna N. for their support and constant encouragement.

A word of thankful mention is deserved by all my friends in the ***CREMA Lab,*** who were always there for me as positive sources of support.

I thankfully acknowledge the sincere co-operation I received from the Library and Administrative staff of the Department.

My heartfelt gratitude goes to my friends Dr. Suja, Dr. Jitha, Dr. Manju and Dr. Shameena who were a constant source of motivation and energy for me.

I am grateful to all of my friends and neighbours at Sri Ram Gardens, Chennai for their immense love and constant encouragement.

This acknowledgment would be incomplete without fondly recording my gratefulness to my loving parents, sisters, brothers-in-law, their children, my in-laws and especially my husband ***Anil*** and our son ***Rishabh*** for their constant loving support and sacrifice in connection with preparation of my thesis. I am sure I could not have completed this blessed task without their support and cooperation.

Prabha C.

ABSTRACT

Underwater target localization and tracking attracts tremendous research interest due to various impediments to the estimation task caused by the noisy ocean environment. This thesis envisages the implementation of a prototype automated system for underwater target localization, tracking and classification using passive listening buoy systems and target identification techniques. An autonomous three buoy system has been developed and field trials have been conducted successfully. Inaccuracies in the localization results, due to changes in the environmental parameters, measurement errors and theoretical approximations are refined using the Kalman filter approach. Simulation studies have been conducted for the tracking of targets with different scenarios even under maneuvering situations. This system can as well be used for classifying the unknown targets by extracting the features of the noise emanations from the targets.

Contents

Page No.

List of Figures

Page No.

List of Tables

Page No.

Abbreviations

AIS	**-**	**Automatic Identification System**
AR	**-**	**AutoRegressive**
ARMA	**-**	**AutoRegressive Moving Average**
AUV	**-**	**Autonomous Underwater Vehicle**
CC	**-**	**Communication Controller**
DOA	**-**	**Direction Of Arrival**
DT	**-**	**Detection Threshold**
GUI	**-**	**Graphical User Interface**
GIBS	**-**	**GPS Intelligent Buoy System**
HA	**-**	**Hydrophone Array**
HAC	**-**	**Hydrophone Array Controller**
HOS	**-**	**Higher Order Spectra**
KF	**-**	**Kalman Filter**
NL	**-**	**Noise Level**
PSD	**-**	**Power Spectral Density**
RAP	**-**	**Radio Acoustic Positioning**
RL	**-**	**Reverberation Level**
ROV	**-**	**Remotely Operated Vehicle**
SL	**-**	**Source Level**
SNR	**-**	**Signal-to-Noise Ratio**
SONAR	**-**	**SOund Navigation And Ranging**
SS	**-**	**Shore Station**
TFR	**-**	**Target Feature Record**
TL	**-**	**Transmission Loss**
TMA	**-**	**Target Motion Analysis**
TOA	**-**	**Time Of Arrival**
TS	**-**	**Target Strength**
VMS	**-**	**Vehicle Monitoring System**

CHAPTER 1

INTRODUCTION

Localization, tracking and classification of underwater targets bear immense significance and has attracted great attention in the past few decades due to its growing importance in various spheres critical to mankind like oceanographic as well as fisheries studies, sonar operations, military applications, research, etc.. This chapter addresses the concepts of underwater acoustics, the types of underwater noises and systems to detect underwater noises. The ensuing chapters of the thesis are also briefly introduced herein.

1.1 *Underwater Acoustics*

Sound is considered as the most suitable form of energy that propagates through the sea, as it is the most robust form of energy against attenuation by underwater conditions, especially when compared to other sources of radiations such as electromagnetic waves. Electromagnetic waves do not propagate over long distances underwater except at extremely low frequencies and is prohibitively expensive because of the large and powerful transmitters required. Over the past few decades, ocean exploration activity has been steadily increasing. The data collected by sensors placed underwater is transmitted to the surface of the ocean, from there, it is possible to relay the data via dedicated communication systems or satellites to a data collection centre [1, 2]. The technique that uses sound propagation underwater to navigate, communicate or detect objects underwater is *SONAR* (SOund NAvigation and Ranging).

An underwater acoustic channel has been characterized as a multipath channel due to signal reflections from the surface and bottom of the sea. Because of wave motion, the signal multipath components undergo time varying propagation delays that result in signal fading. In addition, there is frequency dependent attenuation which is approximately proportional to the square of the signal frequency. The sound velocity is normally about 1500 m/s, but the actual value will vary either above or below the normal value depending on the depth at which the signal propagates.

The ambient ocean acoustic noise is caused by shrimp, fish, and various mammals. Near the harbours, there is also manmade acoustic noise in addition to the ambient noise. In spite of this hostile environment, it is possible to design and implement efficient and highly reliable underwater acoustic systems for different applications including position fixing and identification of underwater noises.

Applications of underwater sound can be classified into civilian and military. Underwater sound originally employed for depth sounding, is now being used for wide variety of purposes like fish finding and spotting fish schools, fisheries aids for counting, luring and tagging individual fish, divers aids, position marking of underwater objects, acoustic flow meters, wave height sensors etc.. Military applications include acoustic mines and mine sweeping. Also, the acoustic radiations of ships and submarines are employed for passive detection of the vessels from a long distance. There are a wide variety of sonars like modern echo-range sonar, towed sonar, homing torpedoes, mine hunting sonar and sonar object locators. A number of special sonar equipments are also available viz., the underwater telephone and sonobuoys.

1.2 *Detection of Underwater Acoustic Signals using Sonar Systems*

Sonar is a device used for remotely detecting and locating objects underwater. They play a key role in ocean research due to the ease with which they can be used as instruments for detection of noise sources underwater. Since its introduction during the early half of the 20^{th} century, it has been undergoing various evolutionary stages and has remained as one of the priority areas of research in developed, developing as well as underdeveloped countries. Sonar uses sound propagation underwater, to navigate, communicate or detect other vessels or targets of interest.

Sonar, which can be used as a means for the detection and localization of underwater targets, can be classified into two broad categories, viz., Active sonar and Passive sonar. Active sonars are those devices that generate sound waves of specific, controlled frequencies and also listen for the echoes of these emitted sound signals returned by remote objects underwater. Passive sonars are, essentially listening devices that record the sounds emitted by the objects underwater. Such devices can be used to detect seismic occurrences, early warning of ships, submarines, torpedoes, etc. and marine creatures that emit characteristic sounds of its own. The received signals in sonars are processed to estimate both the temporal and spatial structure of the received signal field. The sensor arrays in sonar consists of sound-pressure sensing electromechanical transducers known as hydrophones, which are immersed in the underwater medium.

Both active and passive sonars are extensively used in modern naval warfare and surveillance operations from various platforms like water-borne vessels, aircrafts and fixed installations. The usefulness of active and passive sonar systems depends on the characteristics of the target of

interest. Although in World War II active sonar was mainly used, now a days, passive sonar is preferred for early detection and warning applications.

1.2.1 Active Sonar

Active sonar involves the transmission of an acoustic signal which, when reflected from a target, provides the sonar receiver with a basis for detection, estimation and localization of targets underwater as illustrated in Fig. 1.1. A signal, in the form of a sound pulse called ping, is emitted and the wave then travels in various directions and hits the objects on its propagation path [1].

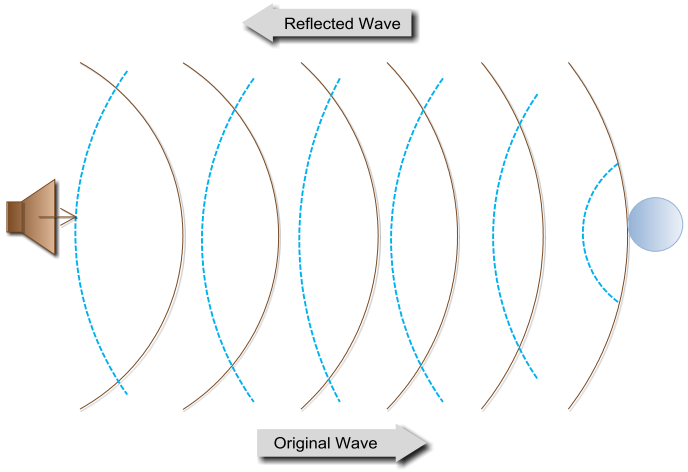

Fig. 1.1 Principle of Active Sonar

Some of the energy reflected will travel back to the transmitting system. The echo, along with other factors such as the frequency, energy of the received signal, depth, water temperature, etc., will enable the sonar system to compute the position of the target of interest, with vanishingly small errors. Ping of acoustic signals generated using a Sonar Projector working in conjunction with the signal generator, power amplifier and

transducer array, possibly with a beam former helps in target detection and estimation as depicted in Fig. 1.2. Acoustic signals can as well be generated underwater by other means such as detonation of explosives.

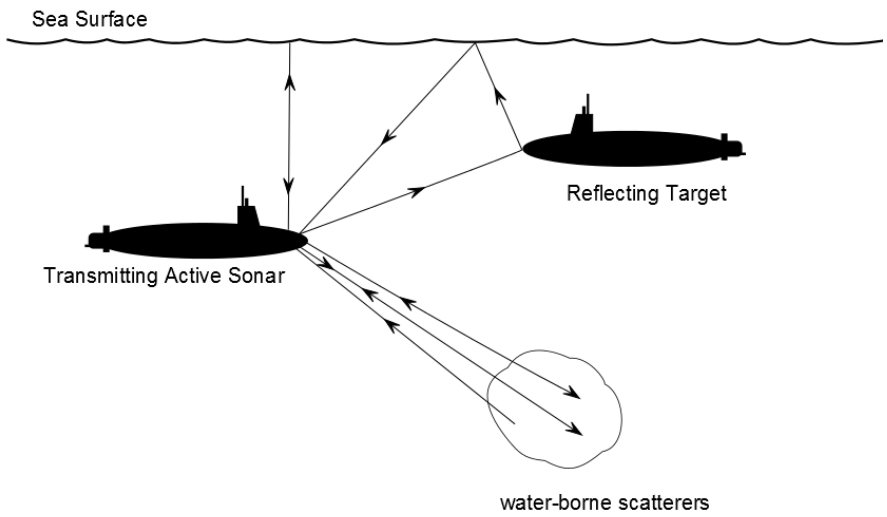

Fig. 1.2 Scenario using Active Sonar

The time elapsed between the transmission and reception of a signal is converted into the range parameter to estimate the distance of the target of interest using the velocity of sound. To measure the bearing, several hydrophones are used, which measure the relative time of arrival (TOA) of the reflected signal to each, or by measuring the relative amplitude of beams formed through beamforming, with an array of hydrophones. Beamforming is a technique that is used to manipulate the directionality, or sensitivity of a radiation pattern. When receiving a signal, it can increase the receiver sensitivity in the direction of the desired signals, while it decreases the sensitivity in the direction of interference and unwanted noises**.**

The use of an array reduces the spatial coverage and hence to achieve wider coverage, multi-beam systems are used. The echo returns together with noise is then subjected to various types of signal processing, which for simple sonars may be just energy detectors. It is then presented to some form of decision device, which will interpret the signal, within certain allowable tolerances. This decision device may be an operator with headphones or a display, or in more sophisticated and fully automated sonar systems, this function may be implemented by special purpose tools or platforms [1].

Simple sonars generally use the TOA technique with a filter, wide enough to cover possible Doppler effects, while more complex ones generally employ the beamforming technique. Military sonars often have multiple beams to perform the surveillance of the entire space, while the simple ones only cover a narrow area. When single frequency transmission is used, the Doppler effect can be utilized to measure the radial speed of a target. The Doppler shift, which is the difference between the transmitted and received frequencies, is estimated and converted into a velocity term. Since Doppler shifts are caused by either the motions of the receiver or target platforms, appropriate correction terms deemed fit need to be taken into account to compensate for the radial speed of the sonar platform. The use of active transmissions from sonars, especially during war time, need to be analysed on the strategic point of view. Active transmissions from such sonars will help the enemy vessels, around the radiating sonar, to infer the clues about the presence of active sonar, its transmitting frequency and its position making use of the received acoustic levels.

Since active sonar platforms are very noisy, such sonars will not allow target identifications with significant success rates. Thus, this type of

detection is used by fast platforms such as planes and helicopters and by noisy platforms like surface ships, but rarely by submarines. When active sonar is used by surface ships or submarines, it is typically activated very briefly at intermittent periods, to reduce the risk of detection by the enemies.

Depending on the number and position of the transmitters and receivers, the active sonar operation can be classified as mono-static, bi-static and multi-static. When the transmitter and a receiver are in the same place, the operation is called mono-static, while in bi-static, they are separated. When more transmitters or receivers are used, it is referred to as a multi-static operation. Generally, most sonars are used mono-statically with the same array often being used for transmission and reception. In certain mono-static system installations, if the platform is moving, it may be considered as bi-static. Multi-static operation is preferred in active sonobuoy field applications.

1.2.2 Passive sonar

The passive sonar which is quite frequently referred to as listening sonar is essentially a listening device that records the sounds emitted by the objects underwater. Such device can be used to detect seismic occurrences, early warning of ships, submarines, torpedoes, etc. and marine creatures that emit characteristic sounds of its own. A passive sonar scenario is depicted in Fig. 1.3. Passive sonar systems, unlike the active sonars, do not radiate any signals. They detect the targets and perform estimations by analyzing the sound signals emitted by the target itself.

The passive sonar has a much greater detection range than active systems and helps in performing the identification of the targets, estimating

the range and bearing as well as tracking of targets. The noise generated by mechanized objects underwater is made use of, for performing the target detection.

Once a signal is detected in a certain direction, referred to as broadband detection, it is possible to zoom in and analyze the signal received, referred to as narrow band analysis. Identification of the target is made possible, as every target generates its own characteristic noises and Fourier Transform techniques can be used to analyze the various frequency components in it. Another use of the passive sonar is to determine the target's trajectory by a technique referred to as Target Motion Analysis (TMA), which will provide the target's range, course, and speed [1].

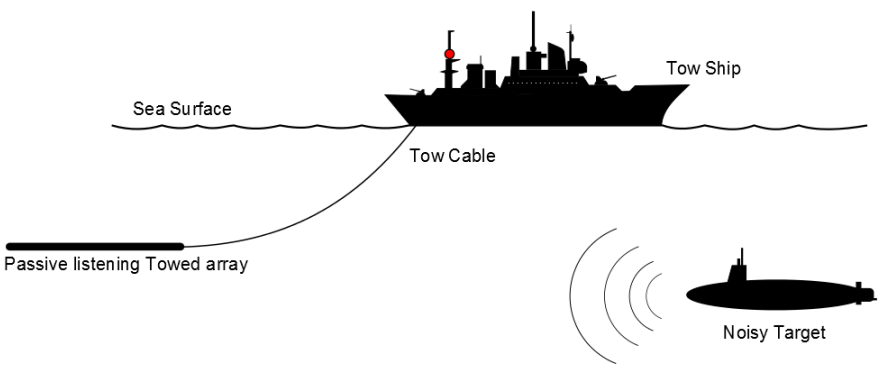

Fig. 1.3 Typical illustration of Passive sonar

Performance limitations arise as a result of the propagation loss and additive noise at the receiver, even though passive sonar is stealthy and very useful. Major limitations result from the imprecise knowledge of the characteristics of the target emanations, and from dispersion in time and frequency of target emissions by the undersea medium.

1.2.3 Sonar Equations

The sonar equations were devised to formulate the relationship between the effects of the medium, target and equipment in decibel levels and found to be useful in design calculations for sonar equipment. The two important practical functions served by them are the prediction of performance of the sonar equipment of known or existing design and the design of the sonar system. The prediction of the performance characteristics, mostly in terms of detection probability, is achieved in sonar by the prediction of range, through the sonar parameter, *Transmission Loss* (TL). The equations are solved for transmission loss, which is then converted to the range through some assumption concerning the propagation characteristics of the medium [1].

The sonar equation is a tool for quantifying the performance of a sonar relating to the signal to noise ratio of the sonar to the source level of the transmitted sound, propagation loss and the background noise level. For finding solutions for the sonar design problems, for a given range, the equation is solved for the particular parameter, whose practical realisation is likely to cause difficulty. For example, the equation can be solved for the directivity required, along with other probable values of sonar parameters, to yield the desired range of detection in sonar.

Once, the directivity needed to obtain the desired range has been achieved, the design continues with the trade-offs between the directivity index and other parameters. The design is finally completed through several computations using the equations and the design engineers' intuition and experience. The sonar parameters are expressed in units of decibels relative to the standard reference levels.

Certain sonar parameters are determined by the equipment, while some others are determined by the medium and the target as detailed below.

- ❖ Parameters determined by the equipment
  - Projector Source Level (SL)
  - Self Noise Level (NL)
  - Receiving Directivity Index (DI) and
  - Detection Threshold (DT)
- ❖ Parameters determined by the medium
  - Transmission Loss (TL)
  - Reverberation Level (RL)
  - Ambient Noise Level (NL)
- ❖ Parameters determined by the target
  - Target Strength (TS)
  - Target Source Level (SL)

It may be worth mentioning the fact that one of the parameters on account of the equipment, *viz.* the self noise level cannot be completely decoupled from the ambient noise level parameter determined by the medium and as such these two parameters are essentially identical and hence represented by the same notation.

A sound source, by appropriate means, produces a *source level* of $\boldsymbol{SL}$ decibels at a 1 m. When the radiated sound reaches the target, its level will be reduced by the *transmission loss,* and becomes $\boldsymbol{SL - TL}$. Upon reflection or scattering from the target of target strength TS, the reflected or backscattered level will be $\boldsymbol{SL - TL + TS}$ at a distance of 1 m from the acoustic centre of the target in the direction back towards the source. In travelling back towards the source, this level is again attenuated by the

transmission loss and becomes $\boldsymbol{SL - 2TL + TS}$. This is the echo level at the hydrophone terminals. Turning now to the background and assuming it to be isotropic noise rather than reverberation, the *background level is* $\boldsymbol{NL}$. This level is reduced by the *directivity index* (DI) of the transducer acting as a receiver or hydrophone so that at the terminals of the hydrophone, the relative noise power is $\boldsymbol{NL - DI.}$ Hence, at the hydrophone terminals, the echo-to-noise ratio is $\boldsymbol{SL - 2TL + TS -}$ $(\boldsymbol{NL - DI})$.

In sonar scenario, a decision will be made by the human observer that a target is present, when the input signal-to-noise ratio is above a certain *detection threshold*, $\boldsymbol{DT}$, satisfying certain probability criteria, else the decision will be made that the target is not present. If the target is present, just at the point of detection, the signal-to-noise ratio will be equal to the detection threshold, and hence the equation becomes,

$$\boldsymbol{SL - 2TL + TS - (NL - DI) = DT} \qquad (1.1)$$

This is the active sonar equation for the *mono-static* case, in which the acoustic returns of the target is back towards the source. In some sonars, a separated source and receiver are employed and the arrangement is said to be *bi-static* and in this case, the two transmission losses, to and from the target, are not the same. Also in some modern sonar, it is not possible to distinguish between $\boldsymbol{DI}$ and $\boldsymbol{DT}$ and it becomes appropriate to refer to $\boldsymbol{DI - DT}$ as the increase in signal-to-background noise ratio generated by the entire receiving system.

For a reverberation background, we will replace the terms $\boldsymbol{NL -}$ $\boldsymbol{DI}$ by an *equivalent plane wave reverberation level* $\boldsymbol{RL}$ observed at the hydrophone terminals. The active sonar equation then becomes

$$SL - 2TL + TS = RL + DT \quad (1.2)$$

In the passive case, the target itself produces the signal by which it is detected, and the parameter source level now refers to the level of the radiated noise of the target at 1 m. In addition, the parameter target strength becomes irrelevant and as only one way transmission is involved, the *passive sonar equation* becomes

$$SL - TL = NL - DI + DT \quad (1.3)$$

1.3 *Factors Affecting the Sonar Performance*

The detection, classification and localization performance of sonar depends on the environmental factors and the capabilities of the receiving equipment. In the case of active sonars, the performance is also determined by the transmitting subsystems, while the radiated noise characteristics also can be a factor that influences the performance of the passive sonar.

1.3.1 Environmental Factors

One factor which affect the sonar operations are variation in sound speed, particularly in the vertical plane. Sound speed is lower in fresh water than in seawater. Density of water affects the speed of sound and temperature, dissolved molecules, salinity and pressure in turn affect the density. As the depth of the ocean changes, the water temperature changes and at depth ranges between 30 and 100 meters, there is often a significant variation in temperature, which is referred to as the thermocline. The thermocline divides the warmer surface water from the cold still waters that make up the rest of the ocean. This will lead to inaccuracies in sonar predictions, as a sound originating on one side of the thermocline tends to be bent or refracted off the thermocline. Since the wave propagation speed

is a time varying function of depth and range, in sonar operations which depend significantly on geographic location and season of the year, the estimations turn out to be cumbersome due to complex refractive phenomenon, more so when the propagating energy interacts with the sea surface or bottom. Motions of the water mass, sea surface, sonar platforms and targets, cause wide variety of channel dispersions in time, frequency and angle.

1.3.2 Reverberation

In active sonar operations, scattering phenomenon occurs from small objects in the sea as well as from the bottom and surface. This is one of the major sources of interference. This scattering is called reverberation and is different from that in room reverberation, which is a reflection phenomenon. The reverberation phenomenon in the ocean is analogically similar to the scattering of light from the car's headlights in a foggy or misty environment. A high intensity pencil beam is able to penetrate the fog and since the car headlights are less directional, these scattering will result in *white-out*, where the return reverberation dominates. Hence, in the active sonar scenario in the ocean, the need is to transmit in narrow beams to reduce the effect of reverberation.

1.3.3 Target Characteristics

In the active sonar scenario, the sound reflection characteristics of the target, known as its *target strength* and in the passive sonar scenario, *radiated noise* characteristics of the target are the two main characteristics of the sonar targets which influence the performance of the sonar. The radiated noise, in general, will consist of an unresolvable continuum of noise with superimposed or resolvable spectral lines on it, the lines or bands in the spectrum aid in classification. Echoes are also obtained from

marine species and other objects in the sea such as whales, wakes, schools of fish and rocks.

1.3.4 Other Noises

The ocean is a propagation medium with full of interfering noise sources like machinery noise from the shipping traffic, flow noise, wave noise, wind noise, noise from biologics and even intentional jammers, all of which may interfere with the desired target returns and emissions.

1.4 *Noise Sources in the ocean*

The ocean environment includes a variety of noise sources, which are of natural as well as manmade in origin. The general back ground noise which has the contributions from all the oceanic noise sources is termed as the ambient noise. The ambient noise has a broad frequency range and its characteristics depends on a number of factors including climate, wind speed, presence of aquatic organisms, etc.. The following sections briefly examine the principal sources of ambient noises and their characteristics.

1.4.1 Natural Sources of Ambient Noise

The natural sources of ambient noise can be broadly classified into the following categories:

- Hydrodynamic sources
- Thermal agitations
- Seismic sources
- Biological sources
- Cracking of ice

1.4.2 Manmade Noises

Various types of human activities also contribute greatly towards ambient noise. The main sources include shipping traffic, seismic surveys, oil and gas exploration / production, military operations, sonars etc.

1.5 *Importance of Localization and Tracking Systems*

Underwater target localization and tracking attracts tremendous research interest due to various impediments to the estimation task caused by the noisy ocean environment. As underwater sound environment is characterized by a multitude of noise like signals and signal like noises, in many occasions a bewildering mix of signal and noise is obtained, which necessitates the need for having specialized systems with sophisticated signal processing techniques for extracting the signals of interest. Many specialized systems have been developed for localizing and tracking underwater noise sources and targets as solutions to definitive problems in active sonar scenario.

Unlike active sonar systems that localize and range by measuring the time elapsed between the transmitted pings and its echo, passive systems rely on the time of arrival (TOA) or direction of arrival (DOA) solutions for localization and tracking of targets in a water body. One resorts to TOA approach, if the target emits known signals synchronized with certain timing information as in the GPS Intelligent Buoy Systems (GIBS) and Vemco Radio Acoustic Positioning systems (VRAP), while the DOA approach is used for the localization and tracking of unknown targets, making use of the target emanations.

A three buoy automated system aids in localizing, tracking and classifying underwater targets using passive listening and target

identification techniques concepts has been developed and discussed in this thesis. The system consists of hydrophone elements and arrays of improved sensitivity and can identify targets with minimally configurable hardware resources.

The noise emanations sampled by the sensors at three locations in the ocean are analyzed for the decision making. The acoustic signals from the targets are used to estimate the direction of arrival of the noises at the nodes of an acoustic network, leading to the estimation of the position of the target of interest. Each sensor node comprises of mechanically steerable hydrophone array and support electronics. This minimally configurable three node network is deployed in the ocean at the vertices of a triangle. The buoys are moored at fixed positions in the ocean with the help of appropriate bottom mooring mechanisms.

The measurement errors and inaccuracies in the localization estimates are refined using the Kalman Filter approach. This system has been developed and field trials have been conducted successfully. Simulation studies have also been conducted for the tracking of targets with different scenarios. This system also features a technique for classifying the unknown targets by extracting the features of the noise emanations from the target and using the classification procedures.

The proposed technique achieves target localization by passive listening. Not many techniques are reported in open literature, for localization of unknown underwater targets using passive listening techniques. If at all some techniques are in use (may be unpublished/ patented), these may be outcomes of certain trial and error or thump rule approaches.

1.6 *Highlights of the Work Carried out*

The salient highlights of the work carried out are briefly outlined in the following sections.

1.6.1 Review of Past Work on Localization Systems

Chapter 2 is devoted to the review of the past research works reported in open literature in the areas of underwater target localization, tracking and classification. Many surveillance systems based on passive listening concepts have been developed and deployed in the past. To overcome the limitations associated with the conventional acoustic sensing and tracking systems, a versatile technique for position fixing and tracking of underwater targets using passive listening concepts has been developed. The highlights of the existing underwater target localization systems are addressed in this chapter along with their limitations.

To overcome the limitations, a new approach using an acoustic three buoy system for localization is presented in this thesis. The localization estimates may vary due to the instabilities of the buoys, measurement errors caused by changes in environmental parameters and theoretical approximations. The inaccuracies in the localization estimates are refined using the Kalman filter approach and the algorithm is also extended for moving targets even under maneuvering situations. The literature survey on the Kalman filter approach is also covered in this chapter. The decision making on the classification of targets is implemented by comparing the extracted target specific features with the ones in the knowledge base. A literature survey on the techniques for the target feature record generation is also included.

1.6.2 Methodology

Chapter 3 addresses the methodologies adopted to perform the localization, tracking and classification of underwater targets based on passive listening concepts. As a prelude to the localization and tracking efforts, a simulation study was carried out, based on which a conceptual approach for a realizable three buoy system for the localization and tracking has been formulated.

This system comprises of mechanically steerable hydrophone arrays and suitable electronics to localize the unknown target in the vicinity of the system which performs the localization, tracking and classification of unknown underwater targets. The angle from which the maximum signal arrives at each of the buoy system differs and from the direction of arrival information, the localization of the unknown underwater target is performed using triangulation techniques.

The Kalman filter approach is implemented to reduce the inaccuracies of the localization estimates. The classification primarily involves the extraction of source specific features by analysing the composite noise data waveforms by the signal processing modules of the surveillance system and compilation of the knowledge base, which forms the backbone of the classifier.

1.6.3 Simulation of Target Localizer

Generally, the underwater surveillance systems depend on the noise emanations from the targets of interest. The proposed three buoy system consists of three mechanically steerable hydrophone arrays which receive the acoustic signals and the required buoy electronics. The automated buoy system carries out the surveillance operations and processes the received

signals as well as manages the communication and power supply. The buoy electronics gather the geographical positions with the help of the GPS receiver attached to them. The buoys are deployed in the ocean with the help of appropriate mooring mechanisms. The buoys are deployed in the ocean with the help of appropriate mooring mechanisms. Buoys comprising of the arrays and support electronics are deployed at the vertices of a triangle. When target emanations are received, the hydrophone arrays get steered to the direction of maximum signal arrival, and the angular position information of the hydrophone arrays are used to estimate the position of the target using triangulation techniques. Applying geodetic latitude and longitude distance computations, trigonometric and triangulation techniques, the position of the target with reference to geomagnetic meridian can be computed. Three different approaches based on the mathematical formulae and software platforms are used for the localization and are summarized in Chapter 4.

1.6.4 Prototype Localizer

The design and development of the prototype localizer is discussed in Chapter 5. To facilitate the localization, tracking and classification of unknown underwater targets, submerged hydrophone arrays should be deployed for capturing the acoustic signals from three different locations with suitable buoy systems. As the buoy needs specialized requirements for this application involving the steering of the submerged hydrophone arrays suspended from the gear assembly, a specialized structural buoy design SWAB (Small Water plane Area Buoy) has been formulated, conforming to the concept of minimizing the water plane area, so that the disturbances the buoy experiences, is brought to the minimum. The buoy electronics performs the vital task of mechanically steering the hydrophone arrays in the submerged buoys for the purpose of estimating the direction of arrival

of the captured signals with the help of the hydrophone array controller. The Direction of Maximum Arrival Estimator is used to compute the power received by the hydrophone array at various angular positions of the hydrophone array.

The heart of the DOA estimation system is the Microchip dsPIC30F6014A, a DSP enabled 16 bit microcontroller with a dedicated DSP Engine. With the DOAs and the distance between the buoys, the distance of the target from the buoy system is computed using triangulation techniques. The prototype three buoy system has been used for validating the technique during the field trials in a Reservoir in Kulamavu, Idukki and the results were promising.

The recoiling effect, caused due to the movement of the array from one position to another, the instabilities of the buoy system caused by the surface waves, etc. will lead to unpredictable errors in the estimates of the direction of arrival of the noise waveforms in each of the hydrophone arrays. With the help of Kalman filter, the imprecision in the estimated position values are reduced by minimizing the mean square error.

1.6.5 Target Tracking

Target tracking systems basically produce a stream of data related to the position of the target. This scenario can be further divided into one dimensional motion of the target with inherent noises of different forms such as process noise and measurement noise. A study of one dimensional system is carried out and then extended to two dimensions, which can further be generalized to a multi-dimensional system depending on the nature of the problem.

In the case of a maneuvering target, the errors observed are more complex in nature compared to the case of a moving target and hence suitable correction measures has to be adopted. In the case of a highly maneuvering target, a chi-square based decision statistics can be applied for effecting necessary corrections to the Kalman filter algorithm, so that the system is capable of tackling such abrupt maneuvers.

1.6.6 Target Classification

The surveillance system, apart from performing the task of localization and tracking, also performs the task of target classification. The noise emanations received by the hydrophone arrays of the buoy system may be of natural origin or man-made in nature. The target specific features of the unknown target are compared with a set of archetypal features of a known pre-recorded sound files which have been previously generated and stored in a knowledge base, leading to the identification of the target.

The various digital signal processing techniques used to extract the signature features, leading to the classification of the noise source are discussed in Chapter 7. The Spectral and Bispectral features are used during the trials on the classifier performance, which yielded acceptable success rates. A Digital Signal processing hardware for the identification of the noise sources in the ocean has also been developed. The system has been realized using a proprietary version of C language evolved for the digital signal processor TMS320C6713 development board. The feature vectors for different noise sources were computed in MATLAB as well as DSP hardware and the results were compared and summarised in this chapter.

1.7 *Summary*

The importance and relevance of underwater target localization, tracking and classification have been discussed in this chapter. The concepts of sonar, different types of sonar systems, the sonar equations as well as the factors affecting the sonar performance are also elaborated. The different types of underwater noises are discussed along with the importance of underwater noises for localizing and classifying the various noise sources in the ocean. The salient highlights of the work undertaken are also briefly introduced.

CHAPTER 2

REVIEW OF PAST WORK

This chapter is devoted to the review of the past work reported in open literature in the areas of underwater target localization, tracking and classification. The highlights of the existing vessel monitoring systems and localization systems are discussed herein. A variety of systems and techniques are in wide spread use for monitoring and tracking of ships, fishing vessels and cargos making use of GPS and AIS. GIB (GPS Intelligent Buoy) systems and VRAP (Vemco Radio Acoustic Position) systems are used for localizing known targets. A system for monitoring air-water borne noise generated by an aircraft flying over a water body and a method for screening the acoustic emissions from the underwater target have been patented. A method for determining the three dimensional location of an acoustic event using five or more sensing elements is also reported. Apart from discussions on existing localization systems, a literature survey on the application of Kalman filters for refining the localization and tracking estimates, including the maneuvering situations are also included. A survey on generation of different target specific features for the classification of unknown targets is also covered.

2.1 *Introduction*

Passive sonar system bases its detection and estimation on sounds, which emanate from the noise source itself, such as the machinery noise, flow noise, etc.. Performance limitations may arise as a result of imprecise knowledge of the characteristics of the noise emanations and dispersion in

time as well as frequency of the noise signals. Moreover, the ocean is full of interfering sound sources, which include machinery noise from shipping traffic, flow noise, wave noise, biologics and even intentional jammers. Since the noise in the ocean is composite in nature, comprising of all the noise sources mentioned above, the localization, tracking and classification of unknown underwater target are challenging tasks.

An approach for unknown underwater target localization, tracking and classification using three moored surface buoys is presented in this thesis. The literature survey undertaken during the design and development of the system is briefly reviewed in the following sections.

Robert J. Urick [1] describes the sonar, active and passive sonar equations as well as the factors that affect the propagation of sound in the sea. Sound propagation is affected by spreading, attenuation, multipath, absorption etc.. Velocity structure and thermocline of the sea, effects of sea surface and sea bottom on sound propagation are also described. Various sources of ambient noises like tides, seismic disturbances, oceanic turbulence, thermal noise, biological noises, etc are considered in detail. The noises like the radiated noise and self noise as well as the methods to reduce them are also described. John G. Proakis discussed about various characteristics of communication signals and systems as well as different coding techniques for various channels [2].

Richard O. Nielson [3] describes the sensor arrays, beamforming, detection and estimation in active and passive sonar. Conventional beam forming in time and frequency domains as well as the effects of quantized delays and other errors are considered. Active sonar signal processing and characteristics of sonar channel are illustrated in detail. An overview of

high resolution beamforming and spectral estimation are also discussed in this book.

Array signal processing by Simon Haykin, is completely devoted to sonar and radar array signal processing [4]. The basic concepts in wave propagation as well as the theory and applications of array signal processing in passive sonar are dealt with, in detail.

William *et al.* [5] describes main stream sonar digital signal processing functions along with the associated implementation considerations. Monson H. Hayes briefs the different filtering problems and their solutions including Kalman filters with example problems in [6]. Digital signal processing theory is explained in [7] by Somanathan Nair, in a simplified manner.

2.2 *Highlights of the Existing Underwater Systems*

The highlights of the existing vessel tracking/monitoring systems and underwater target localization systems are discussed in the following sections.

2.2.1 Vessel Monitoring Systems

A variety of Tracking/Monitoring systems and techniques are in wide spread use for monitoring and tracking of ships, fishing vessels and cargos making use of GPS and AIS.

Vessel Monitoring System (VMS) is a satellite based, near real time, positional tracking system. This system consists of a Global Positioning System (GPS) and a satellite data transmitter that provides information on vessel ID, location and activity. A VMS unit is about the size of a small radio with an antenna. Data is sent to a satellite, relayed to a

station on the ground and then sent to the designated vessel monitoring centre. This system provides important information to manage fisheries resources and improves compliance with fisheries regulations by providing regular positional information of vessel activity. VMS also provides information about the status of fish stocks and fish movement. The VMS unit has a two-way data communication port that can provide email access while at sea [8]. VMS is widely used in many fisheries programmes throughout the world and helps to monitor vessel position, course and speed [9, 10].

AIS (Automatic Identification System) is a onboard broadcast transponder system making use of which, ships continually transmit their ID, position, course, speed and other data to all other nearby ships and port authorities on a common VHF radio channel. AIS is designed to operate in one of the following modes [11] :

- Ship-to-ship mode
- Ship-to-shore mode
- Traffic management tool when integrated with a Vessel Traffic System (VTS).

When integrated with shore-based vessel traffic systems, as shown in Fig. 2.1, AIS provides a powerful tool for monitoring and controlling the movement of vessels through restricted harbours and waterways. The AIS channels can be used to transmit port data, pilot age, berth assignments, shipping agency information, tides and currents, notices to mariners and other information from shore to ship, as well as ship-to-ship and ship-to-shore AIS reports. It is also possible for the VTS to broadcast the complete harbour picture to all ships in the area, so that the masters and pilots all share the relevant information.

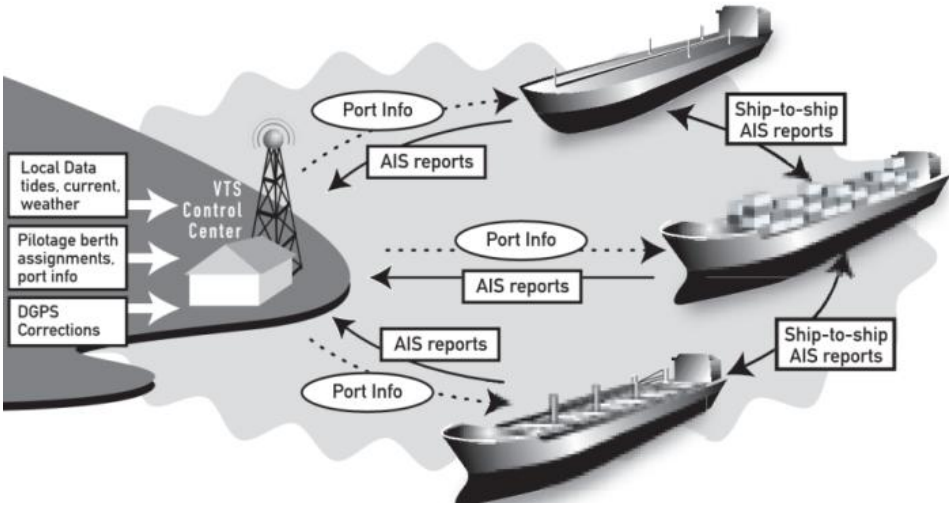

Fig. 2.1 AIS integrated with VTS [11]

Vessel Traffic Monitoring and Management Systems developed by Ledwood Technology Ltd., UK, provide a comprehensive situational awareness information that facilitates efficient management of waterways, ports and harbours as well as helping to improve safety and reduce risk to the environment. They provide remote monitoring and control from a wide range of sensors that assist in the efficient management of waterways. Radar and AIS track data are brought together from multiple sensors to present a traffic view that simultaneously support both marine and Inland standards. CCTV cameras can be tasked to look at or follow any track or location available in the system. All sensor data including Radar, VHF as well as CCTV can be remotely controlled and all available data, traffic information and events are recorded to enable quick and efficient in house training and incident investigation [12].

Another category of VMS, shown in Fig. 2.2, transmits a signal, typically once per hour, for identifying the exact latitude and longitude of a vessel. Such VMS consists of a three step process. First, the system itself,

which includes a mobile transceiver unit placed on the vessel, second, a communications service provider that supplies the wireless link between the unit on the vessel and Fisheries Service's Office for Law Enforcement (OLE), and third, a secure OLE facility where only OLE staff can receive and monitor compliance [13].

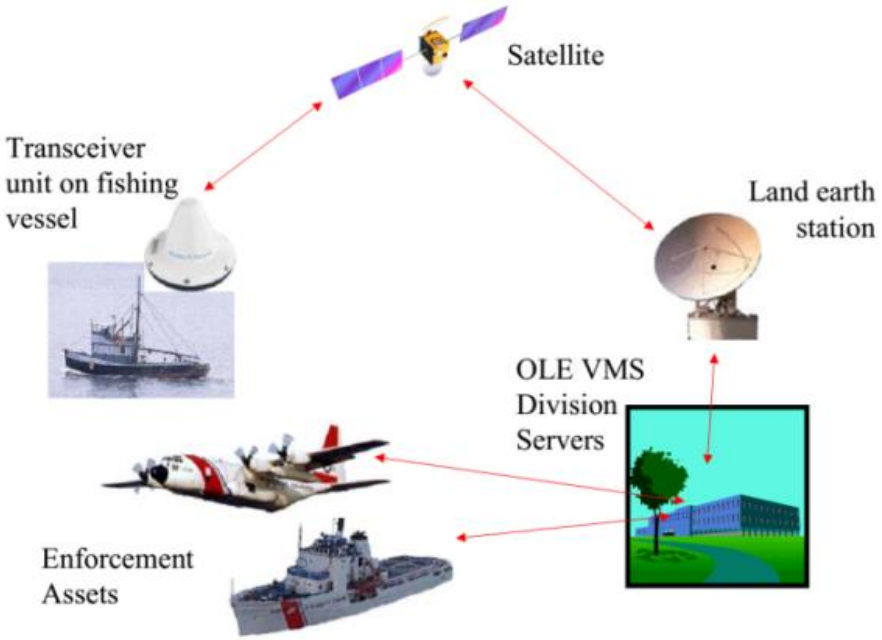

Fig. 2.2 The Vessel Monitoring System reported in [14]

PACTRACS is a Vessel Tracking System that employs AIS and Satellite Communications to aid safe, secure, efficient and environmentally sound maritime operations [14]. This system is designed to track and record the vessel's locations, speed, route, destination etc. in the Pacific. This system is capable of receiving, processing and displaying the positions of vessels using AIS and satellite tracking systems.

The Shipborne Automatic Identification System is a ship and shore based broadcast system, operating in the VHF maritime band [15]. It is

capable of sending and receiving ship information such as ship ID, position, course, speed, ship particulars and cargo information to and from other ships. It uses Self Organizing Time Division Multiple Access (SOTDMA) technology to meet this high broadcast rate and ensure stable and reliable ship-to-ship and ship-to-shore operation. When used with an appropriate graphical display, shipboard AIS enables the provision of fast, automatic and accurate information regarding risk of collision by calculating Closest Point of Approach (CPA) and Time to Closest Point of Approach (TCPA) from the positional information transmitted by target vessels. The principles of SOTDMA is shown in Fig. 2.3.

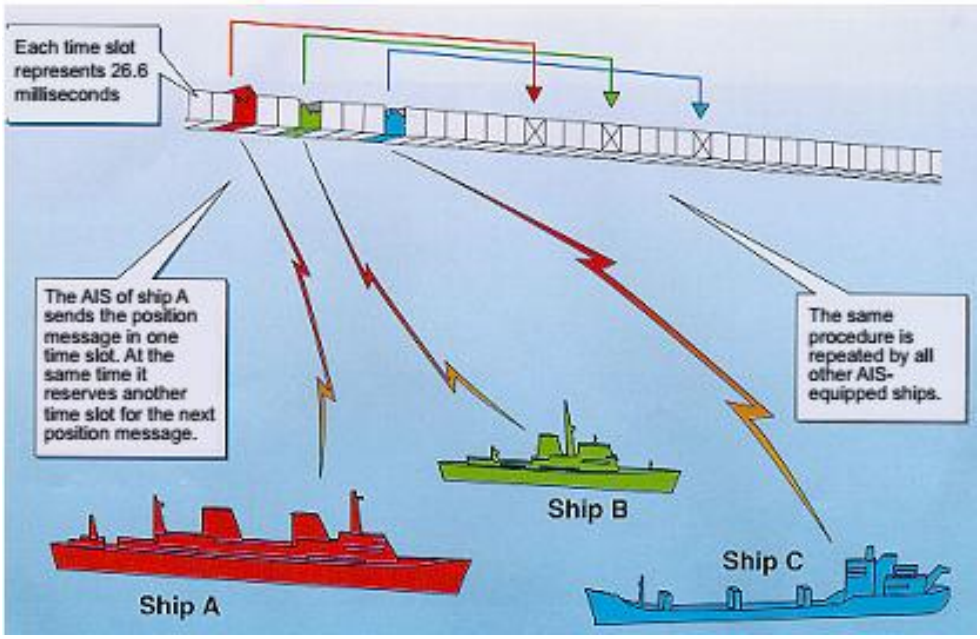

Fig. 2.3 Principles of SOTDMA [15]

M. Redoutey *et al*. discussed the techniques that improve the existing Automatic Identification System by offering better and guaranteed tracking accuracies at lower communication costs. This system, identifies and locates vessels, transmits location related information from vessels to

ground stations that are part of Vessel Traffic Service (VTS), thus enabling these to track the movements of the vessels. This system offers better and guaranteed tracking accuracies and the techniques employ movement predictions that are shared between vessels and the VTS [16].

The RFID based Rolta Command & Control solution for Tracking of Vessels (C2TV) [17] is a fully integrated system for automating the Control Centers of Law Enforcement agencies. The prime objective of this solution is to automate the processes at the local and main Control Centers by creating a shareable Situational Awareness (SA) picture providing operational functionalities amongst the individual members of watch teams at respective Control Centers. Making use of such systems, the Local Control Centers can maintain a very close watch on the activities of fishing boats and other vessels operating in the captive areas.

Applied Weather Technology (AWT), provides a valuable tracking service, which is an indispensable tool for keeping track of a vessel's location and monitoring its estimated time of arrival. AWT will insert vessel's track into the AWT Route optimization system and using proprietary wind and wave data and vessel specific speed down algorithms, AWT can predict when the vessel will arrive at a specified port. The vessel's ETA is continuously updated throughout the voyage as new weather or position data is received. Automated polling service uses the vessel's inmarsat unit to schedule positions to be sent to AWT. This polling service is an ideal tool to keep track of the vessel's latest position and to monitor speed and heading [18].

A new approach using the WERA (WEllen RAdar) system, in order to monitor ship traffic over long distances is discussed in [19]. For ship detection and tracking procedures, the sea clutter can be considered to be an

unwanted, self generated interference which ultimately limit the detection capability of the radar system. To evaluate the quality of radar detection, a data set of GPS-acquired ship locations, provided by the Automatic Identification System was recorded for the same period of time. Due to external noise, radio frequency interference and different kinds of clutter, special techniques of ship detection using the WERA system have to be applied. The WERA HF radar system [20] was developed at the University of Hamburg, Germany in 1996, which allows a wide range of working frequencies, spatial resolution, and antenna configurations in order to operate as a low power oceanographic radar, providing simultaneous wide area measurements of sea surface currents, waves and wind parameters.

The Ship Tracking Service Using Google Earth has been developed by SHIPPOS [21], specifically for shipping companies, offshore support & oil exploration companies and coastal fleet operators to track surface vessels. This tracking system is a web-based service that provides an effective way of automatically tracking and managing vessels in real time. Access from Google Earth is controlled by a password protection scheme, which is administrated through a web interface. The system requirements are, a PC onboard with an attached GPS, and an Internet connection and GPS reader as well as a license to access the service. Another Internet-based Vessel Tracking System (I-TRACK) reported in [22] is a user friendly web-based system, which aims to provide real-time information of vessel Positions in the port to the maritime industry.

The role of AIS for small vessels monitoring has been discussed by Marek Dziewicki in [23]. The AIS, the limitations associated with the use of AIS, HELCOM (Helsinki Committee) AIS network and a rescue boat test with AIS onboard are also discussed.

ORCA Vessel Tracking System [24] for Maritimes Authorities ensures safety, security & efficiency of ship traffic over wide areas or busy waterways and provides a clear traffic picture and advanced automatic tools for traffic management. This is a fully integrated multi-sensor surveillance system providing a complete real-time maritime picture encompassing Radar and AIS. As a key breakthrough in VTS technology, this system offers an innovative interface with a complete set of user friendly displays combined with click and play controls and advanced tools, as shown in Fig. 2.4.

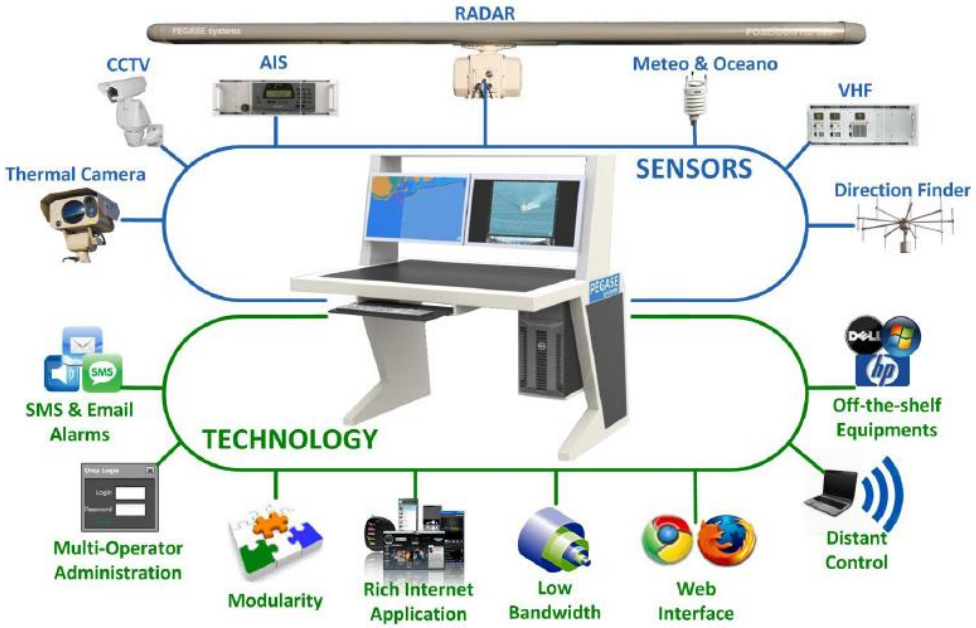

Fig. 2.4 ORCA Vessel Tracking System reported in [24]

Many VMS and VTS systems are used all over the world [25-32]. THEMIS (THEmatic Maritime Information System) [33] is a comprehensive data integration interface and a crucial tool for maintaining 24 hour maritime surveillance based on a variety of data sources.

Kevin Gregory discusses about latest technological developments in vessel tracking and monitoring including usage of traffic image, CCTV applications and VTS charting [34]. Lemoine *et al*. presented an operational vessel detection system based on SAR imagery [35]. The system is capable of near real time delivery of vessel positions for matching to known positional records.

A dynamically positioned (DP) [36] vessel maintains its position (fixed location or predetermined track) by means of active thrusters. The DP system can also be used in combination with mooring and anchoring to form position-mooring systems for energy efficiency. DP-operated vessels possess the ability to operate with positioning accuracy, safety, and reliability. Such systems have gained the trust and acceptance of the industry and the International Maritime Organization and have been successfully applied worldwide. The advantages of fully DP-operated vessels include the ability to operate with positioning accuracy and the flexibility to establish position and leave location fast, without the need for mooring lines to be deployed. In addition, there may be restrictions on the deployment of anchors due to the already installed subsea structures on the seabed. For certain deepwater exploration and production scenarios, DP-operated vessels may be the only feasible solution due to the depth and length of mooring lines required.

2.2.2 Target Localization Systems

Many surveillance systems based on passive listening concepts have been developed and deployed in the past.

The GPS Intelligent Buoy (GIB) System for the position fixing of underwater targets is used for estimating the positions and tracking of

known underwater targets. GPS intelligent buoy systems are devices where the transducers are installed on GPS equipped sonobuoys that are either drifting or moored [37].

The GPS Intelligent Buoy System, developed by Advanced Concepts Systems Architecture, South France, consists of four surface buoys equipped with GPS receivers and submerged hydrophones. A pinger housed onboard the target emits periodic acoustic signals. The hydrophone subsystem in the buoys receive these acoustic signals with different latencies, since all the buoys are positioned at different locations. Each of the hydrophones receives the acoustic impulses emitted periodically by a synchronized pinger installed onboard the underwater target and records their times of arrival (TOA). The buoys communicate via radio with a central station, where the position of the underwater target is computed and displayed. The pinger emits two successive acoustic pulses during each emission cycle, the time delay between the two pulses being proportional to the pinger depth. Accuracies up to 10 cms are reported to have obtained, when the buoys are placed 500 meters apart.

The GIB, the portable tracking system is based on surface buoys network that measures the time-of-flight of acoustic signals emitted by an acoustic transmitter mounted on an AUV, ROV, diver, etc..

A. Alcocer *et al.* presented a method for underwater acoustic positioning systems based on buoys with GPS [38, 39]. This method is used to estimate the position of an acoustic pinger by measuring the times of arrival of acoustic signals at four surface buoys equipped with GPS receivers and submerged hydrophones. Each of the hydrophones receives the acoustic impulses emitted periodically by a synchronized pinger installed on-board the underwater platform and records their TOA. The

pinger emits two successive acoustic pulses during each emission cycle. A constant value for the speed of sound is assumed to translate TOA into distance. The measured TOA data contains range and depth information as well as numerous outliers. It is a critical issue for this kind of systems to be able to identify and properly reject acoustic outliers. If enough number of ranges are available, an instantaneous position solution can be obtained by triangulation or by using more sophisticated algorithms. Assuming that the pinger is synchronized with the buoys and that the speed of sound is constant and known, the measured times of arrival can be converted to distances.

Hubert G. Thomas [40] investigated the GIB buoy systems and discussed different techniques allowing development of underwater applications of GPS. The tracking principle is based on measuring, on a set of buoys, the time of arrival of an acoustic pulse sent by the mobile target at a known time. At regular interval, each buoy transmits to a processing centre, its GPS position and the time of arrival of the acoustic pulses. Knowing the sound velocity, distances from the buoys to the mobile target can easily be calculated.

Another commercial system existing for a similar application, is the Vemco Radio Acoustic Positioning (VRAP) system [41]. This system is similar to the GIB system. This system is also used for locating the known object, using the pinger signal generated from a tag attached to a fish, ROV, etc.. It does not make use of any GPS. The VRAP system measure real-time detailed position information from underwater acoustic transmitters using a series of three buoys and has a two way radio link to a base station. Depending on environmental conditions, the VRAP system is typically able to furnish position information with a resolution in the range

of 1 to 2 meters within the buoy triangle. The Pinger pulse width and frequency are selected in accordance with the depth and some other parameters. This signal is captured by the hydrophones and transmitted to the shore station for further processing.

The VRAP system illustrated in Fig. 2.5, is used to investigate a wide range of species from lobsters to sharks. Applications include ecological impact studies, bioenergetics, spawning aggregate interaction, predator versus prey interaction and site residency studies. It is particularly useful in studying the impact of various environmental conditions such as changing tides, sea state, temperature and storms on the movement of aquatic organisms.

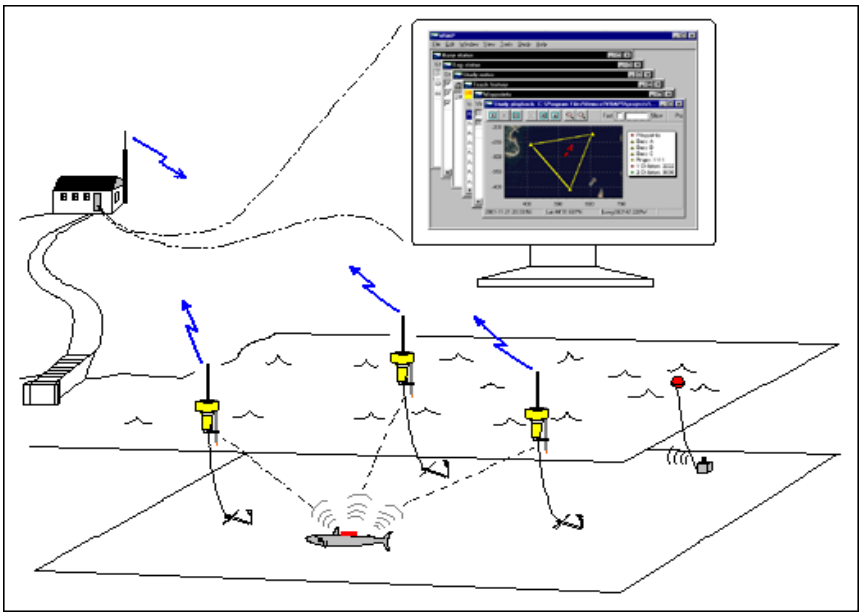

Fig. 2.5 VRAP System [41]

While deploying the Buoys, the geographical information and distance between each buoys has to be noted. Each buoy contains ultrasonic receiver, two way radio links, a microcontroller, solar panel and

rechargeable battery. The RF links of each buoy operate on different mode frequency, for buoy identity. The base station includes a two way communication RF link, timing circuitry and a PC serial data link. The hydrophones on each buoy receive the data from the pinger in the tag attached to the animal that is being tracked. This information is then transferred to the base station through the RF link and the position is computed and displayed in real time.

When the system is initialized, the base station sends a radio command to each of the three buoys to determine 'buoy-to-buoy' distances. Positioning is performed in sequence and each transmitter can be monitored for certain time period (in the order of seconds). Following initialization, each transmitter is positioned based on arrival time of the acoustic ping to each buoy.

In this context, it is worth mentioning the fact that the estimation of position of known targets using the known transmitted data emanating from the pinger onboard the target is quite simple and straightforward.

Sonobuoys are small sonar sets dropped by an aircraft for underwater listening or echo ranging. This compact, expendable device contains miniature radio transmitter for relaying signals picked up by its hydrophone. In submarine hunting from an aircraft, a specially packaged explosive charge is dropped by the aircraft, a sonobuoy is used to receive and transmit echoes and using these, *explosive echo ranging* can be performed. The pressure detonated explosive charge is the sound source for echo ranging and the sonobuoy is the link between the sound underwater and aircraft above [1].

Lock *et al.* [42] discloses an acoustic sensing system, known as a sonobuoy, for detecting underwater acoustic signals of interest. It consists of a hydrophone or array of hydrophones deployed beneath the surface of water and suspended from a float for detecting the acoustic signals underwater. The float also carries an antenna for transmitting the output of the hydrophone array. This sonobuoy is typically operational for one to six hours, after which the float is punctured and the device falls to the seabed. Such devices are used only for sensing or detecting certain targets by dropping the sonobuoys from aircraft, at the desired locations of interest. The sonobuoy for detecting acoustic signals of interest is shown in Fig. 2.6.

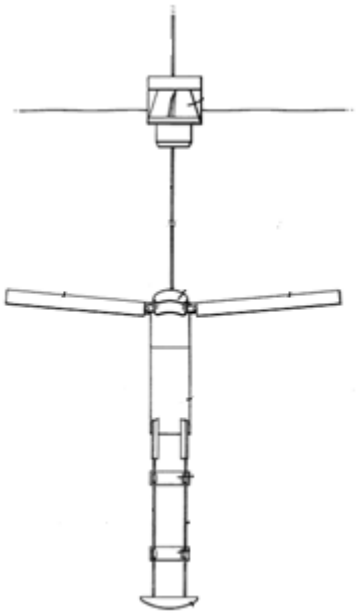

Fig. 2.6 A sonobuoy for detecting acoustic signals of interest
[Courtesy : Lock (European Patent EP 0489593A1)]

A system for monitoring air-water borne noise generated by an aircraft flying over a body of water has been reported in [43]. It comprises of a sonobuoy having a linear array of hydrophones suspended beneath the

surface of water and a radio transponder for locating the surface position of the sonobuoy.

A number of electroacoustic buoys are positioned apart from the sonobuoy and the emitted acoustic pings are detected by the linear array, leading to the determination of the surface position of the sonobuoy. Such systems are used only for sensing or detecting certain targets by dropping the sonobuoys from an aircraft. The Perspective view of the system invented is depicted in Fig. 2.7 and the side elevation view of the data gathering sonobuoy is shown in Fig. 2.8.

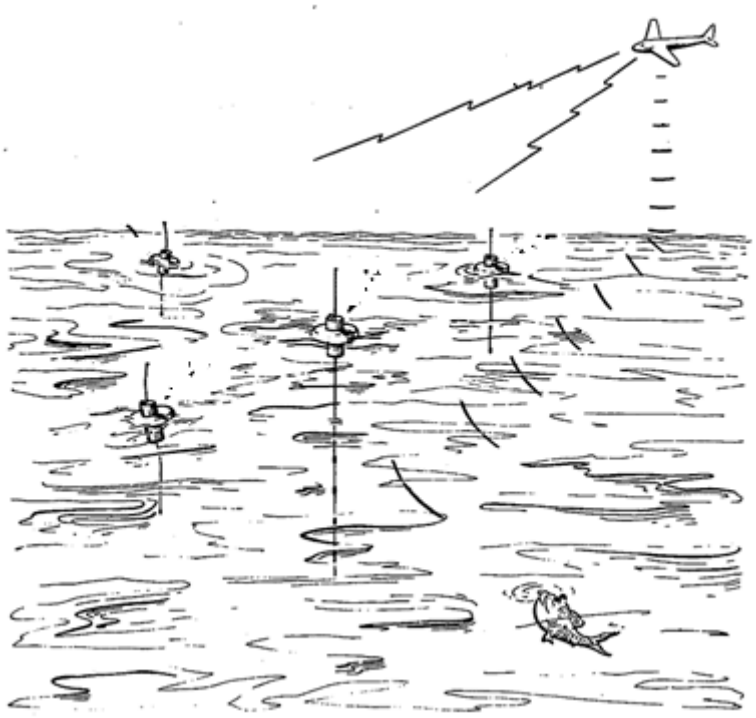

Fig. 2.7 Perspective view of the system for monitoring air-water borne noise [Courtesy : Funk (US Patent 4114135)]

Another system which discloses a method for screening the acoustic emissions, spectral line or narrow band, from the targets underwater from

among many acoustic signals of the same type with a certain threshold energy level [44].

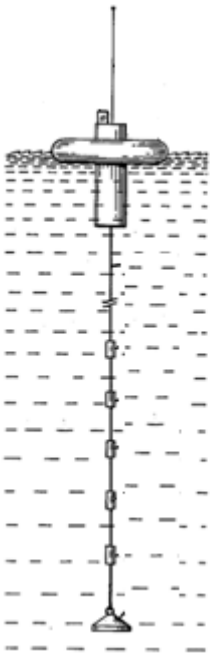

Fig. 2.8 Side elevation view of the data gathering sonobuoy
[Courtesy : Funk (US Patent 4114135)]

This approach helps in reducing the number of unwanted signals interfering with the observation of useful signals, to be detected. It introduces the concept of surveillance cells with two adjacent pickups, each pickup being associated with one or more target detection regions, defined as the geographic areas within which the presence of the target is deemed detectable. This system also defines the conditions under which the noise generator is located and locating it relative to the special areas. This method is a heuristic approach centered around some thumb rules, and will work with targets that are in the neighborhood. For targets which are far away, this will turn out to be inefficient, and will certainly fail as the acoustic

signal levels received by the system from far away targets will be very feeble and much less than the threshold level.

A technique for determining the three dimensional location of an acoustic event using a system of five or more sound sensing elements has been reported [45]. The system using the aforesaid technique is shown in Fig. 2.9.

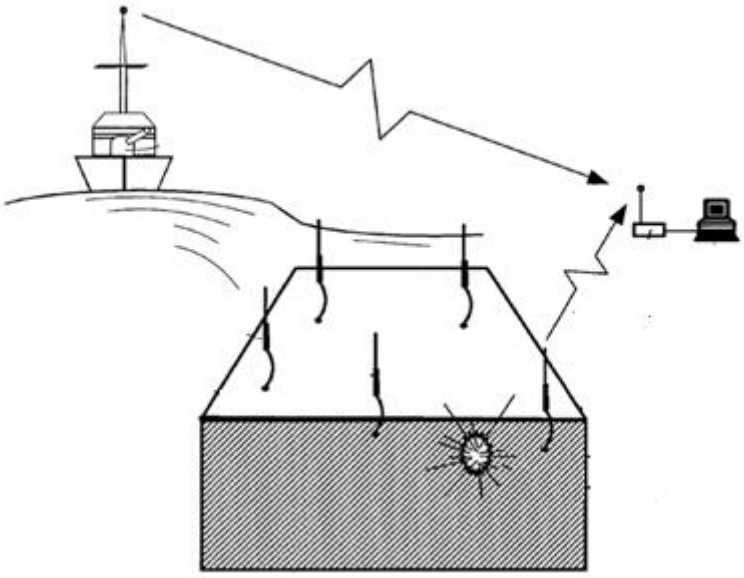

Fig. 2.9 A system for determining the three dimensional location of an acoustic event [Courtesy : Harvey (US Patent 7233545B2)]

The sensing elements generate notification signals indicating the occurrence of the acoustic event. A central processor receives the notification signals and associates the locations of each of the sensing elements with the instants at which each sensing element sensed the sound and computes the three dimensional location of the acoustic event using the speed of sound. Like the GIBS and the VRAP systems, this system also

computes the position using the transit time, associated delays and speed of sound and will work well with acoustic sources, which are generating known and short lived acoustic events. The disadvantage associated with this approach is that the system will fail for acoustic signals that are emitted continuously by the target.

An apparatus for estimating the range of a noise source has been developed by Turgut, utilizing the acoustic measurements carried out at two locations, using which the ratio of the distance of the source from the first passive vertical hydrophone array to the distance of the same from the second vertical hydrophone array is determined [46] and is as shown in Fig. 2.10.

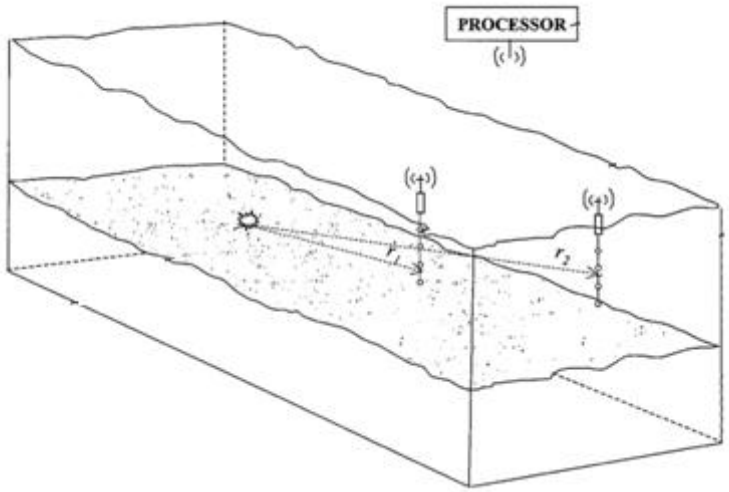

Fig. 2.10 An apparatus for estimating the range of a noise source [Courtesy : Turgut (US Patent 7471592B2)]

Making use of the measured acoustic levels, concepts of mapping the virtual array output as a function of angular frequency or angular frequency shifts, patterns of acoustic intensity level curves and precise application of waveguide invariant theory to form virtual receiver arrays as

well as by generating a two-dimensional parameter space, the system performs acoustic ranging. This system is mainly centered on the concepts of heuristics and suffers from all the limitations and disadvantages arising out of theoretical approximations, consequent to the formation of virtual receivers.

A. Peter Klimley *et al.* [47] described a method, radio acoustic positioning (RAP), for continuously monitoring the movements and behaviour of large marine animals. An ultrasonic transmitter on the mammal can be localized with spatial accuracy of 2m to 10m within an area of 1km^2, based on when the same pulse arrives at three hydrophones on sonobuoys, positioned at the vertices of a triangle as shown in Fig. 2.11.

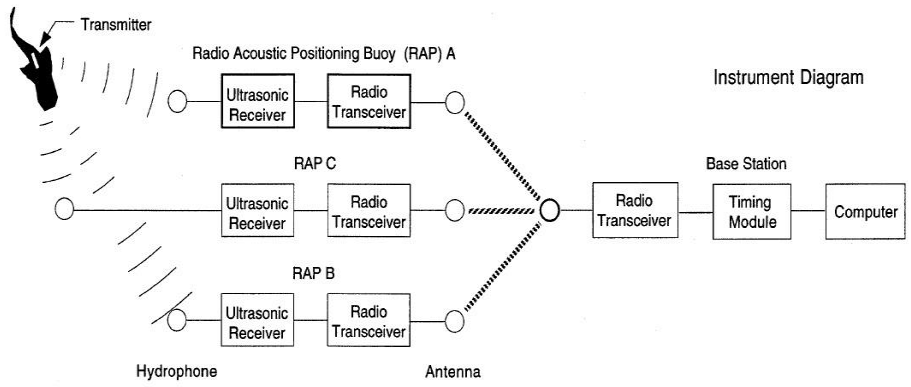

Fig. 2.11 Radio acoustic positioning for studying site-specific behaviour of marine species

Radio transceivers communicate with the base station, where the x and y coordinates of the target are computed. The base station also plots the spatial position of the target and displays the information from the tag sensors in real time on a computer monitor. The base station must be situated either on land or on a vessel within the reception range of the three

buoys. The RAP system was used to monitor the movements and behaviour of white sharks. This type of study throws light into their predatory behaviour because they patrol for seal prey within a zone less than 1300m from shore. The authors describe the implementation and operation of the system including acoustic triangulation, range of detection and positioning, data acquisition and analysis, and positional accuracy.

This thesis envisages a three buoy automated system for underwater target localization, tracking and classification, using passive listening buoy systems and target classification techniques. The system has been designed, developed and field tested. The recoiling effect, caused due to the movement of the array from one position to another, the instabilities of the buoy system caused by the surface waves, etc., will lead to unpredictable errors in the estimates of the direction of arrival of the noise waveforms, which in turn affect the accuracy of the localization system. These inaccuracies in the localization estimates due to changes in the environmental parameters, measurement errors and theoretical approximations are resolved, to a certain extent, by applying the concepts of Kalman filter.

2.3 *Refinement of Localization Estimates*

In 1960, Rudolf E Kalman [48] introduced the Kalman filter theory. In his paper, the classical filtering and prediction problem is re-examined using the Bode-Shannon representation of random processes and the "state transition" method of analysis of dynamic systems. The formulation and methods of solution of the problem are applied without modification to stationary and nonstationary statistics and to growing-memory and infinite memory filters. A nonlinear difference or differential equation is derived for the covariance matrix of the optimal estimation error. From the solution

of this equation, the coefficients of the difference or differential equation of the optimal linear filter are obtained without further calculations. Also, the filtering problem is shown to be the dual of the noise free regulator problem.

In 2006, G. Welch and G. Bishop published papers and discussed the theory of Kalman filters through their website [49, 50]. The purpose is to provide a practical introduction to the discrete Kalman filter. This includes a description and some discussion of the basic discrete Kalman filter, a derivation, description and some discussion of the extended Kalman filter, and a relatively simple or tangible example with real numbers and results.

Dan. Simon and T. Chia discussed Kalman Filtering and Kalman filter with state equality constraints during 2001-2002 [51, 52]. Kalman filters are commonly used to estimate the states of a dynamic system. However, in the application of Kalman filters there is often known model or signal information that is either ignored or dealt with heuristically. For instance, constraints on state values, which may be based on physical considerations, are often neglected because they do not fit easily into the structure of the Kalman filter. A rigorous analytic method of incorporating state equality constraints in the Kalman filter is developed. The constraints may be time varying. At each time step the unconstrained Kalman filter solution is projected onto the state constraint surface. This significantly improves the prediction accuracy of the filter.

Chiman M. Kwan *et al.* discussed [53] a simple qualitative explanation to understand performance of Discrete Kalman Filter (DKF) and Continuous Kalman filter (CKF) which help to clear the misunderstanding that DKF is better than CKF. The three ways of Kalman

filter design depending upon the measurement process are Continuous Kalman Filter, Continuous-Discrete Kalman Filter and Discrete Kalman filter. CKF gives the best performance since there is a continuous flow of measurement data in to the Kalman filter. Also, the DKF and CDKF converge to the CKF as the sampling period tends to zero.

Peter S. Maybeck reviewed Stochastic Models, Estimation and Control in his book [54] and has also discussed the introductory concepts of Kalman filtering, basic assumptions of Kalman filters and a simple example for understanding the working of the Kalman filter.

2.4 *Target Tracking*

Y. T. Chan *et al.* [55, 56] discussed a Kalman Tracker with a Simple input estimator for tracking space targets. Two Kalman filter based schemes are proposed for tracking maneuvering targets. Both schemes use least squares to estimate a target's acceleration input vector and to update the tracker by this estimate. The first scheme is simpler and by an approximation to its input estimator, the computation can be considerably reduced with insignificant performance degradation. The second scheme requires two Kalman filters and hence is more complex. However, since one of its two filters assumes input noise, it may outperform the first scheme when input noise is indeed present. A detector that compares the weighted norm of the estimated input vector to a threshold is used in each scheme. Its function is to guard against false updating of the trackers and to keep the error covariance small during constant velocity tracks.

Samuel S. Blackman investigated Multiple-Target Tracking with Radar [57]. The author explains the basics of multiple target tracking and gives an overview of data association issues. The methods of filtering and

prediction including Kalman filters, its approximations and simplifications are also discussed. This book also covers the details of maneuver detection, gating as well as data associations. Yaakov Bar-shalom *et al.* discussed principles of estimation and tracking along with various techniques used [58, 59].

A Kalman filter in the Cartesian coordinates is described by Radhakisan S. Baheti [60] for efficient approximation of Kalman Filter for Target Tracking and for a maneuvering target when the radar sensor measures range, bearing and elevation angles in the polar coordinates at high data rates. An approximate gain computation algorithm has been developed to determine the filter gains for online implementation. In this approach, gains are computed for three uncoupled filters and multiplied by a Jacobian transformation determined from the measured target position and orientation. The algorithm is compared with the extended Kalman filter for a typical target trajectory in a naval gun fire control system. The filter gains and the tracking errors for the proposed algorithm are similar to the extended Kalman filter, while the computation requirements are reduced by a factor of four.

In 1996, Tokumaru *et al.* published a paper on improved tracking Kalman filter using a multilayered neural network [61]. In 2004, Lee *et al.* discussed an intelligent Kalman filter for tracking a maneuvering target by considering the unknown target acceleration as additive process noise [62].

In 2003, X. Rong Li and Vesselin P. Jilkov conducted a survey of Maneuvering Target Tracking on the basis of tracking space targets and maneuvering problems and published the survey details in 6 parts including dynamic Models and Motion Models of Ballistic and Space Targets [63-71]. It surveys various mathematical models of target motion or dynamics

proposed for maneuvering target tracking, including 2D and 3D maneuver models as well as coordinate-uncoupled generic models for target motion. This survey emphasizes the underlying ideas and assumptions of the models. Interrelationships among models and insight to the pros and cons of models are also provided.

In 2004, M. Isabel Ribeiro [72] discussed Gaussian probability density functions, properties and error characterization. Author further explains normal random variables, normal random vectors, its properties and the concepts of covariance matrix and error ellipsoid.

M. H. Bahari *et al*. [73-76] published papers on tracking a high maneuvering target based on intelligent matrix covariance resetting. In practice the conventional Kalman filters have a fast convergence rate at the beginning. However, after some iterations the Kalman filter steps become very small. To overcome this defect and to make effective use of Kalman filter capabilities, the matrix covariance resetting concept is used. The matrix covariance resetting is usually used to improve the tracking algorithm result, especially for highly maneuvering targets.

In 2009, Zhang *et al.* presented a paper on improving the tracking performance of maneuvering target based on wavelet neural network [77].

2.5 *Classification*

Another aspect that has been investigated during the course of my research work on localization and tracking system is the identification of the target of interest. The identification and selection of features play a crucial role in the realisation of the classifier with acceptable success rates. A number of features extracted from spectral and bispectral methods have been used for implementing various types of classifiers. The methods and

procedures that have been suggested for extracting some of the vital spectrally decomposable features reported are briefly discussed below.

Marple *et al.* [78, 79] summarized the new techniques developed in spectrum analysis and discussed several modern spectral estimation techniques. Author also throws some light on current spectral estimation research trends. In 1996, Ricardo S. Zebulum *et al.* in their work investigated the different spectral analysis models [80].

Chun Ru Wan *et al.* [81] analysed the statistical property of the power spectrum observations and developed a novel tonal detector by optimally integrating the spectral inferences. The results from simulations and open ocean trial data have shown that the proposed detectors have a promising role in detecting tonals.

Luzin *et al*. [82] proposed a high resolution spectral estimation algorithm based on the maximum likelihood approximation. This method allows the design of power spectrum estimating devices having rather simple structure for real time implementations.

The impact of the Fast Fourier Transform on the spectrum of time series analysis has been carried out by Bingham [83]. The paper also discusses the raw and modified Fourier periodograms, bandwidth versus stability aspects and computational approaches to complex demodulation.

Massino Aletto *et al.* [84] carried out a comparison of different spectral estimation techniques applied to nonstationary signals. The comparison examines applications in which spectral analysis is applied to nonstationary signals. Different spectral analysis algorithms were tested in order to compare their behaviour in detecting defined harmonic

frequencies. A method for estimating signal harmonics in the spectrum is presented by Eftestol [85].

Peretto *et al.* [86] describe signal spectrum analysis and a period estimation using delayed signal sampling The procedure relies on the evaluation of the input signal autocorrelation function in different delayed time instants, located at either equispaced or random time instants.

Supriya *et al.* [87-91] discussed the techniques and algorithms towards improving the underwater target recognition using spectral and cepstral features. The author also addresses the implementation of a target classifier for the noise sources in the ocean as the operated assisted classification turns out to be tedious, laborious and time consuming.

A new method for simultaneously estimating a number of power spectra has been suggested by Rodney *et al.* in [92]. It is required that a prior estimate of each spectrum is available and new information is obtained in the form of values of the autocorrelation function of their sum. The method is compared with minimum cross-entropy spectral analysis.

2.6 *Summary*

This chapter presents a state-of-the-art literature in the topic of the thesis on underwater target localization, tracking and classification. The literature survey summarizes the highlights of the existing systems for vessel monitoring and localization applications. The survey includes the Kalman filter approach applied for the refinement of localization estimates. The literature survey also covers the application of Kalman filters on tracking of targets including maneuvering situations. A literature survey on extraction of target specific features is also carried out.

CHAPTER 3

METHODOLOGY

This chapter addresses the methodology adopted for the realisation of the underwater target localization, tracking and classification system based on passive listening concepts. A three buoy system is used for localization of the underwater targets. The localization estimates may vary due to the instabilities of the buoys, measurement errors and theoretical approximations. The Kalman filter approach is implemented to reduce the inaccuracies in the localization estimates and is extended for the tracking of a moving target by generating a time series data of the localization estimates. Modifications have been effected on to the algorithm in order to cater the situations caused by the abrupt maneuvering of moving targets. The classification of unknown target involves the extraction of source specific features by analyzing the composite noise data waveforms and comparing the features with the ones in the knowledge base.

3.1 *Introduction*

Underwater target localization and tracking attracts interest, since a generalized solution has not yet been established, as the noisy ocean environment causes a multitude of impediments to the estimation task. An approach for localization, tracking and classification of underwater targets is discussed in this chapter, together with performance validation results from field trials. This prototype three buoy automated system design, aids in localizing, tracking and classifying underwater targets using passive listening and target identification techniques.

The propagation effects, responsible for the performance limitations in sonar systems are summarised here. The undersea propagation medium is a time-varying channel, which shows clear significant functional dependencies on geographic location, depth, range and season. Moreover, the temperature profile, multiple reflections and inhomogeneties present in the ocean cause a wide variety of channel dispersion effects on time, frequency and angle. The adverse effect of time spreading is due to multipath, while frequency spreading is caused by the wave motion of the sea surface, movement of water masses, underwater currents as well as the motions of the transmitter, receiver and targets. Doppler spread of up to one percent or more are common in sonar.

The sonar detection and estimation problems for signals of considerable spreading are much more cumbersome than the ones for simple systems, due to reasons that are obvious. A wide range of interfering noises are also present in the ocean such as the sea state noise, biological noise, machinery and cavitation noise from the shipping traffic, in addition to the thermal noise.

In passive listening scenario, the sources and kind of noises from the targets are used to localize and identify the targets. The noise signals generated by such noisy targets will form the basis for passive sonar localization and classification. The noise signals are characteristics of target concerned and may vary a great deal with time as well as class and type of target. Targets can be distinguished based on the specific signature feature vector obtained from the detailed analysis of the noise, which in turn can be compared with known signature patterns. Hence, the matching pattern which has a good degree of acceptability can be identified.

Sonar data can be judiciously used to locate and classify underwater targets. Target localization addresses the problem of determining the position of the target while classification addresses the problem of identifying or categorising the target. To facilitate this, knowledge about the way in which typical isolated individual bodies interact with sound wave is essential. In active sonar, such information are quantified by the parameter *Target Strength* and the process of classification is correlated to the localization and tracking functions as the target dynamics is severely affected and controlled by the target types and class. Passive sonars are the listening sonar systems which use sound, usually unwillingly, radiated by the target.

The localization, detection and estimation procedures in sonar involve the computation of various statistics for improving the overall performance of the target localization, tracking and classification capabilities of the end system, taking into consideration all the undesirable propagation effects mentioned above.

3.2 *The Three Buoy Acoustic System*

The three buoy acoustic system for underwater target localization, tracking and classification encompasses the implementation of an automated system, with the help of which underwater targets can be localized, tracked and classified using passive listening buoy systems and target identification techniques. The acoustic signals sampled by the hydrophone arrays at three spatially and non-collinearly distributed locations in the ocean are analyzed for the decision making. Submerged hydrophone arrays should be deployed for capturing the acoustic signals from three different locations with suitable buoy systems.

The electronics modules onboard the buoy, controls the hydrophone arrays, performs the processing as well as manages the communication and power supply units with back up batteries and solar charging systems. The signals from various subsystems are processed and the feature vectors of the targets extracted by the signal processing unit are to be sent to the shore station through the RF link for further processing and initiating appropriate actions for the target identifications, its position fixing and tracking. This system can identify and locate the position of the targets of interests, ranging from marine species to manmade objects.

This system accomplishes position fixing, tracking and classification of unknown underwater targets by continuously triangulating its position using geometrical construction procedures as well as exchanging the feature vector information of probable targets of interest, within the detection range of the buoy system with the shore station. The position information of the buoys, the direction of arrival, the signal level and other relevant information, gathered by the buoys from processing the received noise signals are used for fixing the position of the target.

As a critical part of the implementation of the system, following subsystems are developed, namely Steerable hydrophone arrays, Signal Processor modules which are capable of generating the feature vectors, Autonomous Buoy Systems and DOA Estimator. Suitable algorithms are implemented for localization of the target from the position information and direction of maximum signal arrival at each of the buoys by geometrical constructions.

Fig. 3.1 shows the over view of the entire system, comprising of three Buoys, the shore station and target of interest. Each of the buoy comprise of a submerged hydrophone array, having a receiving sensitivity

of *-200dB re 1V/µPa* as well as the required buoy electronics for surveying the surroundings using the hydrophone arrays.

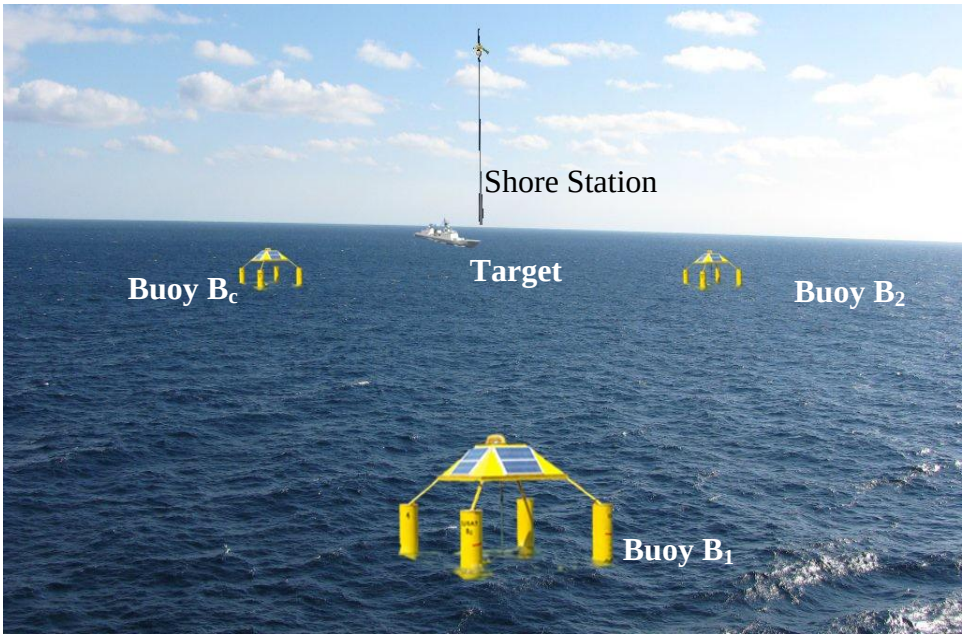

Fig. 3.1 Principles involved in the position fixing and tracking of the underwater targets

The hydrophone array can be rotated in such a way that, it orients itself to the maximum signal energy, at the desired frequencies, from the target of interest. Each of the buoys also has an omni-directional hydrophone for generating an ALERT signal for the system. Upon receipt of an alert command from the shore station, the buoy systems will begin the surveillance operation. The shore station generates the commands either when the operator is suspicious of the presence of a target or the omni-directional hydrophones of any of the buoy systems detect certain types of noise waveforms that are of interest to the deployed system. The signals so gathered by the hydrophone are processed and the feature vector

information will be sent to the shore station, based on which the shore station issues an alert command to the buoy systems.

The buoys are deployed approximately 1 km apart and the signals captured by the hydrophone arrays are pre-processed using the signal conditioning module. The digitized noise data waveforms are fed to the digital signal processor for extracting the target specific features.

Each submerged hydrophone array in the Buoy is mounted on a steering mechanism, which will help in orienting the hydrophone array to the direction of maximum signal arrival (DOA) at the frequencies of interest or in accordance with the commands from the Signal Processor. The angular position information of the hydrophone array is also fed to the DSP processor for onward transmission to the shore station for estimating the position of the target by triangulation and geometrical construction methods.

The earth's magnetic axis is considered as the reference axis. Initially, the hydrophone arrays are aligned along the reference axis. Thus, the total output from the hydrophone array controller unit is the features captured from the signal and the angular position information of the hydrophone array. The GPS receiver in the buoy furnishes the geographical position of the buoy.

The hydrophone array system is also provided with a separate omni-directional hydrophone, making use of which the system can perform effective surveillance of the region surrounding the buoy system. Whenever any of these omni-directional hydrophones capture noise waveforms, above certain threshold value, the buoy systems as well as the shore station

system will be alerted and the shore station initiates commands for performing the surveillance operation.

Finally, the buoys B_1 and B_2 furnish the extracted features, GPS information, angular position information of the hydrophone array and timing information to the coordinator buoy. The coordinator buoy sends its own data along with the data received from the other two buoys to the shore station using the RF communication link. The entire target feature record including the spectral power at the desired tonal(s) or band(s) will be processed in the shore station. Additional controlling commands, regarding a particular feature that needs to be tracked, as well as the angles to which the hydrophone arrays of the various buoys are to be aligned in situations of multiple target scenario are sent to the buoy(s) through the coordinator buoy. The power supply requirements for the system are met by the backup batteries, which are charged from the solar panels.

3.3 *Target Localization Approaches*

Determining the position of the target near the deployed buoy system with reference to the earth's coordinate system is referred as target localization. The global positioning system integrated in the buoy electronic system of the three buoys provide the location of the buoys with reference to the earth's magnetic meridian. Direction of Maximum Arrival of the noise data waveforms from the target is computed by the buoy electronics. Applying geodetic latitude and longitude distance calculations, trigonometric and basic geometric laws, the position of the target with reference to the earth's coordinate system can be computed.

Three different approaches based on the mathematical formulae and software platforms, were used for the computation. The first approach

is using Haversine formula for great-circle distance and performed on AutoLISP platform. The second approach also uses Haversine formula for great-circle distance and is implemented on MATLAB. The third approach is by using Vincenty formulae for ellipsoids and is implemented on MATLAB.

3.4 *Refinement of Localization Estimates*

One of the main requirements of most of the surveillance operations is the precise positioning and ranging of targets, which is implemented using approximate algorithms on real time data from such systems. In the proposed three buoy system, the noise emanations from the sources are used to estimate the direction of arrival of the noise in the three hydrophone arrays of the buoy system, leading to the estimation of the position of the target of interest, using triangulation technique.

For the surveillance operation, the arrays are mechanically steered. Whenever the array moves from one position to another, there will be a recoiling effect on the entire buoy system. This recoiling effect, caused due to the movement of the array from one position to another, will affect the orientation of the buoy, thus leading to inaccuracies in the angular positions of the hydrophone arrays and hence the direction of arrival. The instabilities of the buoy system caused by the surface waves will also lead to unpredictable errors in the estimates of the direction of arrival of the noise waveforms in each of the hydrophone arrays. The estimation of the direction of arrival and range of the target are also influenced by other factors such as effects of reverberation and occurrence of multi-target scenarios. These issues warrant the need and requirement for refining the localization estimation, making use of Kalman Filters.

3.4.1 Kalman Filter

A Kalman filter [48-54] is an optimal recursive data processing algorithm. One aspect of optimality is that the Kalman filter incorporates all information that can be provided to it. It processes all available measurements, regardless of its precision, to estimate the current value of the variables of interest, with the use of knowledge of the system and measurement device dynamics, the statistical description of the system noises, measurement errors, uncertainty in the dynamic models and any available information about initial conditions of the variables of interest.

In 1960, R.E. Kalman published his famous paper describing a recursive solution to the discrete data linear filtering problem. Since then, the Kalman filter has been the subject of extensive research and application, particularly in the area of autonomous or assisted navigation. The Kalman filter is a set of mathematical equations that provides an efficient computational recursive means to estimate the state of a process, in a way that minimizes the mean of the squared error. The filter is very powerful in several aspects: it supports estimations of past, present, and even future states, and it can do so even when the precise nature of the modeled system is unknown. Recursive means the Kalman filter does not require all previous data to be stored and the program inherently incorporates discrete time measurement samples rather than continuous time inputs.

3.4.1.1 **System Model**

A physical system can be represented by a mathematical model that adequately represents some aspects of the behaviour of the system. Through physical insights, fundamental laws or empirical testing, the interrelationships between certain variables of interests, inputs to the

system and outputs from the system can be established. With such mathematical models, the tools provided by the system and the control theories, the system structure and modes of response can be navigated. If desired, compensators that alter these characteristics and controllers that provide appropriate inputs to generate desired system responses also can be designed. In order to observe the actual system behaviour, measurement devices are constructed to output data signals proportional to certain variables of interest. These output signal and the known inputs to the system are the only information that is directly discernible about the system behaviour. If a feedback controller is being designed, the measurement device outputs are the only signals directly available for inputs to the controller.

3.4.1.2 **Introductory Concepts**

Fig. 3.2 depicts a typical situation in which a Kalman filter could be used advantageously. A system of some sort is driven by some known controls, and measuring devices provide the value of certain pertinent quantities. Knowledge of these system inputs and outputs are explicitly available from the physical system for estimation purposes. Often the variables of interest, some finite number of quantities to describe the state of the system, cannot be measured directly and some means of inferring these values from the available data must be generated. This inference is complicated by the fact that the system is typically driven by input other than the known controls and that the relationships among the various state variables as well as the measurements are also uncertain.

Furthermore any measurement also will be corrupted to some degree by noise and other inaccuracies. Kalman filter combines all available measurement data and prior knowledge about the system and

measuring devices, to produce an estimate of the desired variables in such a manner that the error is minimized statistically, where the system can be described through a linear model and the system and measurement noise are white and Gaussian.

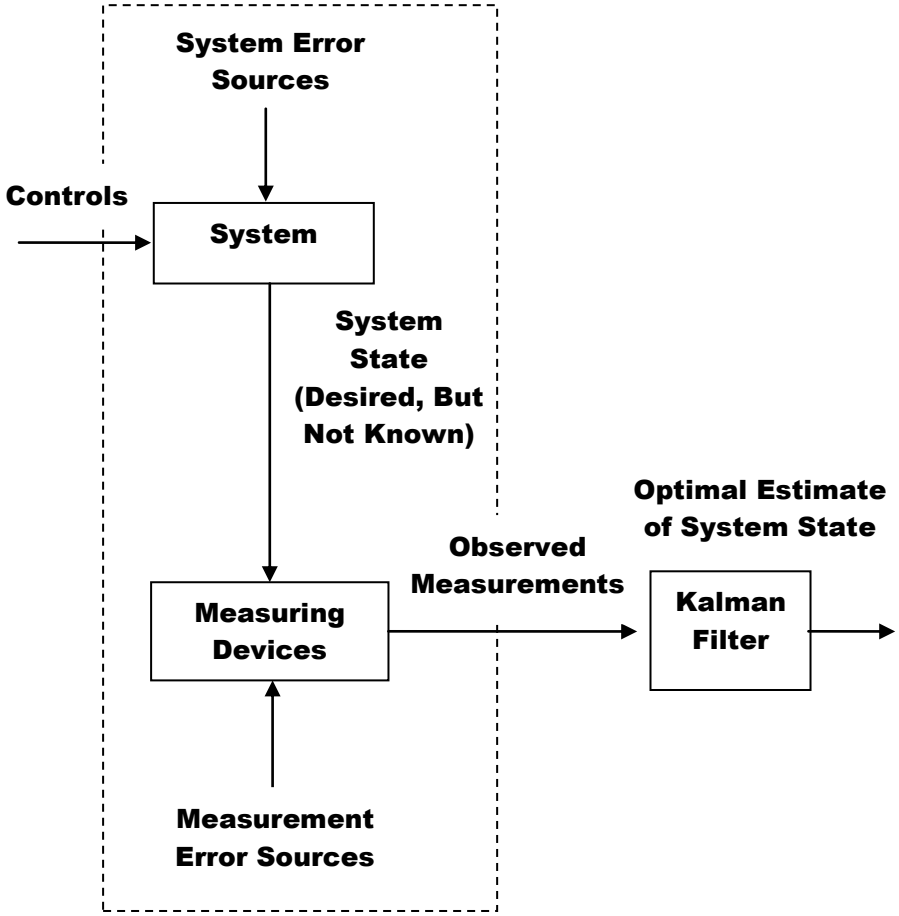

Fig. 3.2 Typical Kalman Filter Application

Linear systems are desirable because they are easy to manipulate with engineering tools and the linear theory is much more complete and practical than nonlinear systems. When nonlinearities do exist the approach is to linearize the system model. Whiteness implies that the noise is not correlated in time and has equal power at all frequencies. Within the band

pass of the system of interest, white noise assumption can be justified. Gaussian assumption can be justified by the fact that a system or measurement noise is typically caused by a number of small sources. When a number of independent random variables are added together, the summed effect can be described very closely by a Gaussian probability density, regardless of the shape of the individual ones and this assumption makes the analysis tractable too.

Many signals can be described in the following way, $y_k = a_k x_k + n_k$ where y_k is the time dependent observed signal, a_k is a gain term, x_k is the information bearing signal and n_k is the additive noise. The overall objective is to estimate x_k. The difference between the estimate $\hat{x}_k$ and x_k itself is termed the error; $f(e_k) = f(x_k - \hat{x}_k)$. The particular shape of $f(e_k)$ is dependent upon the application, however it is clear that the function should be both positive and increase monotonically.

An error function which exhibits these characteristics is the squared error function, $f(e_k) = f(x_k - \hat{x}_k)^2$. Since it is necessary to consider the ability of the filter to predict many data over a period of time, a more meaningful metric is the expected value of the error function, *loss function* $= E [f (e_k)]$, and this results in the mean squared error (MSE) function, $E [e_x^2]$.

3.4.1.3 **The Kalman model**

The Kalman filter uses recursion relations to estimate the state of a dynamic system from a series of incomplete and erroneous measurements. It helps to refine the localization measurements and bring them closer to the target's actual position by taking care of the effect of variances in the measurements. This filter is essentially a set of mathematical equations that implement a predictor-corrector type estimator that is optimal in the sense

that it minimizes the estimated error covariance. Kalman Filter is a recursive filter which means that, unlike most of the data processing concepts, the Kalman filter does not require all previous data to be kept in storage and reprocessed every time a new measurement is taken. This is of vital importance to the practicality of filter implementation.

The Kalman filter addresses the general problem of estimating the state *x*, of a discrete-time controlled random process that is governed by the linear stochastic difference equations (3.1) and (3.2),

$$x_k = Ax_{k-1} + Bu_{k-1} + w_{k-1,} \tag{3.1}$$

with a measurement z_k, that is

$$z_k = Hx_k + v_k \tag{3.2}$$

The matrix *A* in the difference equation relates the state *x* at the previous time step *k-1* to the state *x* at the current step *k*, in the absence of either an optional control function *u* or process noise *w*. The matrix *B* relates the optional control input to the state. The matrix *H* in the measurement equation relates the state to the measurement.

In practice, the matrices might change with each time step or measurement, however here they are assumed to be constant. The random variables w_k and v_k represent the process and measurement noise respectively. They are assumed to be independent, white and with normal probability distributions, $p(w) \sim N(0,Q)$ and $p(v) \sim N(0,R)$. The process noise covariance *Q* and the measurement noise covariance *R* are assumed to be constant. The system model for Kalman filter is shown in Fig. 3.3.

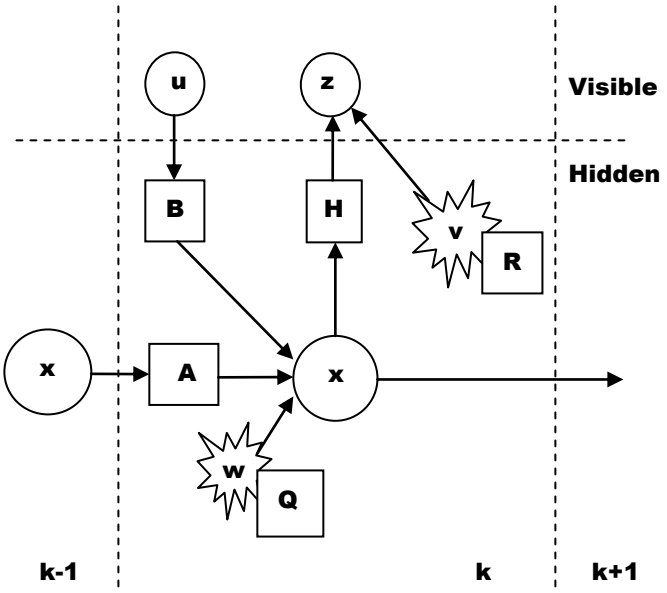

Fig. 3.3 Kalman System Model

3.4.1.4 **Computational and Probabilistic Origins of the Filter**

If random variable $\hat{x}_k^-$ is the *a priori* state estimate at step *k*, given knowledge of the process prior to step *k*, and random variable $\hat{x}$ is the *a posteriori* state estimate at step *k*, given measurement $z_{k,}$ The *a priori* and *a posterioi* estimate errors are $e_k^- = \hat{x} - \hat{x}_k^-$, and $e_k = \hat{x} - \hat{x}_k$.

Then the *a priori* estimate error covariance is,

$$P_k^- = E\,[e_k^-\, e_k^{-T}], \qquad (3.3)$$

and the *a posteriori* estimate error covariance is

$$P_k = E\,[e_k\, e_k^T]. \qquad (3.4)$$

The *a posteriori* state estimate can be written as a linear combination of an *a priori* estimate and a weighted difference between an actual measurement and a measurement prediction as

$$\hat{x}_k = \hat{x}_k^- + K(z_k - H\hat{x}_k^-) \quad (3.5)$$

The difference $(z_k - H\hat{x}_k^-)$ is called the measurement *innovation* or the *residual.* The residual reflects the discrepancy between the predicted measurement and the actual measurement. A residual of zero means that the two are in complete agreement. The matrix *K* is the Kalman gain or blending factor that minimizes the *a posteriori* error covariance.

The minimisation can be accomplished by first taking the derivative of equation for *a posteriori* error covariance after substituting the equations of $\hat{x}_k$ and e_k, with respect to *K*, and setting the result to zero, and then solving for *K*. One form of resulting *K* is given by

$$K_k = P_k^- H^T (HP_k^- H^T + R)^{-1} \quad (3.6)$$

$$= \frac{P_k^- H^T}{HP_k^- H^T + R} \quad (3.7)$$

ie., as the measurement error covariance *R* approaches zero, the Gain *K* weights the residual more heavily. On the other hand, as the *a prori* error covariance P_k^- approaches zero, the gain *K* weights the residual less heavily.

3.4.1.5 **Discrete Kalman Filter Algorithm**

The Kalman filter estimates a process by using a form of feedback control. It also estimates the process state at some time and then obtains the predicted values. As such, the equations for the Kalman filter fall into two groups, *viz.*, the time update equations and measurement update equations. The time update equations are responsible for projecting forward (in time) the current state and error covariance estimates to obtain the *a priori* estimates for the next time step. The measurement update equations are

responsible for mapping the predicted values into the *a priori* estimate to obtain an improved *a posteriori* estimate.

The time update equations can as well be thought of as the *predictor equations*, while the measurement update equations can be thought of as *corrector equations*. Indeed the final estimation algorithm resembles that of a *predictor-corrector algorithm* for solving numerical problems. The following are the Predictor/corrected Kalman Filter Equations.

Predictor Equations:

$$\hat{x}_k^- = A\hat{x}_{k-1} + Bu_{k-1} \tag{3.8}$$

$$P_k^- = AP_{k-1}A^T + Q \tag{3.9}$$

$\hat{x}_k^-$ is the *a priori* state estimate at step *k*, which is the estimate of the state based on measurements at previous time-steps and $\hat{x}_k$ is the *a posteriori* state estimate at step *k*, given measurement z_k. The *a priori* estimate error covariance, $P_k^- = E[e_k^- \; e_k^{-T}]$, and the *a posteriori* estimate error covariance, $P_k = E[e_k \; e_k^T]$, where the *a priori* estimate error, $e_k^- = \hat{x} - \hat{x}_k^-$, and the *a posteriori* estimate error $e_k = \hat{x} - \hat{x}_k$.

Corrector Equations:

$$K_k = P_k^- H^T (HP_k^- H^T + R)^{-1} \tag{3.10}$$

$$\hat{x}_k = \hat{x}_k^- + K_k (z_k - H\hat{x}_k^-) \tag{3.11}$$

$$P_k = (I - K_k H) P_k^- \tag{3.12}$$

A complete picture of the operation of the Kalman filter, with the equations is given in Fig. 3.4.

3.5 *Underwater Target Tracking*

Tracking of underwater targets is an important requirement in ocean surveillance systems. The purpose of target tracking is to accurately estimate the target states based on the observation data.

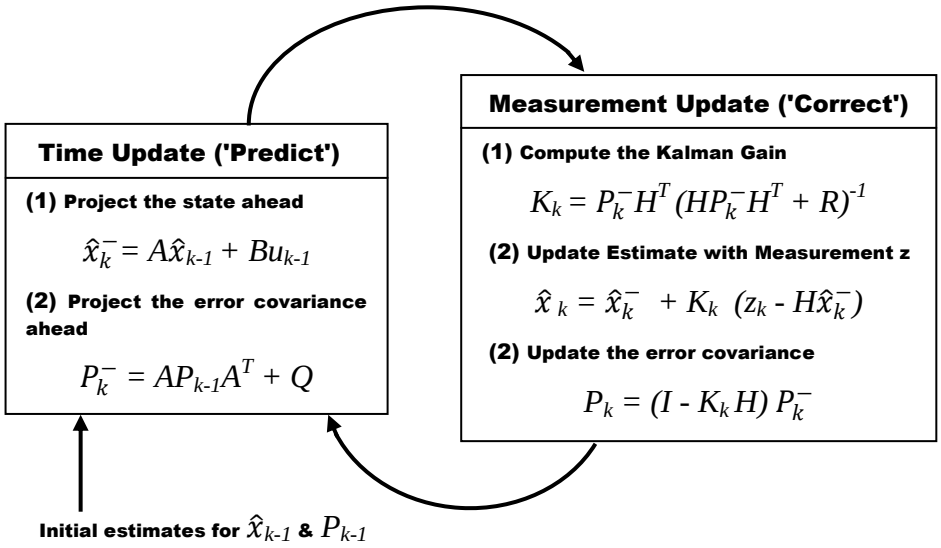

Fig. 3.4 The operation of the Kalman filter

The tracking performance depends on accurate description of the target state. Accurate tracking of the target is achieved when the target state model matches with the target practical state. Among various techniques, Kalman filter tracking devices are getting more attention because of their practicality as this method does not require all previous data to be stored and reprocessed every time a new measurement is taken.

A moving target, represented in Cartesian co-ordinate system is considered for the analysis. Suitable transformations can be used if the measurement data are in a format other than the Cartesian system. However, the tracking system and design challenges are relatively

insensitive to the choice of the co-ordinate system. Methods for tracking and improving the tracking estimates for a target moving in one dimension and two dimensions including the maneuvering situations have been simulated and studied.

When a target is maneuvering, the errors come across are more complex compared to the errors observed for a target moving in a straight line fashion. This imprecision need to be reduced by applying appropriate correction measures. While tracking a maneuvering target, the main issue is to detect the point at which the target is maneuvering. Here a chi-square based decision method using measurement residuals is used. Upon detection, appropriate corrections are made in the Kalman filter algorithm to adapt to the highly maneuvering situation.

3.6 *Target Classification*

The hydrophone array as well as the omni-directional hydrophone element of each of the buoys, is capable of receiving, storing and analyzing the noise emanated from the target of interest. These signals can be used for the classification of underwater targets by comparing their signature features with those available in the knowledge base.

The generalized structure of the target classifier is shown in Fig. 3.5. The noise emanations from the target are received, processed and the target specific features are extracted. These target specific features are compared with the earlier detection or estimation decisions, which are stored in the knowledge base and the target is identified. Over a time period, if a target feature is not updated, that feature will be removed from the target feature record. The most matching signature pattern is identified when the required classification clues are available in the target feature

record, from the known target signatures in the knowledge base, depending on the user defined tolerance.

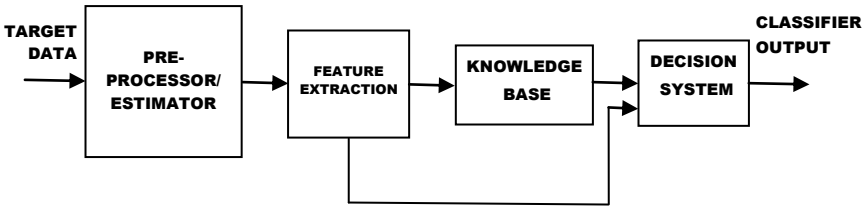

Fig. 3.5 Generalized structure of the target classifier

The methodology suggested to be adopted for realizing the target classifier involves the extraction of source features by analyzing the composite noise data waveforms and identifying the most matching feature vector using template matching technique leading to the identification of the target. For making the system fool proof and full-fledged one, the knowledge base has to be updated with the feature vectors and target dynamics for all the class and type of the targets.

The spectral and bi-spectral features get modified, when the acoustic signal traverses from the radiating source to the receiver through the bounded channel due to many underwater propagation effects in the sea such as multipath, spreading in time, Doppler shifts/spread, as well as disturbances from other sources like the sea state noise, sea micro-organisms and shipping activities in addition to thermal noise. Moreover the signal distortion and interference structure depend on the source and receiver locations as well. This being too complex a problem, the channel distortion effect has not been incorporated while extracting the features.

Moreover the classification function has been implemented as a part of underwater target localization and tracking system. The classifier

function in the proposed system has only limited capabilities and is mainly dedicated to identify and track the targets, making use of the operator provided/system generated target specific features and ignores the other objects in the vicinity of the system. This ensures the tracking of the target of interest by feature matching technique and hence a full-fledged classifier system is not implemented.

3.6.1 Target Specific Signatures

In passive sonar, targets are classified or identified based on the tonal components or signatures present in the frequency spectrum of the noise signals emanating from the targets using spectral estimation techniques.

3.6.1.1 **Spectral Features**

A totally random process with unknown features is normally modelled as a Gaussian random process for decision making purposes. Though the features are unknown, the receiver can have a rough knowledge of the spectral region that the signals may occupy, so that band limiting filters turn out to be a very powerful tool for regenerating the noise signal, devoid of noise power outside the predicted spectral region.

This section presents a summary of some of the features that can be computed from the spectrum of a signal [89].

Spectral Centroid

The spectral centroid, which may also be referred to as the spectral brightness, gives an indication of the spectral shape and is defined as the amplitude-weighted average or centroid of the spectrum. It is a simple, yet efficient parameter, estimated by summing together the product of each

frequency component of the spectrum and its magnitude, which is further normalized by dividing with the sum of all the magnitudes.

Spectral Range

The spectral range or bandwidth refers to the range of frequencies that are present in the signal. It is computed using the spectral magnitude weighted average of the difference between each frequency component and the centroid.

Spectral Roll off

Another spectral feature, which gives a measure of the spectral shape, is the spectral roll off and is defined as the frequency below which 85% of the magnitude distribution of the signal is concentrated.

Spectral Flux

This is a measure of the amount of local spectral change. This is defined as the squared difference between the normalized magnitude spectra of successive frames. Spectral flux is a measure of how quickly the power spectrum of the signal is changing and computed by comparing the power spectrum of one frame with that of the previous frame.

Spectral Slope

The spectral slope is also identified as one of the prominent signatures in the suggested algorithm and refers to the average slope of the power spectral density variation.

Number of Peaks and the Peaking frequencies

The total number of peaks in the power spectral density variation, which will help in identifying the tonal as well as continuous frequency components, is treated as one of the significant spectral features. For better

results, only the significant peaks above a certain preset threshold value are taken into account. The peaking frequencies, rising as well as falling slopes of the power spectral response of the target emanations are also considered for fine tuning the classification clues.

3.6.1.2 **Bispectral Features**

Conventionally, techniques like power spectral estimation is widely being used for the analysis of various acoustic sources in the ocean including that of marine origin. However, power spectral analysis is phase blind and cannot fully characterize the nonlinear signals as well as the noise generating mechanisms. Thus most of the signals are approximated as linear and analysis is carried out, which results in loss of many valuable information in the signal. As the demand for more detailed and accurate analysis as well as modelling has increased, researchers are now mainly focusing on techniques based on higher order spectra.

Analysis using Higher Order Spectra, in particular the third order spectra called bispectrum, is being evolved as a powerful technique in the field of digital signal processing and allied areas. Bispectrum is a third order frequency domain measure, capable of providing more information than the conventional tools like power spectrum. While power spectrum can efficiently estimate the power of different frequency components of a signal, it in general fails to quantify any non-linear interactions between the component frequencies. Such interactions induced by the second order nonlinearities give rise to certain phase relations called Quadratic Phase Coupling (QPC). Bispectral analysis can reveal the presence of phase couplings as well as can provide a measure to quantify such couplings.

Bispectrum is the two-dimensional Fourier Transform of the expected value of a signal at three time points. The use of bispectrum is

highly motivated by the fact that it can provide information regarding deviations from Gaussianity as well as presence of nonlinearities and phase information.. In situations where the stationary signals has non-Gaussian properties and the additive noise process is stationary Gaussian, the use of bispectral analysis become advantageous in estimating the signal features. Such an analysis is important, since all periodic, quasi-periodic as well as many of the signals emitted from various machineries and mechanical systems can be considered as non-Gaussian.

Bispectral analysis can play a key role in the analysis of acoustic noise sources. A normalized form of bispectrum, called the bicoherence is found to be more appealing since its variance is independent of the energy content of the signal. Analysis of noise data wave forms generated by the noise sources in the ocean using bicoherence can reveal the deviation of the signals from Gaussianity as well as linearity, which is usually hidden in the traditional spectral analysis. Such information may be effectively utilized for generating certain target specific features, which can aid in the identification and classification of underwater targets

3.6.2 Compilation of Knowledge Base

The performance of the classifier relies on the target features available in the knowledge base. To generate the features of a target, the long-term spectra of the specific target class are to be collected and averaged. The average spectrum so obtained is the characteristic spectrum for the specific target class or type under consideration.

The information bearing signals sensed by the hydrophone array, on an average, is white in nature, comprising of a wide range of frequencies. By computing the noise spectral level, over the available frequency range,

one can infer the nature of the noisy target and by correlating this information with the available classification clues, it is possible to effectively identify the targets, within the limits of the variances of the classification clues.

3.6.3 Decision making

3.6.3.1 **Feature Vector**

A feature vector is an *n*-dimensional vector of numerical features that represent an object and facilitates processing and statistical analysis. The vector space associated with these vectors is often called the feature space. In general, feature extraction involves simplifying the amount of resources required to describe a large set of data accurately. When performing analysis of complex data, one of the major problems stem from the number of variables involved. Analysis with a large number of variables generally requires a large amount of memory and computational power. In order to reduce the dimensionality of the feature space, a number of dimensionality reduction techniques can be employed. The feature extraction is a generic term for methods of constructing combinations of the variables to override these problems while describing the data with sufficient accuracy.

3.6.3.2 **Feature Selection**

Upon extracting a set of features, which forms the basis for classification, only those features are selected, that can indeed improve the performance of the classifier. This process, known as feature selection, may lead to loss of information and is in many cases based on singular transformations. The feature selection process is significant because of the following reasons.

More specific features are collected together in order to reduce noise generated by irrelevant features. Many classifiers are sensitive to irrelevant features, and will degrade their performance when such features are included. Distance based classifiers, such as the ones used in this work, are particularly sensitive to this. If a random feature is included, it will contribute to the distance measure just as much as any other feature. If the features were not scaled, they may contribute even more than a relevant feature. Thus, due to this distortion, a pattern may appear as similar to patterns of a different class.

By selecting the relevant features, the risk of over fitting the training data can be reduced. The larger the number of features used, the more detailed the classifier will be. But if a classifier has too many degrees of freedom, it may adjust itself perfectly to the training data, but perform poorly when used with other data. By reducing the number of features, and thus the degrees of freedom of the classifier, it is possible to improve generalization for a given scenario.

The classifier made computationally feasible by selecting appropriate features**.** The selection of too many features will demand substantial computing power for the purpose of feature extraction, training as well as classification process. Hence, the smaller the number of features the lesser will be the computational complexities of the classifier.

Thus, the classification function operates in a multidimensional space formed by the various components of the feature vector. For the purpose of classification, an efficient inference system, capable of performing template matching by correlating the generated target features with the feature components available in the knowledge base, has to be realized. The classification decision becomes too hard and inappropriate if

too many features are considered for the decision making. The practical methods for the classification always involve a heuristic approach intended to find a *good-enough* solution to the optimization problem.

3.6.3.3 **Euclidean Distance Model based Identifier**

A classifier system for identifying the noise sources in the ocean using the target specific features extracted from the noise emissions needs to be implemented for alleviating the inefficiencies in the operator assisted classification system. Though signal analysis can be carried out even in the time domain, most of the target specific signatures are extractable from the frequency domain representation and its variants. The process of feature extraction can be carried out through various signal processing techniques, so that the raw data is transformed into new data sets that can be used by the classifier for the purpose of target identification.

A simple and efficient classifier system could be implemented to find out the nearest match using Euclidean distance model, making use of the feature vector. The weights for the feature vector components have been selected based on heuristics, the knowledge gained from the training examples as well as trial and error procedures. The Euclidean distance between the feature vectors of the unknown target and that of the various targets in the knowledge base is computed for the purpose of feature vector based classification. Normalization of vector components is done by standard deviation or the range of the features, across the knowledge base. After normalization, each feature is weighted in proportion to its significance in the similarity estimation.

3.7 *Platforms Used:*

3.7.1 AutoLISP

AutoLISP is a dialect of Lisp programming language built specifically for use with the full version of AutoCAD, which is a software application for computer aided design (CAD) and drafting, developed by Autodesk. The software supports both 2D and 3D formats. AutoLISP is a dynamically scoped, dynamically typed list of programming dialect, records definition facilities, arrays, functions with variable number of arguments or let bindings. Aside from the core language, most of the primitive functions are for geometry, accessing AutoCAD's internal DWG database, or manipulation of graphical entities in AutoCAD. AutoCAD loads AutoLISP code from .LSP files. AutoLISP code can interact with the user through AutoCAD's graphical editor by use of primitive functions that allow user to pick points, choose objects on screen, input numbers and other data. AutoLISP also has a built-in GUI mini-language, the Dialog Control Language, for creating modal dialog boxes with automated layout, within AutoCAD. AutoLISP is one of a number of Application Programming Interfaces (APIs) built into AutoCAD but it is probably the easiest to use and therefore the most productive.

3.7.2 MATLAB

MATLAB, which is developed by MathWorks, is a numerical computing environment and fourth-generation programming language. MATLAB allows matrix manipulations, plotting of functions and data, implementation of algorithms, creation of user interfaces, and interfacing with programs written in other languages. Although MATLAB is intended primarily for numerical computing, an optional package, Simulink, adds graphical multi domain simulation and Model Based Design for dynamic

and embedded systems. MATLAB is widely used in academic and research institutions as well as industrial enterprises.

3.8 *Summary*

The methodology used for the development of underwater target localization, tracking and classification system, and the elaborate description of the three buoy system scenario including the approaches for the localization are detailed in this chapter. The Kalman filter theory, which is used for the refinement of the localization estimates and target tracking, is also looked into. The feature vector extraction methods as well as the classification algorithm used for the detection of unknown underwater targets are also discussed. The platforms used for the simulation purposes are also briefly touched upon.

CHAPTER 4

SIMULATION OF TARGET LOCALIZER

Model studies on the localization of underwater targets have been presented in this chapter. Simulation of a localizer system comprising of three buoy systems, each consisting of steerable hydrophone arrays and support electronics, positioned at the vertices of a triangle, is implemented to estimate the position of the target. The system picks up the noise emanations from the targets and the hydrophone arrays of each node gets aligned to the direction of maximum signal arrival. Using the Direction of arrivals for the three hydrophone arrays, the distances of the target from the three nodes are computed. Three different approaches for generating the localization estimates based on the mathematical formulae and software platforms have been implemented.

4.1 *Introduction*

Most of the underwater surveillance systems rely on the acoustic signals emanating directly from the targets of interest. The ultimate requirement of surveillance systems is the precise position fixing and ranging of targets, making use of the real time data captured by the hydrophone arrays, with the help of suitable algorithms. In underwater scenario, certain inherent errors due to the characteristics of the medium like reverberation, multipath effects, scattering and fading can affect the overall performance of the system. This is highly prominent in underwater scenario especially when the system is passive. These errors can be minimized to some extent by incorporating appropriate models of the

channel characteristics. An acoustic network of at least two nodes can be used for the localization of underwater targets. Additional nodes placed non-collinear with respect to the position of the target can significantly improve the accuracy of the measurement. This chapter discusses the simulation models for localization of underwater targets using different approaches for range estimation using Haversine and Vincenty formulae. The Haversine formula for great circle distance calculation assumes the earth's geometric plane to be spherical whereas Vincenty formula assumes the plane to be elliptical.

4.2 *Simulation of Target Localizer*

The minimally configurable system consists of three, mechanically steerable hydrophone arrays of high sensitivity and directivity as well as the required electronic modules for carrying out the surveillance operations using the hydrophone arrays, processing the received signals, managing the communication and power supply. The arrays gather the geographical positions with the help of the GPS receiver attached to them. Buoys comprising of the arrays are deployed at the vertices of a triangle. The buoys are deployed in the ocean with the help of appropriate mooring mechanisms. The hydrophone arrays can be steered in such a way that, they orient themselves to the direction of maximum signal energy, from the targets of interest.

For estimating the direction of arrivals to each array accurately, it is essential to have a reference orientation for the hydrophone array system. The geomagnetic meridian is considered as the reference axis and the angular position information of the hydrophone array is gathered with respect to the magnetic meridian using a magnetic compass. Initially, the hydrophone arrays are aligned along the reference axis. When target

emanations are received, the hydrophone arrays get steered to the direction of maximum signal energy as depicted in Fig. 4.1. The angular position information of the hydrophone arrays are used to estimate the position of the target using the triangulation technique. To gather the direction of maximum signal arrival from the target of interest, the array is mechanically steered through small steps and in each step the signals are captured and analyzed using signal processing techniques.

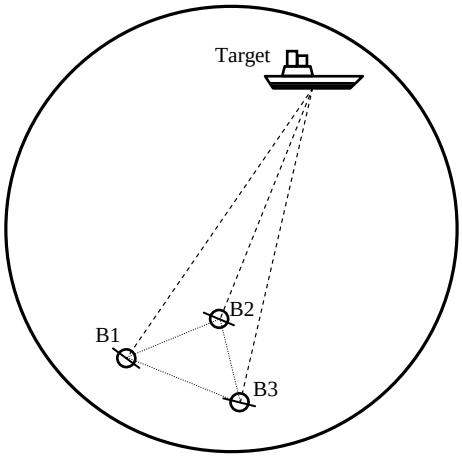

Fig. 4.1 Horizontally deployed sensor arrays get aligned to the DOAs when the target enters in the vicinity of the sensor network

4.3 *Target Localization Approaches*

Target localization refers to determining the position of the target near the deployed buoy system with reference to the earth's coordinate system. The GPS modules integrated in the buoy electronic system of the three buoys provide the location of the buoys with reference to the earth's magnetic meridian. Direction of Maximum Arrival of the noise data waveforms from the target can be computed by the buoy electronics. Applying geodetic latitude/longitude distance calculations, trigonometric and basic geometric laws, the position of the target with reference to

earth's coordinate system can be computed. Three different approaches based on the mathematical formulae and software platforms are used for the computation.

The approaches and mathematical formulae used are:

Approach 1. Using Haversine formula for great-circle distance on AutoLISP

(i) Haversine formula

(ii) Sine Law

(iii) Inverse Trigonometric Ratios

Approach 2. Using Haversine formula for great-circle distance on MATLAB

(i) Haversine formula

(ii) Sine Law

(iii) Cosine Law

(iv) Inverse Trigonometric Ratios

Approach 3. Using Vincenty formula for ellipsoids on MATLAB

(i) Vincenty Direct formula for Ellipsoids

(ii) Vincenty Inverse formula for Ellipsoids

(iii) Trigonometric Ratios

(iv) Inverse Trigonometric Ratios

(v) Sine Law

(vi) Cosine Law

4.3.1 Range Estimation using Approach 1

The GPS modules attached with the system give the latitude and longitude values of the locations of the hydrophone arrays [93-95]. If latitude and longitude values of two locations on the earth are known, the distance and bearing between the locations can be computed as detailed below. If La_1, La_2, Lo_1 and Lo_2 are the latitude and longitude values of the two locations, then,

$$\Delta La = La_2 - La_1 \text{ and } \Delta Lo = Lo_2 - Lo_1$$

If R is the radius of the Earth, then the distance, d between the two locations can be computed using the Haversine formula as

$$d = R.c \tag{4.1}$$

where $$c = 2\tan^{-1}\frac{\sqrt{a}}{\sqrt{(1-a)}}$$

and a is computed as

$$a = \sin^2(\Delta La/2) + \cos(La_1).\cos(La_2).\sin^2(\Delta Lo/2)$$

The bearing, θ between the two locations with respect to the true north of the Earth can be computed as

$$\theta = \tan^{-1}\frac{y}{x} \tag{4.2}$$

Where $y = \sin\Delta Lo.\cos La_2$ and

$$x = \cos La_1.\sin La_2 - \sin La_1.\cos La_2.\cos\Delta Lo$$

If La_n and Lo_n are the latitude and longitude values of one node, the latitude of the target, La_t is given by

$$La_t = \sin^{-1}(\sin La_n.\cos\frac{d}{R} + \cos La_n.\sin\frac{d}{R}.\cos\theta) \tag{4.3}$$

and the longitude of the target, Lo_t is given by,

$$Lo_t = Lo_n + \tan^{-1}\left[\frac{\sin\theta.\sin\frac{d}{R}.\cos La_n}{\cos\frac{d}{R} - \sin La_n.\sin La_t}\right] \tag{4.4}$$

The longitude and latitude values of the target position can be computed, if the distance to the target is known, using the equations (4.3) and (4.4).

The procedures involved in the estimation of the range of the target from each of the nodes are described below.

4.3.1.1 **Computation of DOA**

The Direction of Maximum Arrival of the signal, with respect to the geomagnetic meridian can be estimated by comparing the power levels at different orientations of the hydrophone array. As the array is linear and broad side in nature and is mechanically steered, it will receive maximum signal energy when the acoustic axis of the array is along the line joining the target and the centre of the array. The direction of maximum signal arrival can be obtained by computing the received power levels at various orientations of the array. Knowing the DOAs and the angles and distance between the nodes, the position of the Target can be computed using triangulation techniques. The flowchart for estimating the position of the target is depicted in Fig. 4.2.

4.3.1.2 **Triangulation Technique**

Triangulation technique can be adopted for estimating the range of the target from the distance between the two buoys furnished by the GPS and the angle between the line joining the nodes and the direction of arrivals.

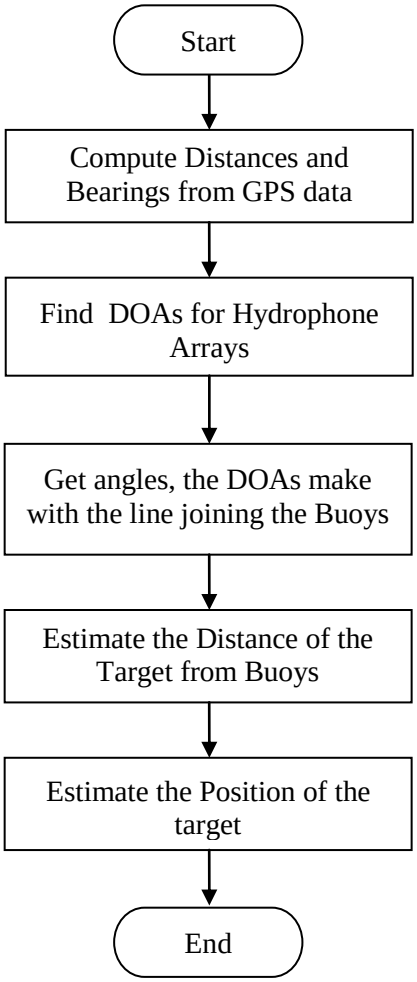

Fig. 4.2 Flowchart for localization of the Target

Consider a section of the buoy system, comprising of two buoys and the target as shown in Fig. 4.3, that perfectly position the target according to the maximum signal arrival criterion or the direction of arrival of noise waveforms that contain the desired band of frequencies as specified by the shore station system. The angles corresponding to this position be represented as Φ_1 and Φ_2, which refers to the angular positions of the hydrophone arrays in Nodes B_1 and B_2 respectively, when the

maximum signal arrival condition is satisfied. The known distance D between B_1 and B_2 could be corrected with the help of GPS receivers, whenever required.

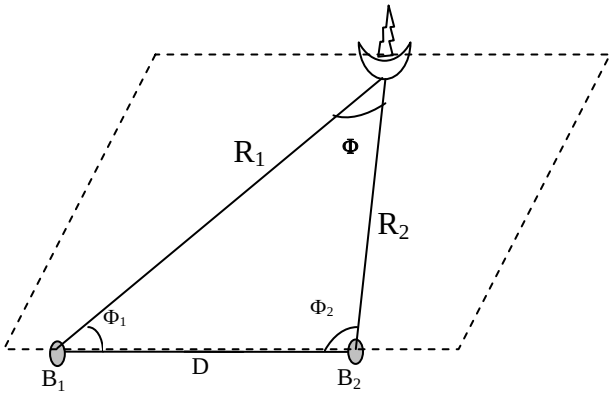

Fig. 4.3 The proposed scenario for computing the ranges using two nodes

Knowing the values of Φ_1, Φ_2 and Φ, the distance R_1 and R_2 of the target from the Buoys B_1 and B_2 can be computed. Similarly, using the other sections of the sensor system, R_1 and R_3 as well as R_2 and R_3 can also be computed. From these, the distance of the target from B_1, B_2 and B_3 are obtained, using which the position of the target can be estimated.

4.3.1.3 **Simulation**

Simulation of this model is carried out using AutoLISP programming. The buoys are positioned by calculating the distances and bearings between them by using Haversine formula. All the bearings between the buoys are with respect to the true north. Then, for the simulation of the source, Inverse beamforming is used to generate the appropriately delayed signals. The directions of maximum signal arrivals towards each buoy are estimated by taking the power spectrum of the signals and hydrophone arrays are oriented to that direction. After getting

the three DOAs from the three arrays, distances from the buoys to the target are calculated using triangulation techniques.

The simulation starts at an assumption that the GPS readings of the three Buoys are available and calculates the distances and bearings between the three Buoys from the corresponding GPS values and places the Buoys along with the hydrophone arrays in position. The hydrophone arrays (HA) are aligned to the magnetic axes, here x- axis of the graphical plane. Now a noise source is introduced as target, and the hydrophone arrays automatically rotate and aligned along the acoustic axes. The angular movements of the hydrophone arrays are noted and these angular measurements are used to estimate and display the absolute positions and the distances to the target from the buoys. The simulation is done using AutoLISP programming which is a supplement to AutoCAD. The buoy distances are verified with Google Earth and distances to the target from the buoys are verified with scaled drawing.

Algorithm for Simulation of Localizer in AutoLISP

```
        START
        Create Diagrams for Buoys, HAs and Target
LABEL1 : Read GPS values for the Buoys
        Compute the Buoy Positions
        Place Buoys and HAs in the Computed Positions
        Align HAs to Magnetic Meridian
LABEL2 : Insert Target in the vicinity of the Buoys
        Align Hydrophone Arrays towards Target
        Find the DOAs
        Estimate the Position of the Target
```

To change Target Position, goto LABEL2

To repeat Simulation, goto LABEL1

STOP

4.3.1.4 **Results and Discussions**

The proposed model for the localization of targets using the 3-node buoy system has been simulated in AutoLISP environment. The GPS data for the three hydrophone arrays are furnished as the input of the program, which computes the node to node distances and using the directions of arrivals, depending on the position of the target, the range of the target from the nodes are computed. Fig. 4.4 depicts the GUI for setting the position data of the nodes and the estimated distances are generated as shown in the screen shot furnished in Fig. 4.5.

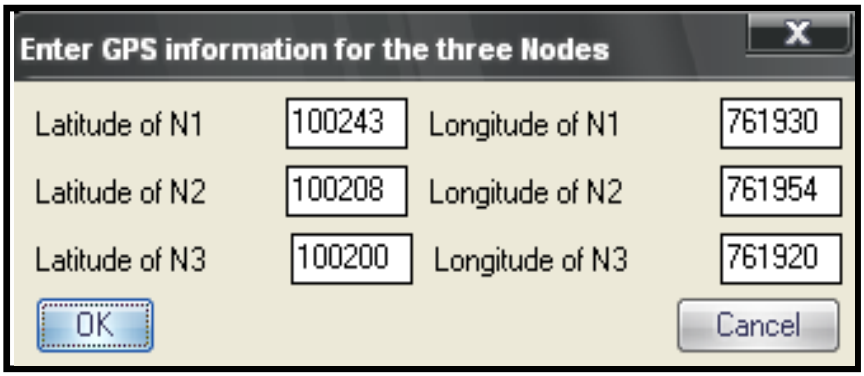

Fig. 4.4 GUI for furnishing the latitude and longitude values of the three Nodes

Fig. 4.6 depicts the scenario in which the hydrophone arrays of all the nodes are aligned to the direction of the geomagnetic meridian, just before commencing the surveillance operation, while Fig. 4.7 depicts the case in which the hydrophone arrays have got aligned to the direction of maximum signal arrival, from the target of interest.

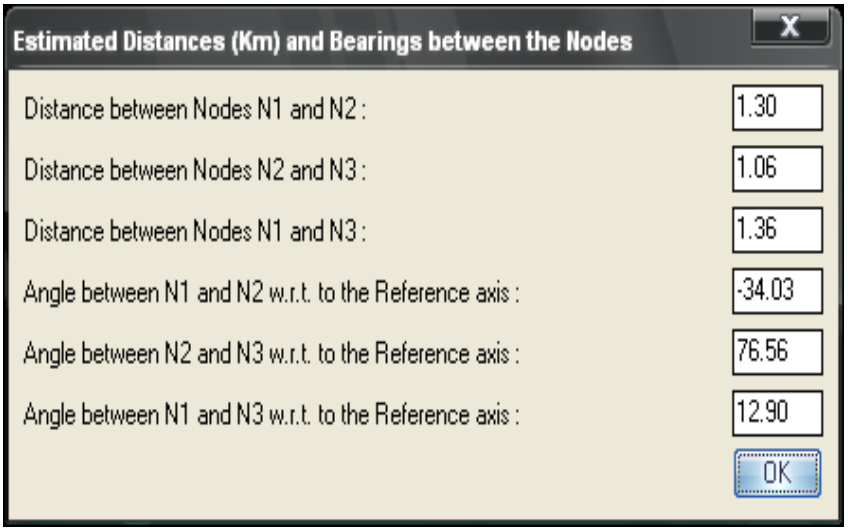

Fig. 4.5 Screen shot of the estimated distances and bearings from the GPS data

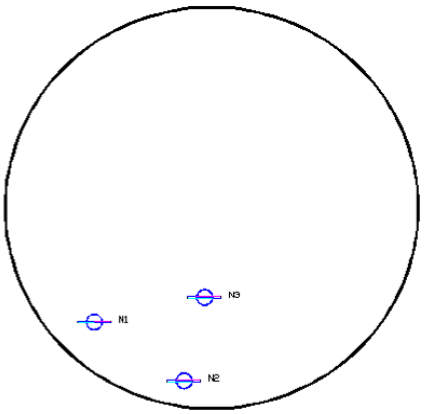

Fig. 4.6 Initial alignment of the arrays

The estimated directions of the maximum signal arrival are furnished in the screen shot shown in Fig. 4.8 while Fig. 4.9 depicts the screen shot of the position estimates of the target from the three nodes.

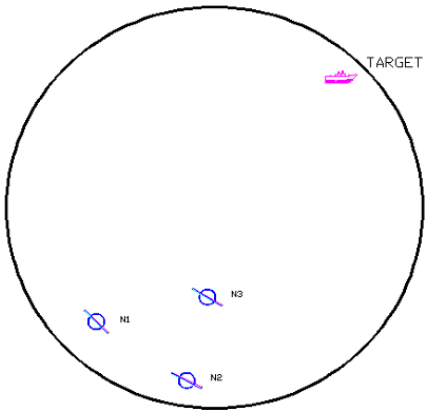

Fig. 4.7 Arrays aligned to the DOA

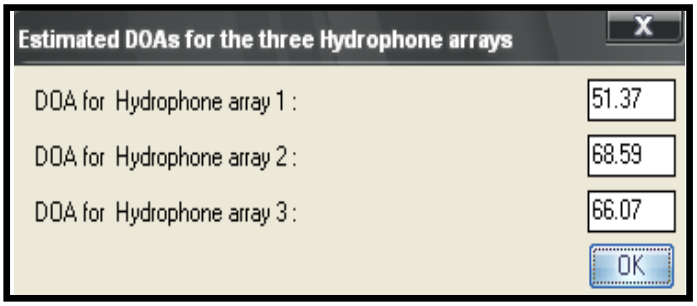

Fig. 4.8 Estimated DOAs for the three hydrophones

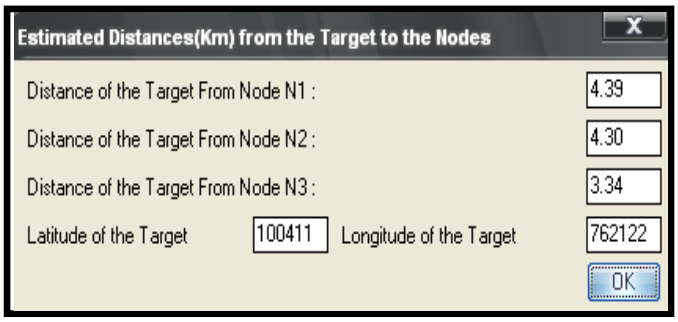

Fig. 4.9 Estimated Position of the Target

4.3.2 Range Estimation using Approach 2

Approach 2 uses the Haversine formula for great circle distance and different triangulation techniques. Fig. 4.10 shows the scenario of the three buoys and the target across the earth's geomagnetic plane.

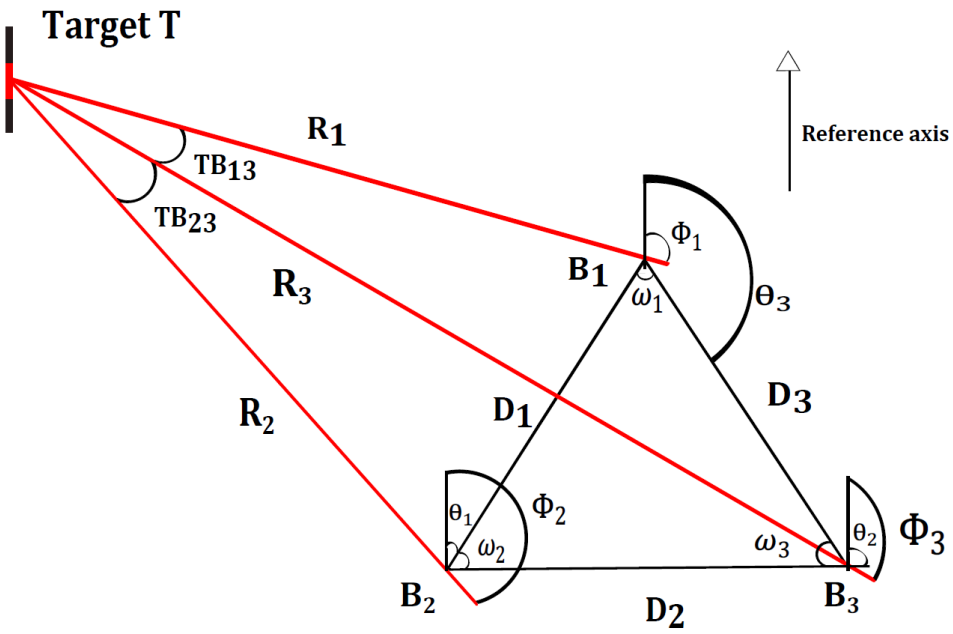

Fig. 4.10 Scenario depicting the buoys and the target

As depicted, B_1, B_2 and B_3 are the three buoys with the GPS coordinates as (La_1, Lo_1), (La_2, Lo_2) and (La_3, Lo_3) respectively. The known parameters are La_1, La_2, La_3, Lo_1, Lo_2, Lo_3 and the direction of arrival angles, Φ_1, Φ_2 and Φ_3 respectively. The radius of Earth, R is assumed as *6371 km* approximately.

4.3.2.1 **Computation**

Let, $\Delta La = La_2 - La_1$ and $\Delta Lo = Lo_2 - Lo_1$

$$a = sin^2(\Delta La/2) + cos(La_1)\, cos(La_2)\, sin^2(\Delta Lo/2) \quad (4.5)$$

$$c = 2\, tan^{-1}[\sqrt{a}/\sqrt{(1-a)}] \quad (4.6)$$

$$d = R*c \ \textbf{\{Haversine Formula\}} \quad (4.7)$$

where R is the radius of Earth

d_1, d_2 and d_3 are the distances between the buoys which can be computed using (4.7)

$$y = \sin(\Delta Lo)\cos(La_2)$$

$$x = \cos(La_1)\sin(La_2) - \sin(La_1)\cos(La_2)\cos(\Delta Lo)$$

$$\theta = \tan^{-1}(y / x) \quad \textbf{\{Haversine Formula\}} \qquad (4.8)$$

θ_1, θ_2, and θ_3 are the bearings of the buoys with respect to the reference which can be computed using (4.8)

$$\omega_1 = \cos^{-1}[(d_1^2 + d_3^2 - d_2^2) / (2d_1d_3)] \quad \textbf{\{Cosine Law\}} \qquad (4.9)$$

ω_2 and ω_3 are calculated using (4.9)

$$TB_{12} = \omega_1 - \Phi_1 + \Phi_2 - \theta_1 + \theta_3 - 180 \qquad (4.10)$$

[Angle B_1TB_2 in diagram]

$$TB_{23} = -\omega_2 + \Phi_2 - \Phi_3 - \theta_1 + \theta_2$$

[Angle B_2TB_3 in diagram]

$$TB_{13} = -\omega_3 - \Phi_1 + \Phi_3 - \theta_2 + \theta_3$$

[Angle B_1TB_3 in diagram]

Distance towards the target from B_1 computed using triangle B_1TB_2 is r_{11} and distance towards the target from B_1 computed using triangle B_1TB_3 is r_{12}

$$r_{11} = d_1 \sin(\Phi_2 - \theta_1) / \sin(TB_{12}) \quad \textbf{\{Sine Law\}} \qquad (4.8)$$

$$r_{12} = d_3 \sin(\omega_3 - \Phi_3 + \theta_2) / \sin(TB_{13})$$

$$r_{21} = d_1 \sin(\omega_1 + \theta_3 - \Phi_1) / \sin(TB_{12})$$

$$r_{22} = d_2 \sin(\Phi_3 - \theta_2) / \sin(TB_{23})$$

$$r_{31} = d_2 \sin(\Phi_2 - \theta_1 - \omega_2) / \sin(TB_{23})$$

$r_{32} = d_3 \sin(\theta_3 - \Phi_1) / \sin(TB_{13})$

Distance of the target from the three buoys are computed as:

$R_1 = (r_{11} + r_{12}) / 2$

$R_2 = (r_{21} + r_{22}) / 2$

$R_3 = (r_{31} + r_{32}) / 2$

The target coordinates are computed using,

$$La_t = \sin^{-1}(\sin La_1 . \cos\frac{R_1}{R} + \cos La_1 . \sin\frac{R_1}{R} . \cos\Phi_1)$$

$$Lo_t = Lo_1 + \tan^{-1}\left[\frac{\sin\Phi_1 . \sin\frac{R_1}{R} . \cos La_1}{\cos\frac{R_1}{R} - \sin La_1 . \sin La_t}\right]$$

4.3.2.2 **Algorithm for Target Localization using Approach 2**

START

Read the GPS coordinates of the buoys and DOAs of the target

Do necessary conversions on the inputs for computation

Find the distances between the buoys using Haversine formula

Find the angles between each of the buoys using the Cosine law

Apply geometric rules and trigonometric laws

Find the various angles of the triangle

Compute the distances to the target by applying Sin law

Take the mean of two sets of distances

Compute the target coordinates

END

4.3.3 Range Estimation using Approach 3

The digital signal processing unit of the buoy electronics estimates the direction of maximum arrival of the signals captured by the hydrophone array associated with each of the buoys. The DOA furnished by the buoy system gives the orientation of hydrophone array with respect to the geomagnetic meridian. The GPS system integrated with the buoy electronics provide the information about the location of the buoys. The distances between the buoys are computed from the GPS data using the Vincenty formula for ellipsoids [95-98].

4.3.3.1 **Vincenty formulae for Ellipsoids**

In 1975, Thaddeus Vincenty published a geodesic computation technique called the Vincenty distance formulae for ellipsoids. It is an efficient technique used for GPS based computations involving parameters relating to the earth's latitude, longitude and bearing angles with reference to the earth's magnetic poles.

The following two Vincenty distance formulae are in widespread use.

- Vincenty Direct formula
- Vincenty Inverse formula

Notations

a, *b*, Semi major axis and semi minor axis of ellipsoid

f, flattening = *(a-b)/a*

φ, geodesic latitude, positive north of the equator

L, difference in longitude, positive east

s, length of the geodesic

$\alpha_1, \alpha_2,$ azimuths of the geodesic, clockwise from north α_2 in the direction P_1 P_2 produced

α, azimuth of the geodesic at the equator

$u^2 = cos^2\ \alpha\ (a^2\ - b^2\ )/b^2$

U, reduced latitude, defined by tan $U\ =\ (1-f)\ tan\ \varphi$

λ, difference in longitude on an auxiliary sphere

σ , angular distance $P_1\ P_2$ on the sphere.

σ_1 , angular distance on the sphere from the equator to P_1

σ_m , angular distance on the sphere from the equator to the midpoint of the line.

Direct formula

$$tan\ \sigma_1 = tan\ U_1\ /\ cos\ \propto_1 \quad (4.14)$$

$$sin \propto = cos\ U_1\ sin \propto_1 \quad (4.15)$$

$$A = 1 + \frac{u^2}{16384}\{4096 +\ u^2\ [-768 + u^2\ (320 - 175u^2\ )]\} \quad (4.16)$$

$$B = \frac{u^2}{1024}\{256 +\ u^2\ [-128 + u^2\ (74 - 47u^2\ )]\} \quad (4.17)$$

$$2\sigma_m\ =\ 2\sigma_{1\ +}\ \sigma \quad (4.18)$$

$$\Delta\sigma\ = B\ sin\ \sigma\ \ \{cos\ 2\sigma_m + \frac{1}{4}B[cos\sigma$$

$$(-1 + 2\ cos^{\ 2}\ 2\sigma_m) - \frac{1}{6}\ B\ cos\ 2\sigma_m\ \ (-3 + 4\ sin^2\ \sigma)(-3 +$$

$$4\ cos^2\ 2\sigma_m\ )]\} \quad (4.19)$$

$$\sigma = \frac{s}{bA} + \Delta\sigma \quad (4.20)$$

Equations (4.18), (4.19) and (4.20) are iterated until there is a negligible change in σ. The first approximation of σ is the first term of (4.20).

$$tan\ \varphi_2 = \frac{sin\ U_1\ \cos\sigma\ + \cos U_1 \sin\sigma\ \cos \propto_1}{(1-f)[sin^{\,2}\ \propto\ +(sin\, U_1 \sin\ \sigma -\ cos\ U_1\ \cos\ \sigma\ \cos \propto_1)^{\,2}]^{\frac{1}{2}}} \tag{4.21}$$

$$\tan\ \lambda = \frac{\sin\ \sigma\ \sin\ \propto_1}{\cos\ U_1\ \cos\ \sigma - sin\ U_1 \sin\ \sigma\ \cos \propto_1} \tag{4.22}$$

$$C = \frac{f}{16}\ cos^{\,2} \propto [4 + \mathrm{f}\,(4 - 3\cos^2 \propto)] \tag{4.23}$$

$$L = \lambda - (1-C) f \sin \propto \{\sigma + C \sin\sigma[\cos\ 2\sigma_m + C \cos\sigma\ (-1 + 2\cos 2\, 2\sigma m)]\} \tag{4.24}$$

$$\tan \propto_2 = \frac{\sin \propto}{-sin\ U_1 \sin\ \sigma + cos\ U_1\ \cos\ \sigma\ \cos \propto_1} \tag{4.25}$$

Inverse Formula

$\lambda = L\ (first\ approximation)$

$$sin^{\,2}\ \sigma\ = (cos\ U_2\ sin\ \lambda)^2 + (cos\ U_1\ sin\ U_2 - sin\ U_1\ cos\ U_2\ cos\ \lambda)^2 \tag{4.26}$$

$$cos\ \sigma = sin\ U_1\ sin\ U_2 + cos\ U_1\ cos\ U_2\ cos\ \lambda \tag{4.27}$$

$$tan\ \sigma = \sin\sigma\ /\ cos\ \sigma \tag{4.28}$$

$$sin \propto = cos\ U_1\ cos U_2\ \sin\lambda / \sin\sigma \tag{4.29}$$

$$\cos\ 2\sigma_m = cos\ \sigma\ - 2\ \sin U_1\ sin U_2\ / cos^2 \propto \tag{4.30}$$

λ is obtained by equations (4.23) and (4.24). This procedure is iterated starting with equation (4.26) until the change in λ is negligible.

$$s = bA(\sigma - \Delta\sigma\ ), \tag{4.27}$$

where $\Delta\sigma$ comes from equations (4.16), (4.17) and (4.19)

$$\tan \propto_1 = \frac{\cos U_2 \sin \lambda}{\cos U_1 \sin U_2 - \sin U_1 \cos U_2 \cos\lambda} \tag{4.28}$$

4.3.3.2 **Vincenty Direct Formula**

Given a geodesic point (φ_1, λ_1) on the surface of the ellipsoid along with the starting azimuth α_1 and geodesic distance *'s'*, Vincenty direct formula can be used to find the destination point (φ_2, λ_2) and reverse azimuth α_2 of the geodesic at (φ_2, λ_2). For example, given the starting coordinate X(10°02'43"E, 76°19'30"N), distance to reach destination Y, XY = 4277.5m and bearing angle from starting point to destination, θ = 94.25°. On applying Vincenty direct formula, the destination coordinate Y is computed as (10°02'32.67", 76°21'50"), as shown in Fig. 4.11.

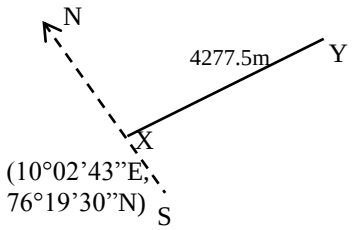

Fig. 4.11 Vincenty Direct Formula

4.3.3.3 **Vincenty Inverse Formula**

Given two geodesic points *(φ_1, λ_1)* and *(φ_2, λ_2)* on the surface of the ellipsoid where φ refers to the latitude and λ refers to the longitude, Vincenty inverse formula can be used to find the geodesic distance 's' between them and the forward azimuth *$\alpha 1$* and reverse azimuth *$\alpha 2$* of the geodesic at *(φ_1, λ_1)* and *(φ_2, λ_2)* respectively. For example, given two GPS coordinates, A(10°02'43", 76°19'30") and B(10°02'08", 76°19'54"). Vincenty inverse formula calculates distance AB and finds the angle 'θ'

which is the deviation of line AB from magnetic North in the North – South plane through East of the earth's magnetic field. On applying Vincenty inverse formula, the distance AB is computed as 1300.198 m as illustrated in Fig. 4.12.

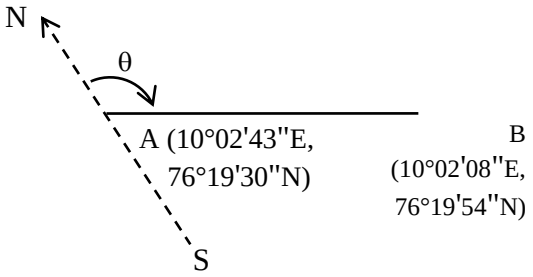

Fig. 4.12 Vincenty Inverse Formula

The sine law can be used to determine the angles of the triangle formed by the three buoys and knowing the distances between the buoys computed from the GPS values, the cosine law can be used to compute the distances between the target and the buoys.

4.3.3.4 **Algorithm for Target Localization using Approach 3**

START

Read the GPS coordinates of the buoys and DOAs of the target

Do necessary conversions for the inputs

Find the distances between the buoys using Vincenty Inverse formula

Find the angles between each of the buoys using the Cosine law

Apply geometric rules and trigonometric laws

Find the various angles of the triangle

Compute the sides of the triangles using Sin law

Take the mean of two sets of distances

Compute the target coordinates using the Vincenty Direct formula

END

4.3.3.5 **Simulation**

For the simulation, the known data are GPS location of each buoys and the DOAs and the parameters to be computed are distances between the three buoys, angles between the lines joining the buoys, distance of the target from each of the buoys and the target coordinates. The GUI for the simulation of the localizer is given in Fig. 4.13.

Input to the Localizer

GPS coordinate of buoy B_1 = (10°02'43",76°19'30")

GPS coordinate of buoy B_2 = (10°02'08",76°19'54")

GPS coordinate of buoy B_3 = (10°02'00",76°19'20")

DOA of buoy B_1 = 51.37°

DOA of buoy B_2 = 68.59°

DOA of buoy B_3 = 66.07°

Output of the Localizer

Distance between Target and Buoy B_1, = 4277.5m

Distance between Target and Buoy B_2, = 4410.3m

Distance between Target and Buoy B_3, = 3354.7m

Coordinates of Target = (10°04'10"N, 76°21'20"E)

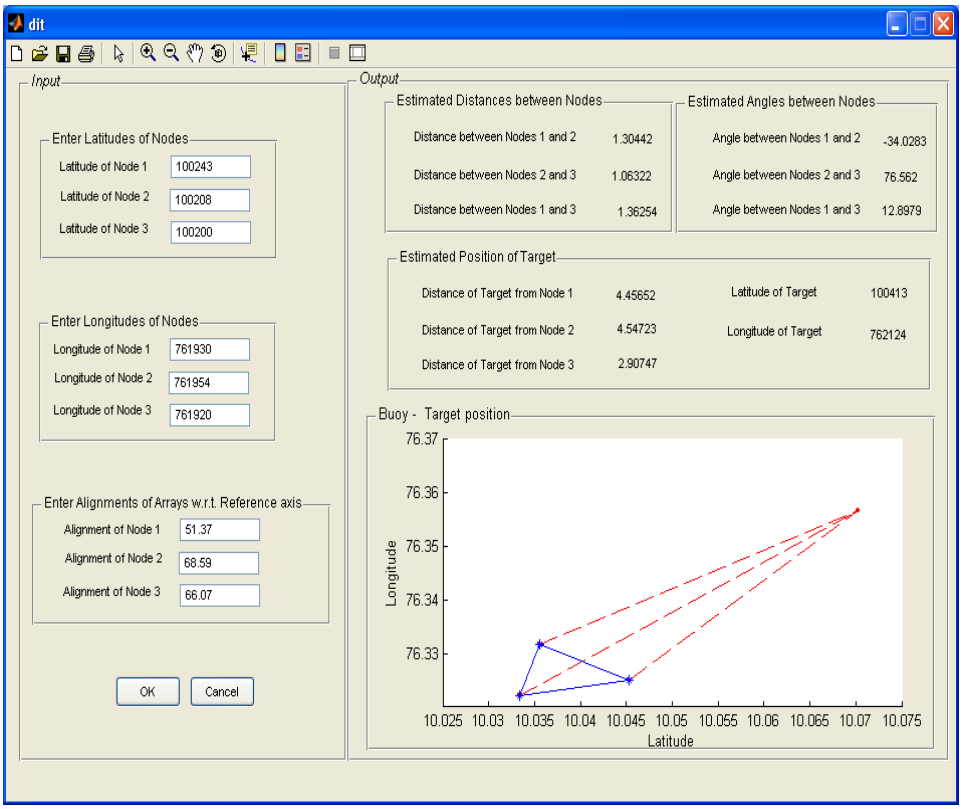

Fig. 4.13 GUI for the Simulation of localizer

4.4 *Results and Discussions*

The results of simulation studies carried out for localizing underwater targets using the Vincenty, Haversine and triangulation techniques have been consolidated and tabulated in Table 4.1. Angular position values for all the computations are considered with reference to the earth's magnetic meridian. The Haversine formula for great circle distance computation assumes that the earth's geometric plane is spherical, whereas the Vincenty formula assumes that the plane is elliptical. As an attempt to minimise the error variances, it is proposed to make use of Kalman filter approach for generating a fairly acceptable localization estimate.

Table 4.1 Consolidated Simulation Results using the Three different Approaches

Parameters	Haversine Approach (AutoLISP)	Approach using Haversine and triangulation techniques	Vincenty Approach
Distance between Target and Buoy B_1	4.39 km	4.46 km	4.28 km
Distance between Target and Buoy B_2	4.30 km	4.55 km	4.41 km
Distance between Target and Buoy B_3	3.34 km	2.91 km	3.35 km
Latitude of Target	10°04'11"N	10°04'13"N	10°04'10"N
Longitude of Target	76°21'22"E	76°21'24"E	76°21'20"E

(The GPS coordinates of B_1, B_2 and B_C are (10°02'43"N, 76°19'30"E), (10°02'08"N, 76°19'54"E) and (10°02'00"N, 76°19'20"E) respectively)

4.5 *Summary*

A model for localization of underwater target has been simulated using MATLAB and AutoLISP environments. The results have been verified using GOOGLE EARTH and scaled drawings. All the approaches for range estimation have been implemented and the results are consolidated. The methodology adopted in this chapter has been used to localize the target within the field of view of hydrophone arrays, which capture the signals emanating from the target.

CHAPTER 5

PROTOTYPE LOCALIZER

A prototype system for the localization of unknown underwater targets using three moored surface buoy systems is presented in this chapter. Each buoy consists of steerable hydrophone array and support electronics for control and processing. The hydrophone arrays of the localizer system pick up the noise emanations from the targets and the arrays of each node gets aligned to the direction of maximum signal arrival. Using the direction of arrivals at the three hydrophone arrays, the distances of the target from the three nodes are computed. The prototype localizer model has been field tested and the validation tests yielded encouraging results within the limits of theoretical approximations and measurement errors, which necessitated the need for refining the estimates using Kalman filter.

5.1 *Introduction*

An approach for the localization of underwater targets using a minimally configurable three buoy system has been prototyped and presented together with performance validation results from the field trials. This prototype three buoy automated system aids in localization, tracking and classification of underwater targets using passive listening concepts and target identification techniques. The acoustic signals sampled by the sensors at three spatially and non-collinearly distributed locations in the ocean are analyzed for the decision making. The system comprises of three fixed surface buoy systems, each consisting of steerable hydrophone arrays and support electronics, positioned at the vertices of a triangle. The sensor

system picks up the noise emanations from the targets of interest and the hydrophone arrays of each node gets aligned to the direction of maximum signal arrival (DOA). Using the DOAs measured at each buoy system, the distances of the target from the three nodes are computed using the triangulation technique. The unpredictable errors in the estimates of direction of arrivals due to the recoiling effect of the rotating hydrophone arrays and the instabilities of the buoy systems caused by surface wave etc. will affect the accuracy of the localization estimates. These inaccuracies are resolved to a certain extent by smoothing the estimates using the concepts of Kalman filters.

5.2 *Methodology*

An acoustic network of at least two nodes can be used for the localization of underwater targets. Additional nodes placed non-collinear with respect to the position of the target can significantly improve the accuracy of the measurement. A three node network deployed as minimally configurable autonomous buoy systems, each consisting of a mechanically steerable hydrophone array of high sensitivity and directivity along with necessary support electronics, moored in such a way as to form a triangle, has been implemented for carrying out the ocean surveillance operations. The buoy systems are capable of initiating the surveillance operations when the ambient acoustic activity crosses a threshold limit. Since the buoys are meant to operate in remote areas of the ocean, it has been powered using solar panels, with adequate backup and suitable charging circuits.

The buoy systems remain in dormant mode to conserve the limited power available onboard. An Omni directional hydrophone element of very high sensitivity, which forms a part of the submerged hydrophone

system, constantly listens to the ambient noise. Any approaching target adds up to this ambient noise level, which alerts the buoy systems and triggers the surveillance operations, once these levels cross a set threshold limit. An alert warning will also be sent to the shore station, indicating the activity through an RF link.

Initially, all the hydrophone arrays are aligned along a reference axis which is the geomagnetic meridian of the Earth. The hydrophone arrays are then mechanically steered through finite steps over the horizontal plane and the spectral power of the ambient acoustic noise captured by the hydrophone array at each step is computed to obtain a pattern of the noise power variation. The power spectra over the horizontal plane are then analyzed to find the direction of maximum signal arrival using signal processing techniques. The information gathered by the onboard GPS of the buoy systems together with the direction of maximum signal arrival is passed on to the shore station, where the localization of the target is computed using triangulation techniques. The localization estimates furnished by the system vary in accordance with the variations in the medium and environmental conditions and hence it is appropriate to make use of adaptive filters like Kalman filter to generate an efficient and effective means to mitigate the errors of random nature.

The buoy system was field tested in a reservoir. The main objective of the field trial was to verify the direction of arrival of each of the buoys and hence the localization of the target using the three buoys setup. The trial was conducted using various noise sources including the pre-recorded acoustic signals and engine noises.

5.2.1 Estimation of Direction of Arrival

Estimation of direction of arrival of the noise waveform at two or more distinct positions using the buoy system is used to evolve the techniques for the localization and tracking of noise sources in the ocean using passive listening concepts. The signal processing hardware for obtaining the direction of arrival of noise waveforms emanating from the target under consideration, making use of the 20-element hydrophone array, which is mechanically steered by a hydrophone array controller, computes the signal power of a source, within a user selectable band of frequencies. The hardware can be set for various gains, bandwidths and integration cycles. The flowchart for extracting the direction of arrival is depicted in Fig. 5.1. The direction of maximum arrival of the signal with respect to the geomagnetic meridian can be estimated by comparing the power levels at different orientations of the hydrophone array. As this linear array is broad side in nature and is mechanically steered, it will receive maximum signal energy when the acoustic axis of the array is along the line joining the target and the center of the array. The direction of maximum signal arrival can be obtained by computing the received power levels at various orientations of the array.

5.2.2 Estimation of Range of the Target

The GPS modules attached to the buoy electronics give the latitudes and longitudes of the locations of the buoy systems. If latitudes and longitudes of two locations on the earth are known, the distance and bearing between the locations can be computed and if the direction of maximum signal arrival of two or more nodes is known, the distance to the target can be computed using triangulation techniques.

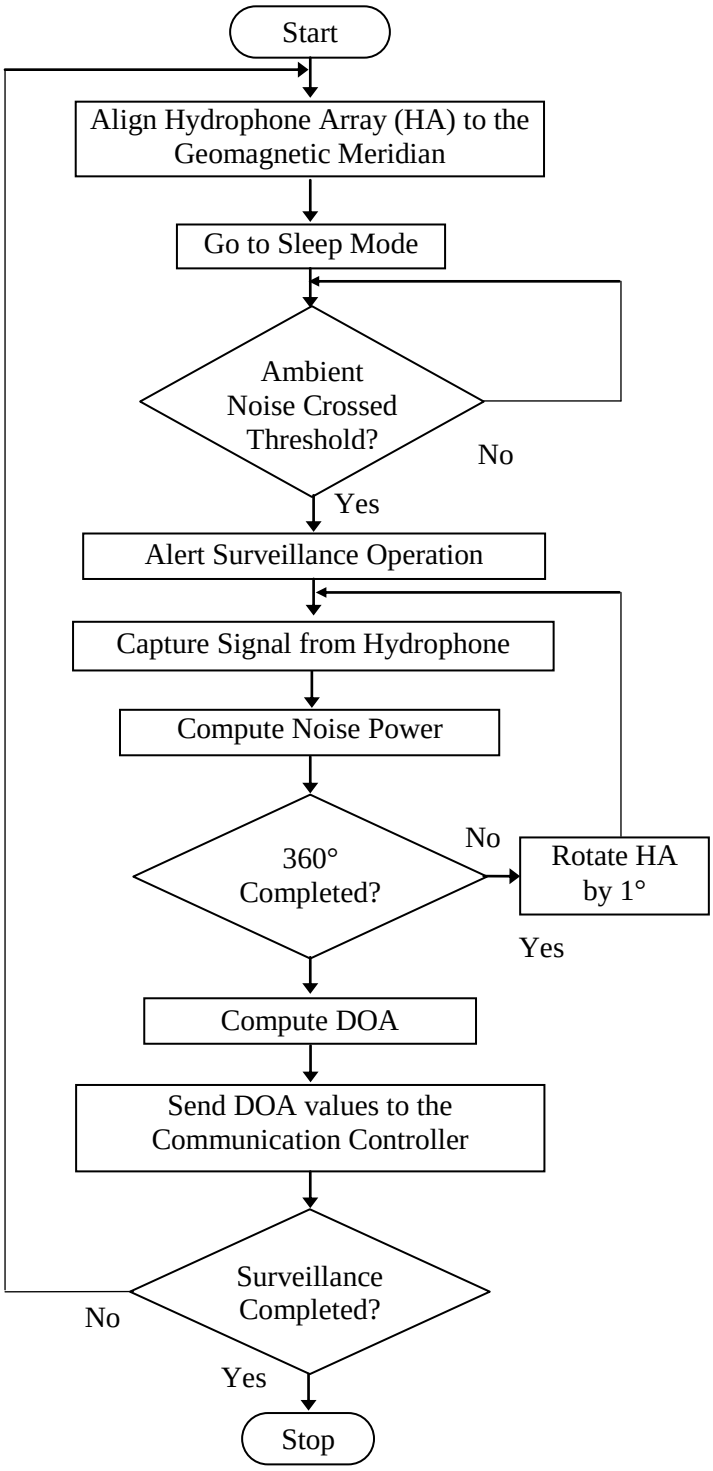

Fig. 5.1 Estimation of Direction of Arrival

5.3 *Specifications of the Buoy System*

To facilitate the localization, tracking and classification of underwater targets, submerged hydrophone arrays should be deployed with suitable buoy systems. As the buoy needs specialized requirements for this application involving the steering of the submerged hydrophones mounted to the gear assembly, a specialized structural buoy design SWAB (Small Water plane Area Buoy) has been formulated, conforming to the concept of minimizing the water plane area, so that the disturbances that the buoy experiences, is brought to the minimum.

5.3.1 Design Considerations

The buoy is intended to be a floating platform to house the electronic equipments, battery, solar panels, DC motor with shaft and the submerged rotating hydrophone array. The basic design requirements are listed below.

- The motions of the buoy due to wave, wind and current action should be minimized, especially yaw, roll, heave and pitch in order to achieve accurate target tracking
- The size and structure of the buoy should be optimized such that the submerged structural components of the buoy do not cause any significant interference to the receiving of acoustic signals.
- The buoy should have adequate stability in free floating and moored conditions.
- A minimum of 3 buoys are required for accurate target positioning and tracking.
- The cost of the buoy should be minimized.

5.3.2 Selection of Buoy Type

Conical or cylindrical buoys are the easiest to design and fabricate. However, such buoys suffer from high motions in waves, especially heave, due to the large water plane area. It was therefore decided to adopt a semi-submersible type buoy, which is relatively transparent to waves and current and with a small water plane area. The basic buoy configuration will consist of four completely submerged cylindrical floats joined to form a square and four partially submerged cylindrical vertical struts and the struts provide the required buoyancy. They also act as the support for the framework on which the payload and the electronics chamber is mounted.

5.3.3 Design of the Electronic Chamber

The payload and the electronics chamber was designed with a view to minimizing its size, weight and surface area leading to minimization of wind loads, lowering of the overall centre of gravity of the buoy and a consequent improvement in stability. The floor area of the cabin should be sufficient to accommodate the electronic equipment, motor and battery. The height of the cabin should be sufficient to accommodate the solar panels mounted on its sidewalls. Adequate access to install and maintain the Buoy Electronics in the chamber has been provided at the top.

5.3.4 Sizing of the Floats and Struts

The diameters of the floats and struts are initially estimated so as to provide the required buoyancy, which should be equal the total weight of the buoy for equilibrium. The diameters and thicknesses of floats and struts are optimized to achieve the design objectives, subject to the constraints of buoyancy and stability. The design details, stability considerations as well as the mooring details are given in Appendix I.

5.4 *Buoy Electronics*

The buoy electronics perform the vital task of mechanically steering the hydrophone arrays in the submerged buoys for the purpose of estimating the direction of arrival of captured signals with the help of the hydrophone array controller. The block diagram of buoy electronics is depicted in Fig. 5.2.

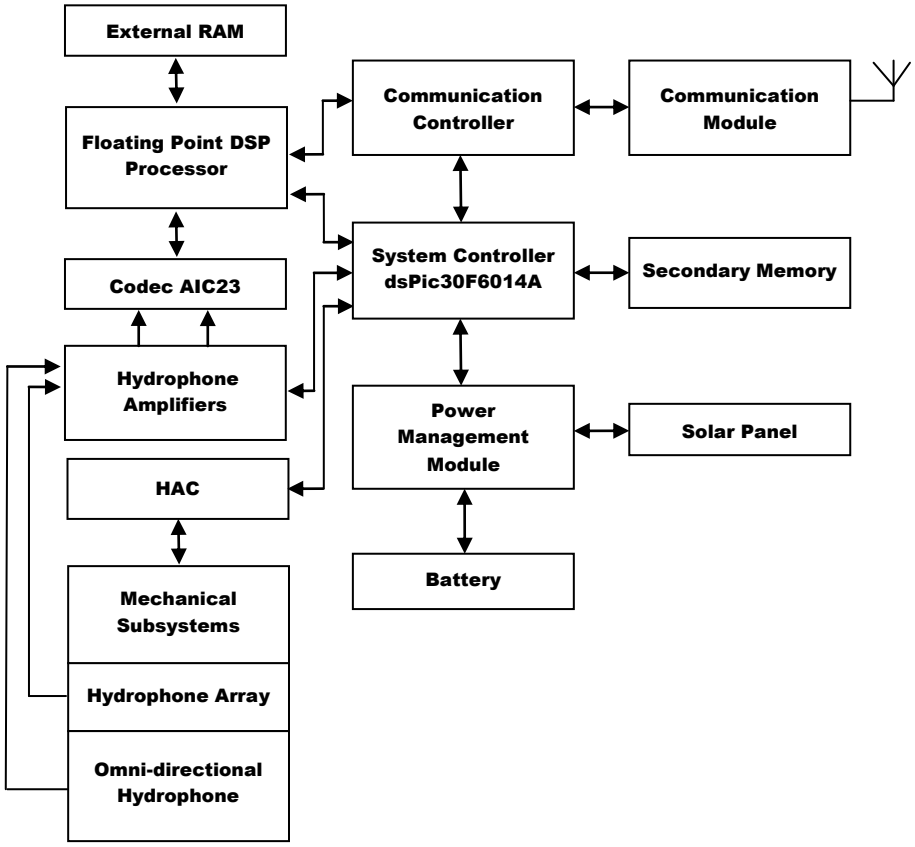

Fig. 5.2 Block diagram of Buoy Electronics

5.4.1 Hydrophone Array

The hydrophone array system used in this model comprises of 20 element linear array [1, 5] and the elements are spaced 15 cm apart, so that the total length of the array is approximately 3 meters. The

arrangement of elements in the array is depicted in Fig. 5.3. A hydrophone pre-amplifier has been provided at the centre of the array. When 20 elements are separated with a distance of 15cms and operating at 2500 Hz (n = 20, d=15 cm and f=2500 Hz), the generated beam pattern of the array is shown in Fig. 5.4, which is more narrower than the beam pattern of the 10 element linear hydrophone array.

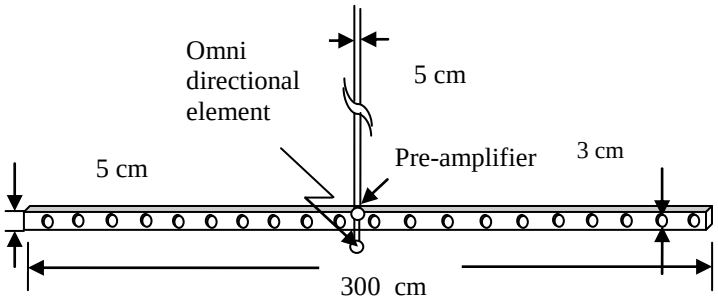

Fig. 5.3 The arrangement of elements in the 20-element hydrophone array

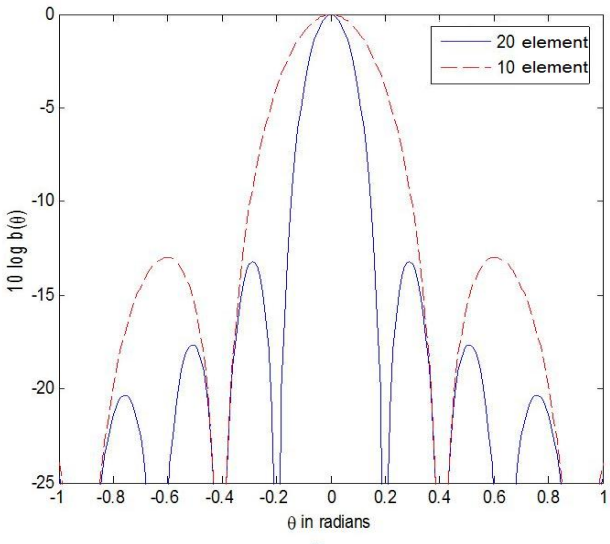

Fig. 5.4 The beam pattern of the 20-element and the 10-element hydrophone arrays at 2500 Hz

5.4.1.1 **Specifications of the hydrophone array**

Number of Elements : *20*

Element Dimensions	: Cylindrical with *30mm* diameter & *26mm* height
Receiving Sensitivity	: *-200dB re 1 V/µPa*
Frequency Response	: *5Hz to 10 kHz*
Preamplifier Response	: *5Hz to 12 kHz*

5.4.2 Hydrophone Array Controller

The hydrophone array controller (HAC) controls the angular position of the hydrophone array, which is horizontally suspended with help of a Brushless DC Motor and a Gearbox. The hydrophone array can be mechanically steered through 0˚ to 360˚ in steps of 1˚ with reference to the direction of the geomagnetic meridian using the hydrophone array controller. In each position, the noise emissions are captured and processed by a processing module so as to gather the direction of maximum signal arrival. The block diagram of the hydrophone array controller and noise acquisition system is shown in Fig. 5.5. The pictorial representation as well as the photograph of the gearbox assembly are given in Fig. 5.6 and Fig. 5.7. The DSP enabled microcontroller manages and controls the hydrophone array controller function.

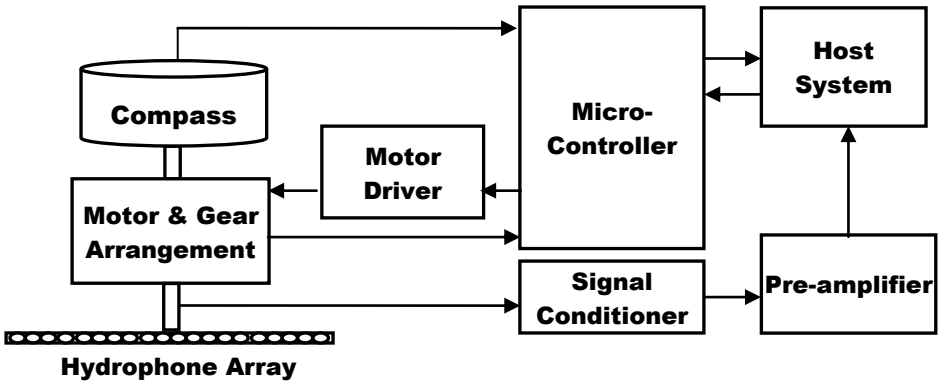

Fig. 5.5 Block diagram of the HAC and noise acquisition system

The hydrophone array subsystem also houses an omni-directional hydrophone, making use of which the system can perform effective surveillance of the region surrounding the buoy system. Whenever any of these Omni-directional hydrophones capture noise waveforms, above certain threshold level, the buoy systems as well as the shore station system will be alerted and the shore station initiates commands for performing the surveillance operation.

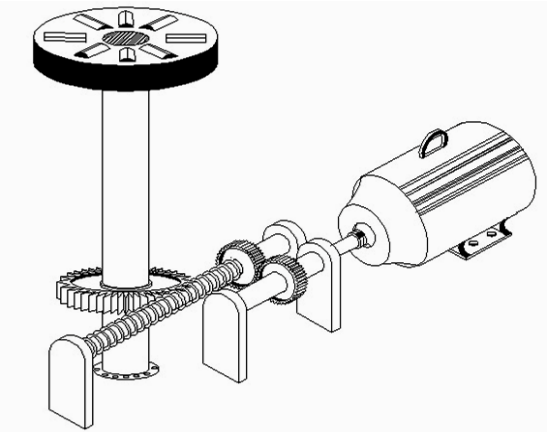

Fig. 5.6 Pictorial representation of the gear arrangement

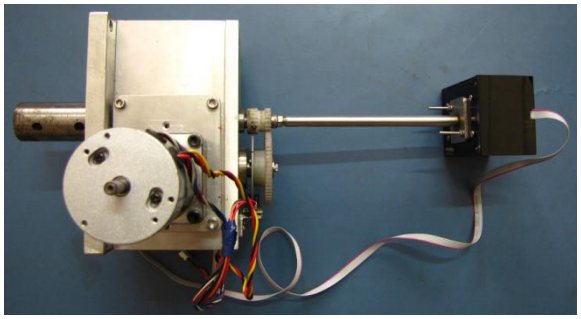

Fig. 5.7 Photograph of the Gearbox assembly

A Digital Magnetic Compass placed on the shaft senses the angular position of the hydrophone array with reference to earth's magnetic meridian. The relative displacement of the array from its initial position is

read back from shaft encoder. Optical proximity limit switches are attached to the anticlockwise and clockwise limits of the setup, which are 720° apart, so that the encoder can make absolute references of the angles and prevent the hydrophone array cable from entangling on the shaft setup.

The hydrophone array controller is interfaced with the GPS module, thus making available the position of the buoys. The RS-232 communication port of the hydrophone array controller receives and transmits data to the RF Link controller, which is one of the integral parts of the buoy electronics. The hydrophone array controller makes use of the communication controller and communication unit of the buoy electronics to pass the data and commands between the hydrophone array controller and the remote station.

5.4.2.1 **Working of the Array Controller**

On power up, the microcontroller initializes the array towards the anticlockwise limit. This is fed back by the optical limit sensor provided in the gearbox. Upon reaching this limit, the array is rotated clockwise 360 degrees to attain the centre position of the allowable rotational limit of 720 degrees.

All the operations commence from this point. The angle that the array makes with reference to the magnetic meridian at this position is read back from the digital magnetic compass attached to the array shaft, which is vital for DOA of any target by the buoy electronics. The array controller works with the DOA estimator by issuing commands and processes the results to create a complete 360° track for the purpose of estimating the direction of maximum signal arrival.

5.4.2.2 **Mechanical Steering System**

Beam steering is achieved by mechanically rotating the hydrophone array by the hydrophone array controller. Communication and control of the HAC by a remote shore station is carried out through an RF link. The three meter long linear hydrophone array is immersed underwater using a 40 mm stainless steel shaft, 6 meters long, connected to a gearbox with worm-gear arrangement driven by a brushless DC motor. The whole setup is kept afloat on the platform of a buoy. The motor is controlled by a driving circuitry built with the hydrophone array signal controller using its built-in motor control PWM (Pulse Width Modulation) module [99, 100].

Angular position of the array is fed back from a shaft encoder which makes use of the integrated Hall Effect switches of the BLDC (brushless DC) motor, reducing the complexity and cost. The mechanical steering system of the buoy consists of a gearbox with a suitable reduction ratio (750:1 or 540:1) and a Brush Less DC motor of 4000 rpm.

The gearbox is specially constructed with a worm gear arrangement limiting the maximum speed of the end shaft to 5.3 rpm, which can further be reduced with the help of the PWM driving circuitry, making slow and precise movements. Angular movements to the extent of 1°, even less are possible. PWM signals are generated by the digital signal controller of the HAC in synchronization with the position feedback from the integrated Hall Effect sensors of the Brushless DC Motor. The mechanical steering system takes about 11.2 seconds for a complete 360 degrees of rotation of the end shaft together with the hydrophone array, which apparently is limited to avoid stress on the shaft and hence to the buoy platform.

5.4.2.3 **Pre-processing Module**

This module is a set of hardware and software filters implemented in the system to avoid unwanted spectral noises from the signals received by the hydrophone array. The module consists of an analog hardware signal conditioner and filter, an analog to digital conversion stage and a high order software filter, designed to work with the other subsystems of signal processing module within the buoy electronics.

5.4.2.4 **Communications Controller**

The communication controller of the buoy system, which is vital for establishing the communication between the shore station and the buoys as well as between each of the buoys transfers data using data packets in a predefined format under the control of the main system. As the whole system is powered by solar energy, power consumption of the communications controller should be minimal and power management is critical.

The formatted data are furnished to the communication module through its RS232 port. The HAC and the power management controller are connected to the Xbee-Pro communication module. When the controller specific commands from the shore station are received, the corresponding controller responds.

5.4.3 Signal Power Computing Hardware

The analog output of the 20-element hydrophone array is directly coupled to the power computing hardware. The array carries within itself an internal amplifier, powered through external circuits, so that the amplified signals can be transmitted from the array to the receiving side, which helps in reducing the noise effects. The array is designed to work on

$6.8V_{DC}$, with a simple driving circuit. The signals from this driving circuit are directly fed to the preamplifier and signal conditioner of the power computing hardware. The block diagram of the analog section of the power computing hardware is shown in Fig. 5.8.

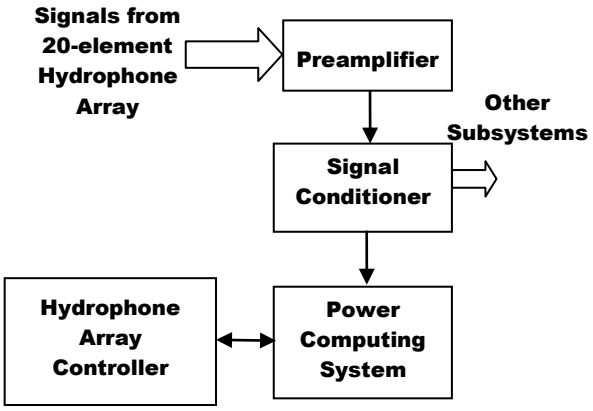

Fig. 5.8 Block Diagram of the Power Computing Hardware

Signals from the hydrophone array need to be amplified to the dynamic range of the built in ADC of the microcontroller. The output from the hydrophone preamplifier is an inverted signal varying from a few micro volts to milli volts, depending on the source level of the noisy target. A level shifting, amplification and filtering must be performed on this signal to generate a compatible signal for the ADC. Since the signal processing module has a bandwidth of 0~5 kHz, higher frequencies can cause problems like aliasing in DSP operations. Hence, a fifth order Butterworth filter has been implemented in hardware. The filter has been built in 3 stages, two of which are second order Butterworth filters in Sallen-Key topology, while the third stage is an inverting active low pass filter of first order.

The analog section of the power computing hardware is built around a low power, matched quad op amp IC. The input and output parameters

for all the four stages are matched. The Unity Gain Bandwidth product of each amplifier is 3 MHz, with a slew rate of 13V/µs. The CMRR and PSRR values are above 70dB. The op amp also features high impedance JFET inputs and short circuit protection at the output, rendering it fit for the proposed application.

5.4.3.1 **Direction of Maximum Arrival Estimator**

The direction of maximum arrival estimator is used to compute the power received through the hydrophone array at every rotation step of the hydrophone array. The DOA estimator constitutes both hardware and software, the heart of the system being Microchip dsPIC30F6014A, a DSP enabled 16 bit microcontroller with a dedicated DSP Engine [101-103].

The input of the analog section of the microcontroller can accept signals with $5V_{PP}$ and needs to be filtered in hardware to around 5 kHz to avoid problems like aliasing in the digital domain. A signal conditioner is designed and incorporated with the DOA Estimator to condition the signals received from the hydrophone array for the input of the microcontroller by applying necessary level shifting and amplification. A fifth order Butterworth filter hardware is also used to set a cutoff at 5 kHz before feeding the signal to the microcontroller, which is then fed to the analog input of the microcontroller, where the signals are sampled at a rate of 10.24 kHz and encoded digitally.

The computation of power within the selected band of frequencies is performed using the microcontroller. The microcontroller has a maximum throughput of 30 MIPS and has many integrated peripherals, including a 12 bit ADC with a maximum conversion rate of 100 kbps and two UART modules. The processor is configured to run on an internal RC oscillator at 14.74 MHz. The ADC module is configured to operate at a

sampling rate of 10.24 ksps, giving a bandwidth of 5.12 kHz. The UART module in the DSP controller is configured to operate at 9600 baud, making it compatible for communicating with the hydrophone array controller.

Normally, the DSP hardware is in power down mode, until data capture or surveillance operations are initiated through the command interface. Upon reception of a valid command, the ADC begins sampling the output of the signal conditioner, and records samples of 100 ms duration in a buffer. When this buffer is full, the 12-bit integer data is converted to double precision values and transferred to a separate buffer for further processing. An FFT is performed on this data, and the results are used to compute the power in the desired band of the signal.

5.4.3.2 **DOA Estimator Software**

The microcontroller based power computing software performs various procedures, based on user selectable parameters. The hydrophone array controller issues the commands to the power computing hardware through the communication module of the microcontroller. The software recognizes six commands, for the spectral power estimation and averaging count, selecting the gain, selecting the upper and lower cutoff frequency of the desired spectrum, for extracting the previous direction of maximum signal arrival and step angle. Each command results in responses, which specify the actions already initiated.

The microcontroller program is divided into the Communication Service and the Data Sampling service. In line with the power management considerations, the power estimator hardware is required to consume least power possible. Hence, the hardware is kept in power down mode unless any surveillance operation is being undertaken. Powering down the hardware during data sampling enhances the performance of the data

sampler by minimizing clock switching that can cause high frequency noises. The communication module receives and transmits predefined commands and responses respectively. On receiving a valid command block, this service identifies and verifies the validity of the command, and extracts the parameters from the block, while initiating necessary actions.

Powering up the DOA estimator system and all other operations can be handled remotely. The system initially aligns the array to a position which is 360° away from both clockwise and anticlockwise rotational limits when the power is up. The system is now ready to begin the surveillance operations. The remote station can request for a spectral power computation, which is carried out in the power computing controller. The spectral power is then transferred to the remote station along with the GPS reading and the alignment angle of the array with reference to the magnetic axis of the Earth.

5.4.4 Power Management System

The buoy electronics works solely on the solar power tapped using the solar panels installed on the dome of the buoy. Solar power can be optimally utilized only with sophisticated drivers for managing the charging and discharging of the batteries. A dedicated microcontroller, PIC16F88, power efficient with Nano-Watt technology, is used to manage the charging cutoff and the power supplies in the buoy [104-106]. Solar power is tapped using 8 solar panels, connected in parallel as series pairs, providing a 24V source for charging the batteries. The charging process is fully controlled by the power management system, and the charging voltage is cut off when the batteries are fully charged. The power stored in the batteries is discharged through four different SMPS voltage levels of 12V,

5V, -5V and 3.3V generated by SMPS1 and SMPS2, for usage of the buoy electronics.

The power management controller maintains the battery voltage at levels greater than 22V while discharging and less than 30V while charging. If the battery voltage goes below a low battery early warning level of 23V, the situation is monitored and the matter will be indicated to the shore station. If the battery again discharges to a low battery cut off level (22.5V) it switches off the SMPS2, which powers the HAC and hence suspends any further array steering. The communication link is kept operating even at this situation, as it is powered from SMPS1 and will shut down only at low battery critical shutdown level of 22V, when all communication with the shore station is suspended.

5.5 *Deployment of the Three Buoy system*

The test was conducted in a reservoir at Kulamavu, Idukki, at a depth of around 30-40 meters. The test facility houses the necessary systems such as a barge and a floating platform facility with crane, power supply connections and generators. The buoys brought to the test site were unloaded from the trucks using the crane of the floating platform facility, and the floating platform can be moved anywhere in the reservoir with the help of a barge. The platform can also be linked to power supplies from the shore. The photograph of the buoys boarded on the floating platform prior to deployment is shown in Fig. 5.9.

The three buoys were loaded on to the floating platform using the crane of the platform. The buoy electronics, the motor assembly and the first shaft section of the hydrophone array were mounted on the buoys while the platform was near the shore. The platform was then tugged to a

viable point at around the centre of the reservoir for conducting the experiment. The preliminary installation of parts were completed, and the buoys were tugged one by one to the designated locations of deployment in the reservoir using the barge.

Fig. 5.9 The three buoys are being taken for deployment

The hydrophone array was fixed to the motor shaft using the connecting shaft after the buoy was firmly tied to the barge at the point of deployment. The connection of the hydrophone arrays were confirmed to avoid any damage to the hydrophone array setup, while tugging the buoy through water. Each buoy was tested for communication and basic functionality at the point of deployments.

The buoys were deployed approximately 400 meters apart and the signals captured by the hydrophone arrays were pre-processed using the signal conditioning module. The digitized noise data waveforms were fed to the digital signal processor for extracting the target specific features.

The buoys B_1 and B_2 deployed at locations (9°48'41"N, 76°53'10"E) and (9°48'10"N, 76°53'19"E) are shown in Fig. 5.10 and Fig. 5.11 while Fig. 5.12 shows the coordinator buoy B_C deployed at location (9°47'56"N, 76°53'19"E).

Fig. 5.10 Buoy B_1 deployed at the location (9°48'41"N, 76°53'10"E)

Fig. 5.11 Buoy B_2 deployed at the location (9°48'10"N, 76°53'19"E)

Fig. 5.12 Buoy B_C deployed at the location (9°47'56"N, 76°53'19"E)

5.6 *Field Testing of The Buoy System*

A shore station, which identifies the buoys and continuously gathers the status of each buoy, by sending appropriate commands with the buoy address in a time slotted manner, was emulated within the fair reach of the RF link. One of the Buoys B_C acts as a Coordinator Buoy, which is responsible for relaying the information from the other two buoys to the shore station as well as coordinating all the surveillance operations autonomously. A communication controller is used to establish such a communication link between the shore station and the buoys. This subsystem which is based on the RF link is also capable of transferring the target feature records and status data from the buoys to the shore station.

The three-meter long linear hydrophone array of each buoy was immersed underwater using a 40 mm stainless steel shaft which measured 6 meters long and connected to a gearbox with worm-gear arrangement driven by a brushless DC motor. The buoy platform keep the whole setup afloat. The buoys were moored at positions to form a triangle and the noise

generated by the barge, high speed boat and other engines were used for localizing the target during the localization trials.

The hydrophone array was rotated in steps for capturing and preprocessing the noise signals. In each step the target features were extracted. The process is continued till it covers the entire 360°. The angular position at which the power in the characteristic band peaks up is taken as the direction of arrival of the noise signal. Fig. 5.13 depicts the graphical user interface (GUI) used to estimate the direction of arrivals.

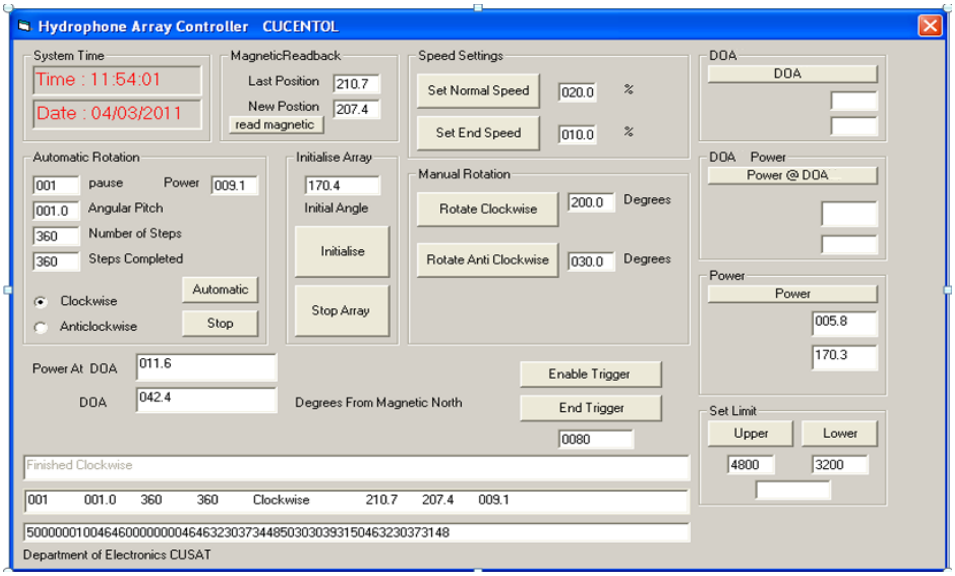

Fig. 5.13 GUI for DOA Estimation Field Trials

The shore station identifies the buoys by unique addresses 0x31, 0x32 and 0x33 respectively for the buoys, B_1, B_2, and B_c. The necessary commands were issued using the frame format shown in Fig. 5.14. The shore station always gathers the status of each buoy by sending appropriate commands with the buoy address in a time slotted manner. The buoys cannot initiate any transaction by itself. It responds in accordance with the command received from the shore station. During idle conditions, the shore

station frequently collects the status of the buoys. Whenever the status data indicates that the buoy has encountered with a trigger event, then the shore station issues commands to the buoys to initiate necessary actions.

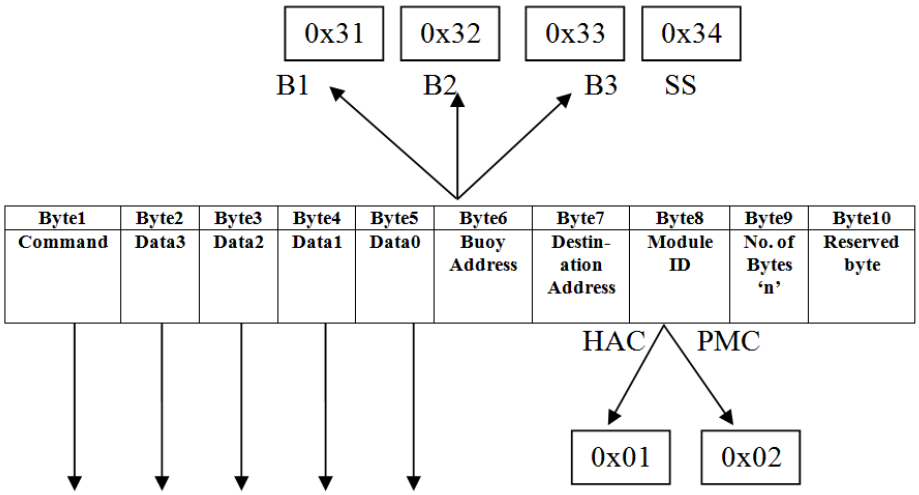

Command	Data3	Data2	Data1	Data0	Description
F	1	1	0	5	Forward array 110.5
R	1	1	0	5	Reverse array 110.5
I	x	x	x	x	Initialize array to anti-clockwise limit
F	x	x	x	x	Stop array
K	0	0	1	0	Start DOA with step size of 1.0
E	x	x	x	x	Stop DOA

Fig. 5.14 Frame format used for Gathering the DOAs during the Field Trials.

All the operations including powering up the HAC can be handled remotely. When the power is up, the HAC initially aligns the array to a position, which is 360° away from both clockwise and anticlockwise rotational limits. The system is now ready to begin the surveillance operations. The remote station can now request the HAC for a spectral power computation, which is carried out in the power computing controller. The spectral power is then transferred to the remote station along with the GPS reading of the HAC and the alignment angle of the array with reference to the magnetic axis of the Earth. Since the HAC is responsible for all remote communications, it remains active even if the battery power

level is critically low. Under critically low battery conditions, the HAC shuts down itself, and all communications with the remote station are relinquished till power is replenished. The GUI for the HAC and Buoys are shown in Fig. 5.15 and Fig. 5.16.

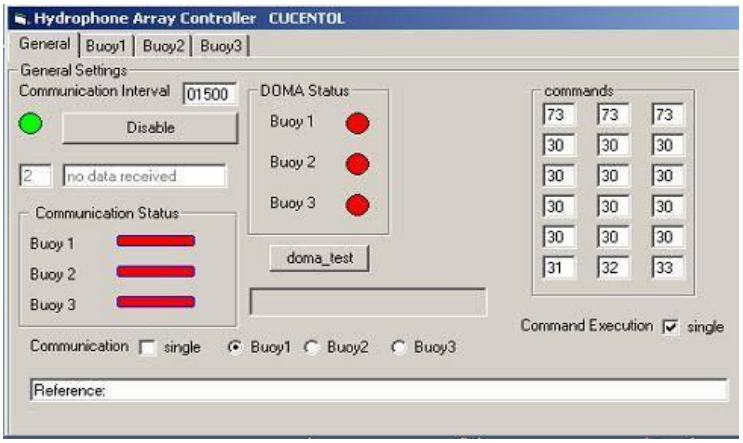

Fig. 5.15 Hydrophone array controller

Noise generated from the barge, the high speed boat and ITC 1007 projector were used as targets. The barge was moved to a distance of about 250m away from the platform. The noise signals were generated from the ITC 1007 projector, using the recorded wave file after due amplification using the B&K 2713 power amplifier. The engine of the barge was turned off to minimise the ambient noises. The pre-processor hardware at the platform was tuned to the characteristic band of the target and the hydrophone array was rotated in steps for capturing and pre-processing the noise signals. In each step, the target features are extracted and frequencies were computed for estimating the direction of arrival. When the DSP hardware for feature extraction is interfaced to the Buoy Electronics, the frame format of the specified type has to be used. The process is continued till it covers the entire 360°. The angular position at which the power in the characteristic band peaks up is taken as the direction of arrival of the noise

signal. Similarly, the directions of arrival of engine noises of barge and high speed boat were also estimated.

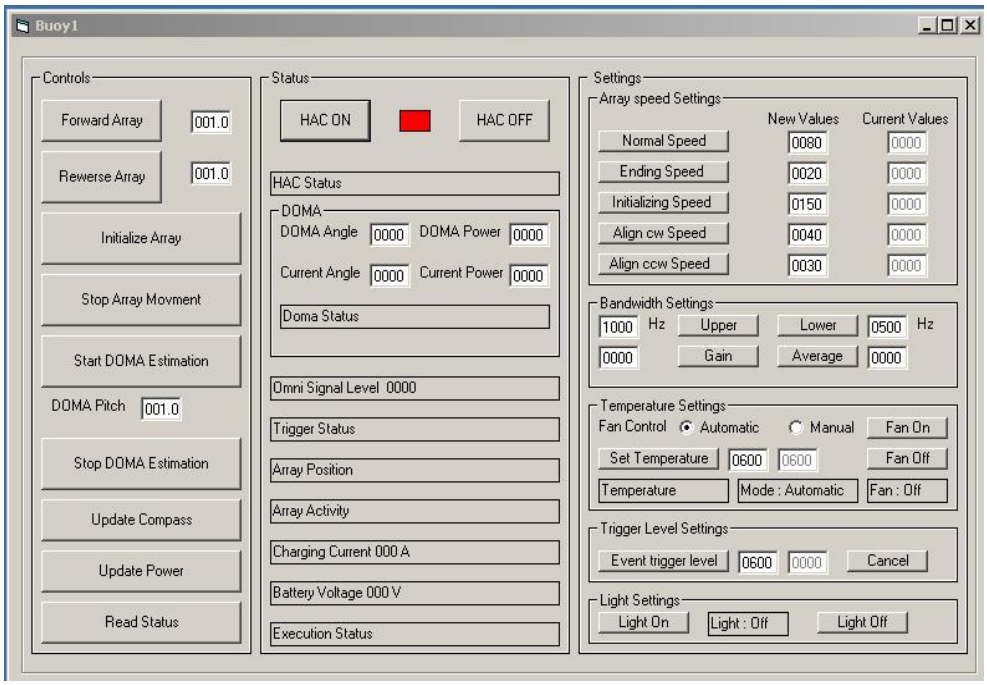

Fig. 5.16 GUI for Buoys

The preliminary test results were successful and when the communication was established, all the buoys reported their status and internal parameters. The system was initially programmed to remain in the idle mode, so that all the internal parameters of the buoy and the signal level at the Omni directional hydrophone will be available at the control station and can be closely monitored.

The buoys were then tested for the trigger event generation. With the full system working, and the buoys in idle state, a boat was started and maneuvered along the reservoir to find out the strength of the signal it produces on to the omni directional hydrophone element. The signal levels were noted in all the three buoys in the idle state. Later a value close to the

strength previously obtained was set as the trigger threshold level of the buoys and the boat was made to move in the reservoir. The buoys successfully indicated that trigger events were generated as expected.

The direction of arrivals as sensed by the three buoy systems were used for localizing the target under consideration. The necessary commands are issued for estimating the direction of arrivals using the predefined frame format. The shore station will sample the DOAs of all the buoys periodically and gathers the information as and when it is ready.

5.7 *Results and Discussions on Localizer*

A suitable test site for conducting the field trials in a hydroelectric reservoir was identified. The three buoy system for localizing the unknown underwater targets was deployed and the performance of the system was validated. The field trial was conducted by deploying the three buoys in the reservoir at the locations (9°48'41"N, 76°53'10"E), (9°48'10"N, 76°53'19"E) and (9°47'56"N, 76°53'19"E) by mooring them to the bottom and placing the noisy target at the location of (9°47'55"N, 76°53'18"E). The DOA estimates for different trials, the spectrum computed at the shore station for different noise sources and the localization estimates computed are listed in the following sections.

5.7.1 DOA Measurements

The directions of arrival of the noise waveforms emanating from the noise sources were estimated using the DOA estimator in a hydroelectric reservoir and the DOAs as seen by the buoy hydrophones were estimated with reference to the magnetic meridian.

The Signal Power Estimator Module has been realized and field tested with the hydrophone array controller and the estimator is capable of reporting the DOA, which is the absolute angle with reference to the Earth's magnetic meridian during the field trials. The DOAs measured by the buoy systems will help in fixing the position and ranging of underwater targets of interest. The absolute ranges and positions of the targets will certainly depend on the precision of the GPS data and the magnetic compass readouts. The angular variations of the estimated power from 0 to 360 degrees for various targets have been recorded and three of which are depicted in Fig. 5.17, Fig. 5.18 and Fig. 5.19. As illustrated in Fig. 5.17, the DOA for the Barge engine has been estimated as 39° with reference to the geomagnetic meridian.

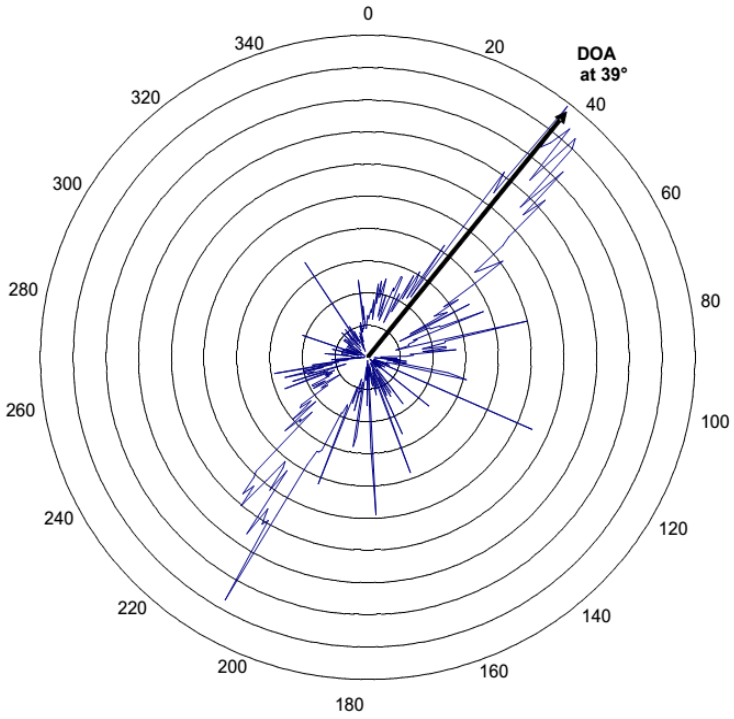

Fig. 5.17 The estimation of DOA as 39° for the Barge engine

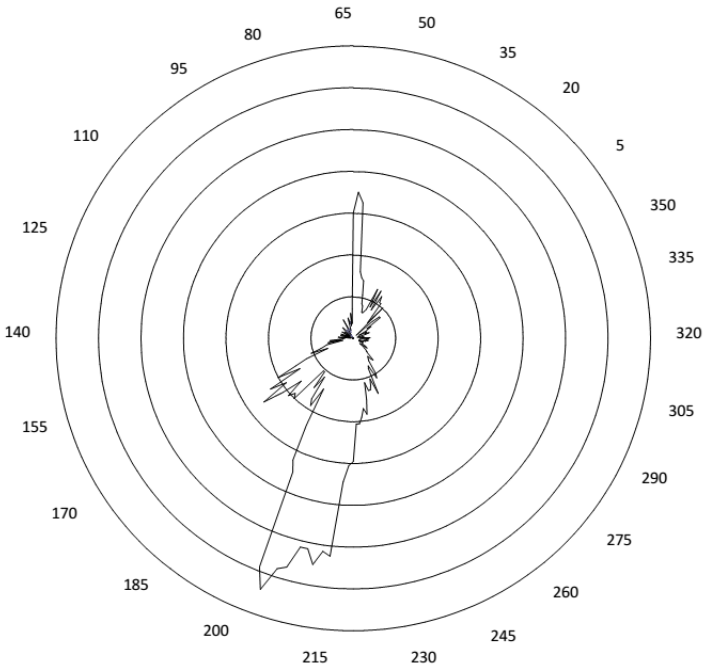

Fig. 5.18 The estimation of DOA as 203° for the Engine noise

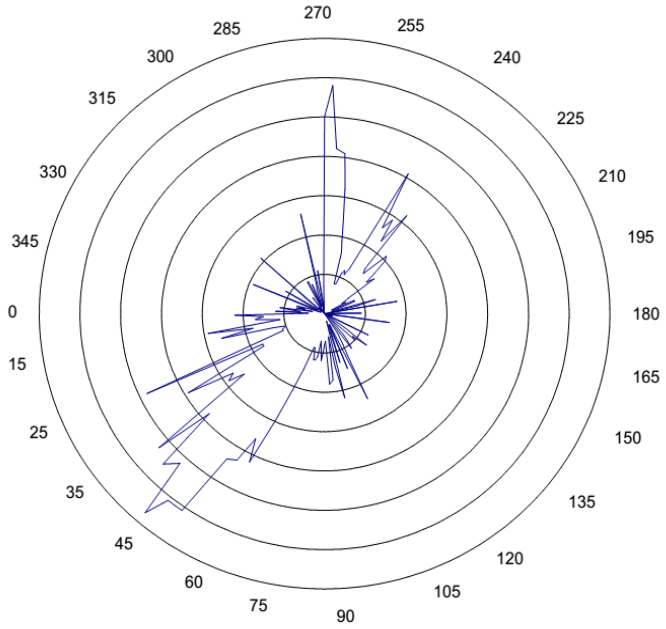

Fig. 5.19 The estimation of DOA as 45° for idling Boat engine

The angular power variation for the Engine noise is illustrated in Fig. 5.18 for which the DOA is estimated as 203°. Fig. 5.19 depicts the angular power variation and DOA estimation of Idling Boat Engine and the DOA is found to be 45°.

The spectrum of pre-recorded Engine noise transmitted using ITC 1007 projector, Idling Barge Engine and Idling Boat Engine, over the band 0 Hz to 5 kHz, are depicted in Fig. 5.20, Fig. 5.21 and Fig. 5.22 respectively.

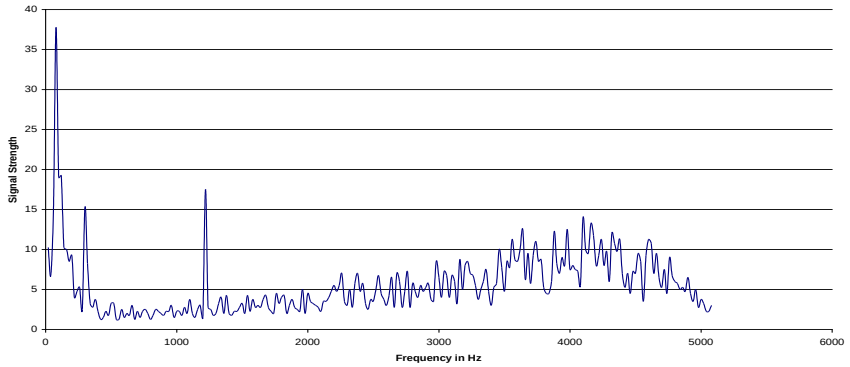

Fig. 5.20 Spectrum of Engine noise transmitted using ITC 1007 projector

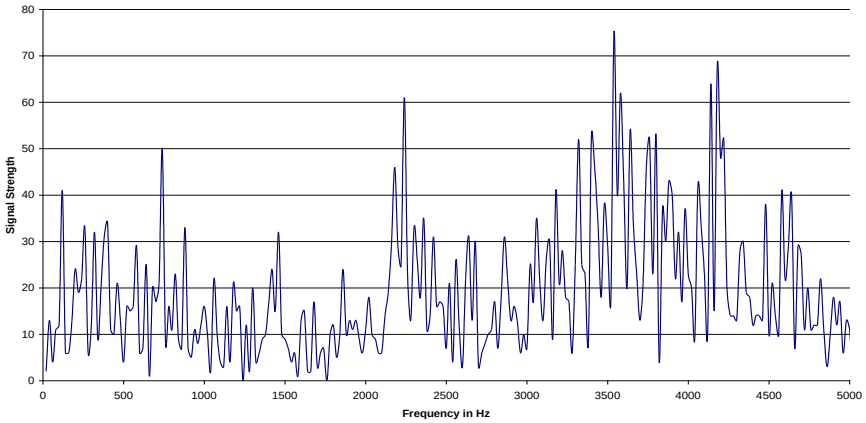

Fig. 5.21 Spectrum of idling Barge Engine

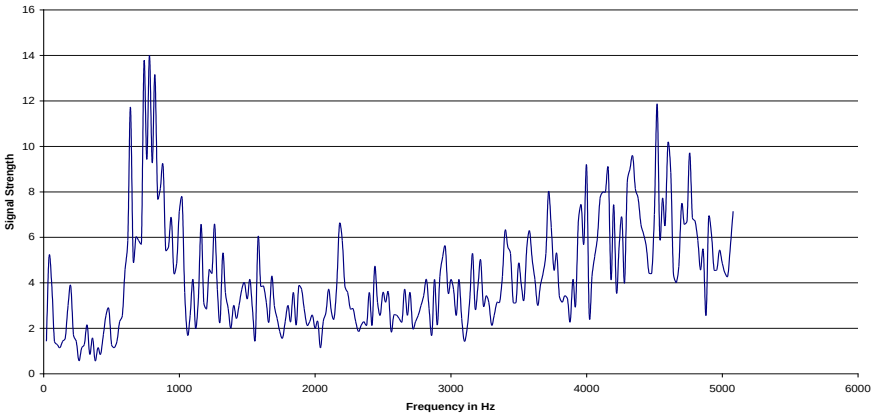

Fig. 5.22 Spectrum of idling Boat Engine

5.7.2 Localization Estimates

The field trial was carried out by deploying the three buoys in the trial site, in a hydroelectric dam at predetermined locations and fixing the position of the noisy target located at (9°47'55"N, 76°53'18"E). Repeated localization trials yielded the positional values of the target as (9°47'50"N, 76°53'15"E), (9°47'50"N, 76°53'11"E), (9°47'56"N, 76°53'25"E), (9°47'48"N, 76°53'10"E), (9°48'04"N, 76°53'09"E), (9°47'54"N, 76°53'19"E), (9°47'57"N, 76°53'22"E) and (9°47'56"N, 76°53'10"E).

The results of the field trials were quite encouraging, as far as the basic functionality is concerned, except for the small discrepancies in the localization estimates. The discrepancies and inconsistencies in the localization estimates are assignable to the fact that the buoys were deployed at close distances. Efforts are also made for further improving the consistencies in the localization estimates.

5.7.3 Need for Refinement of Localization Estimates

The model developed makes use of linear hydrophone arrays for deriving the directions of arrival of the noise waveforms emanating from

the target under consideration. The system can perform the surveillance operation in the horizontal plane only. Though it captures the noise waveforms from the targets located outside this plane, as the beam is roughly omni directional in the vertical plane, it cannot provide any depth information of the target. Due to the lack of depth information, the position estimates furnished by the system are likely to be slightly erroneous. The inaccuracies in the position estimates, consequent to the lack of depth information can be resolved by replacing the linear hydrophone arrays with planar arrays or at least with a cross arrays formed by combining two mutually bisecting linear arrays at right angles.

Also, as the array is mechanically steerable, whenever the array moves from one position to another, there will be a recoiling effect on the entire buoy system. This recoiling effect, caused due to the movement of the array from one position to another, will affect the orientation of the buoy, thus leading to inaccuracies in the angular positions of the hydrophone arrays. The instabilities of the buoy system caused by the surface waves will also lead to unpredictable errors in the estimates of the direction of arrival of the noise waveforms in each of the hydrophone arrays. These issues warrant the need and requirement for refining the range estimation making use of Kalman Filters.

5.8 *Improving Localization Estimates Using Kalman Filters*

The values of latitude and longitude of the target estimated may not be accurate due to the inherent errors in the estimation of DOAs, due to the recoiling effects of the buoy systems, varying environmental conditions and the mathematical approximations which are involved in the range computations.

These inaccuracies can be resolved to some extent by applying the concepts of Kalman filter, making use of which an accurate position of the underwater target is estimated by reducing the mean square error. The flowchart and the graphical user interface for improving the localization and tracking estimates are depicted in Fig. 5.23 and Fig. 5.24 respectively.

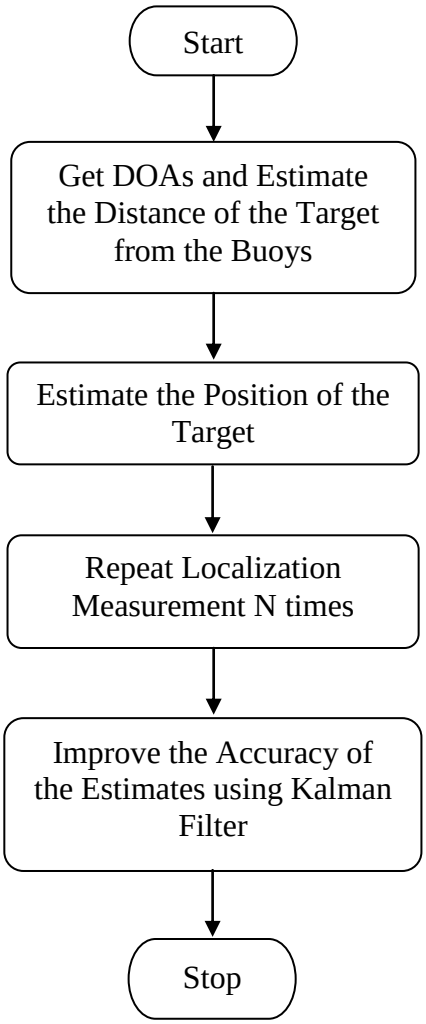

Fig. 5.23 Flowchart for improving the accuracy of Localization estimates

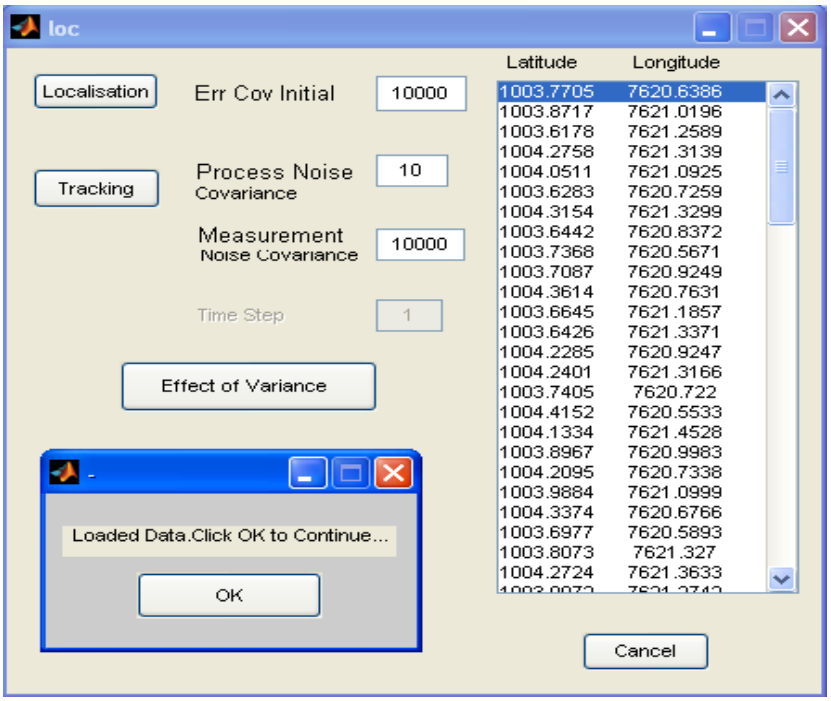

Fig. 5.24 GUI for Target localization and tracking

5.8.1 Results and Discussions on Refinement

The simulation of improving the localization estimates has been carried out using MATLAB. As the data from the localizer output is assumed to be erroneous, its latitude and longitude values are taken as X and Y dimensional values separately and filtered using Kalman filter for reducing the error in both the dimensions. In this simulation, the assumed values of latitude data and longitude data are $10^{o}04'00"$ and $76^{o}21'00"$, respectively. 100 distinct measured values for the latitude with error distributed around zero and a deviation of 1', were fed to the Kalman filter. The Kalman filter iterates these values, by minimizing the error covariance and eventually converges.

For improving the estimation of target localization, the erroneous latitude data is simulated and given to the Kalman filter and the output is

shown in Fig. 5.25. It can be seen that the error in the latitude data is minimized using the Kalman filter. The estimated output of the Kalman filter is generated from the particular iteration, where the Kalman Gain and the estimated error covariance converge and remain stable as depicted in Fig. 5.26.

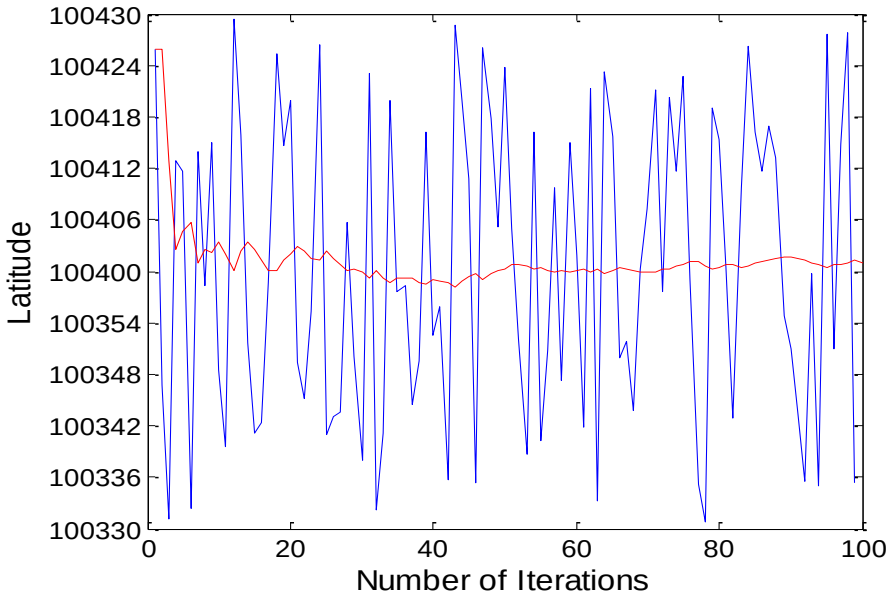

Fig. 5.25 Kalman filter output for the latitude data

From this variation, it can be seen that after 31 iterations, the filter converges and the estimated output of the Kalman filter for the latitude data is $10^{o}04'02''$. The same algorithm is extended to the erroneous longitude values too. The output of the Kalman filter for the longitude data is shown in Fig. 5.27.

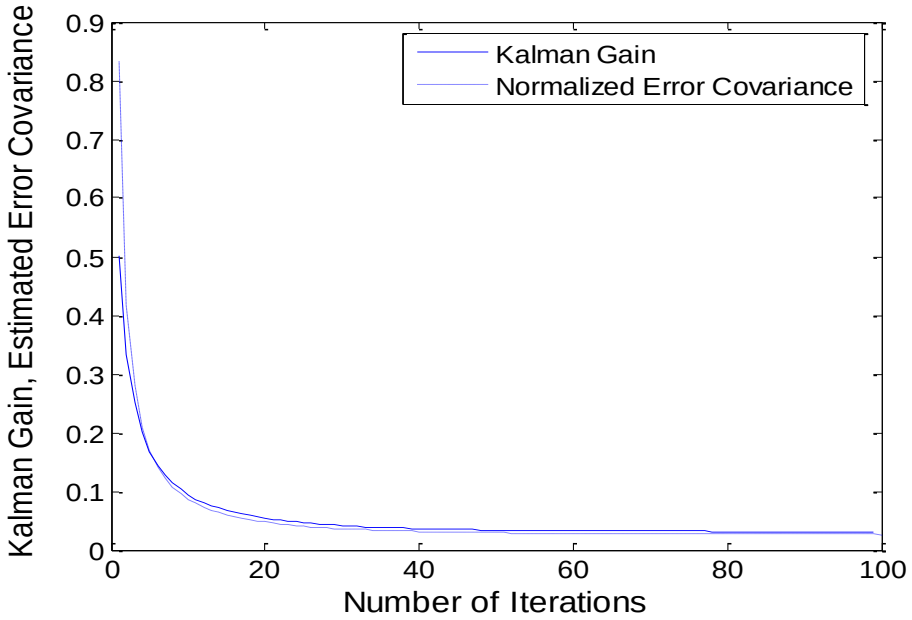

Fig. 5.26 Convergence of Kalman Gain and estimated error covariance

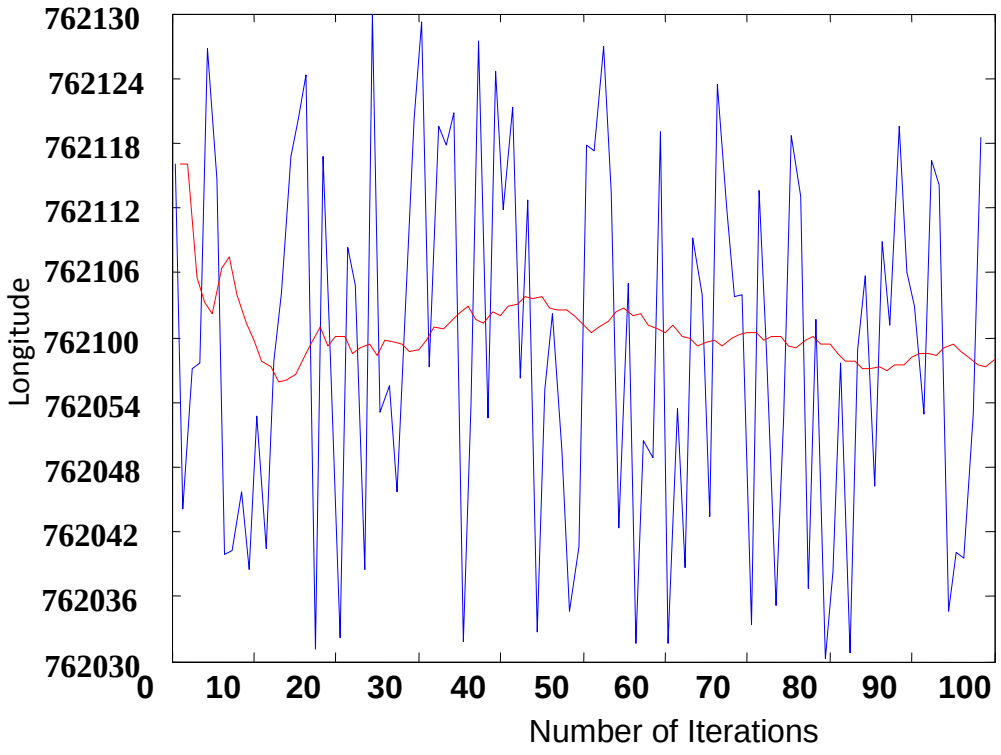

Fig. 5.27 Kalman filter output for the longitude data

A set of randomly fluctuating positional values indicated by 'o' markings, in Fig. 5.28 have been used for generating the corrected positional values by the Kalman filter. These values are simulated by adding random error to the assumed values of latitude and longitude data, $10^{o}04'00''$ and $76^{o}21'00''$ respectively. The Kalman output comprise of the points marked with '•' markings within the circled region in Fig. 5.28. The filter converges and the estimated output of the Kalman filter is the position with latitude $10^{o}04'02''$ and longitude $76^{o}21'01''$.

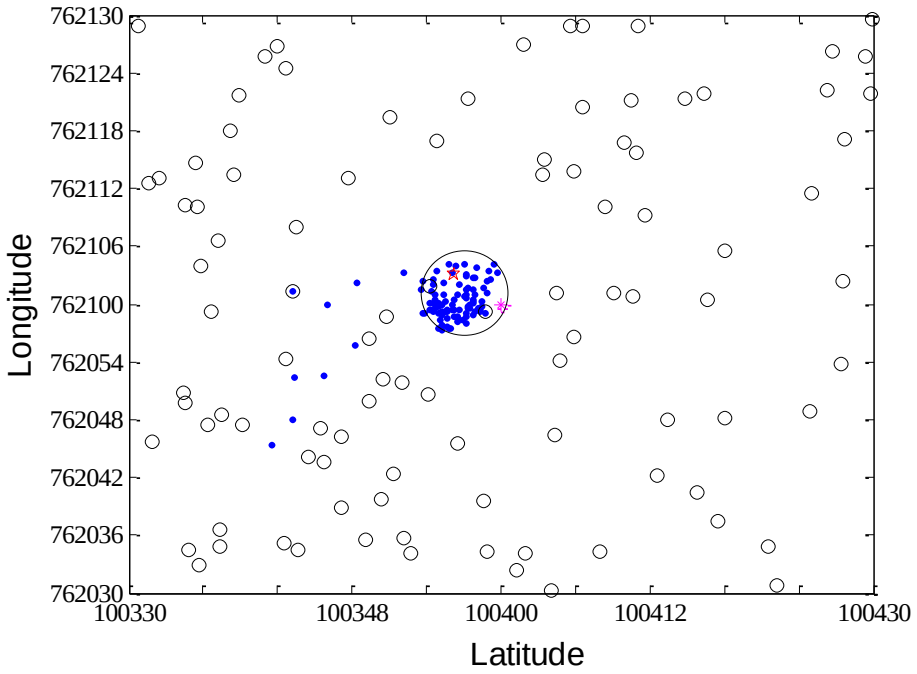

Fig. 5.28 Kalman filter applied to the noisy measurements of stationary target

Moreover, at the test site, repeated localization trials yielded the positional values of the target as (9°47'50"N, 76°53'15"E), (9°47'50"N, 76°53'11"E), (9°47'56"N, 76°53'25"E), (9°47'48"N, 76°53'10"E), (9°48'04"N, 76°53'09"E), (9°47'54"N, 76°53'19"E), (9°47'57"N, 76°53'22"E) and (9°47'56"N, 76°53'10"E) for a noisy target located at

(9°47'55"N, 76°53'18"E). When these positional values were fed to the Kalman filter, the estimated position output of the Kalman filter for the position of the target was seen to be (9°47'54.63"N**,** 76°53'17.5"E) as depicted in Fig. 5.29.

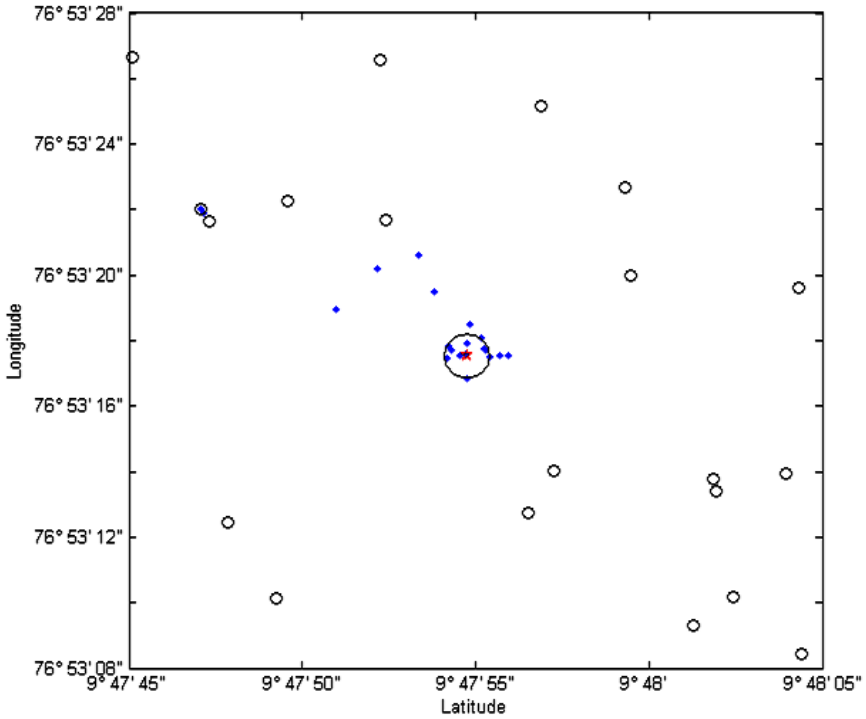

Fig. 5.29 KF gives the position of the target as (9°47'54.63"N, 76°53'17.5"E)

5.9 *Multi-Target Scenario*

The system works satisfactorily with one or two targets, whereas in multi-target scenario, the Shore Station System may have to issue commands to the buoy systems to align their hydrophone arrays to the targets that are emitting certain tonals or bands of frequencies as detected by either any one of the omni-directional hydrophones or the hydrophone arrays in the system. Execution of such missions by the buoys in a two-target scenario is comparatively easy, because in such situations, in all

probability, the target feature vectors generated by two of the buoy systems are likely to be in agreement. If this is the case, making use of geometrical reconstructions, the shore station system can compute the likely orientation to which the hydrophone array of the third buoy system, which disagreed in the target feature vector, has to be steered for acquiring the noise waveforms from the target under consideration. The action to be initiated by the concerned buoy system for handling multi target scenario is illustrated in the flowchart furnished in Fig. 5.30.

5.10 *Summary*

A prototype for the localization of underwater targets, using a buoy system with passive listening concepts has been developed and deployed. The field trials for the localization of the underwater targets has been carried out by mooring three buoys in a trial site at predetermined locations and by fixing the position of the noisy target. The performance of the system was evaluated and the localization estimates were found to be acceptable within the limits of the mathematical approximations and experimental errors [107-110]. The inconsistencies in the localization estimates have been reduced, to a certain extent, by minimizing the measurement errors using Kalman filters.

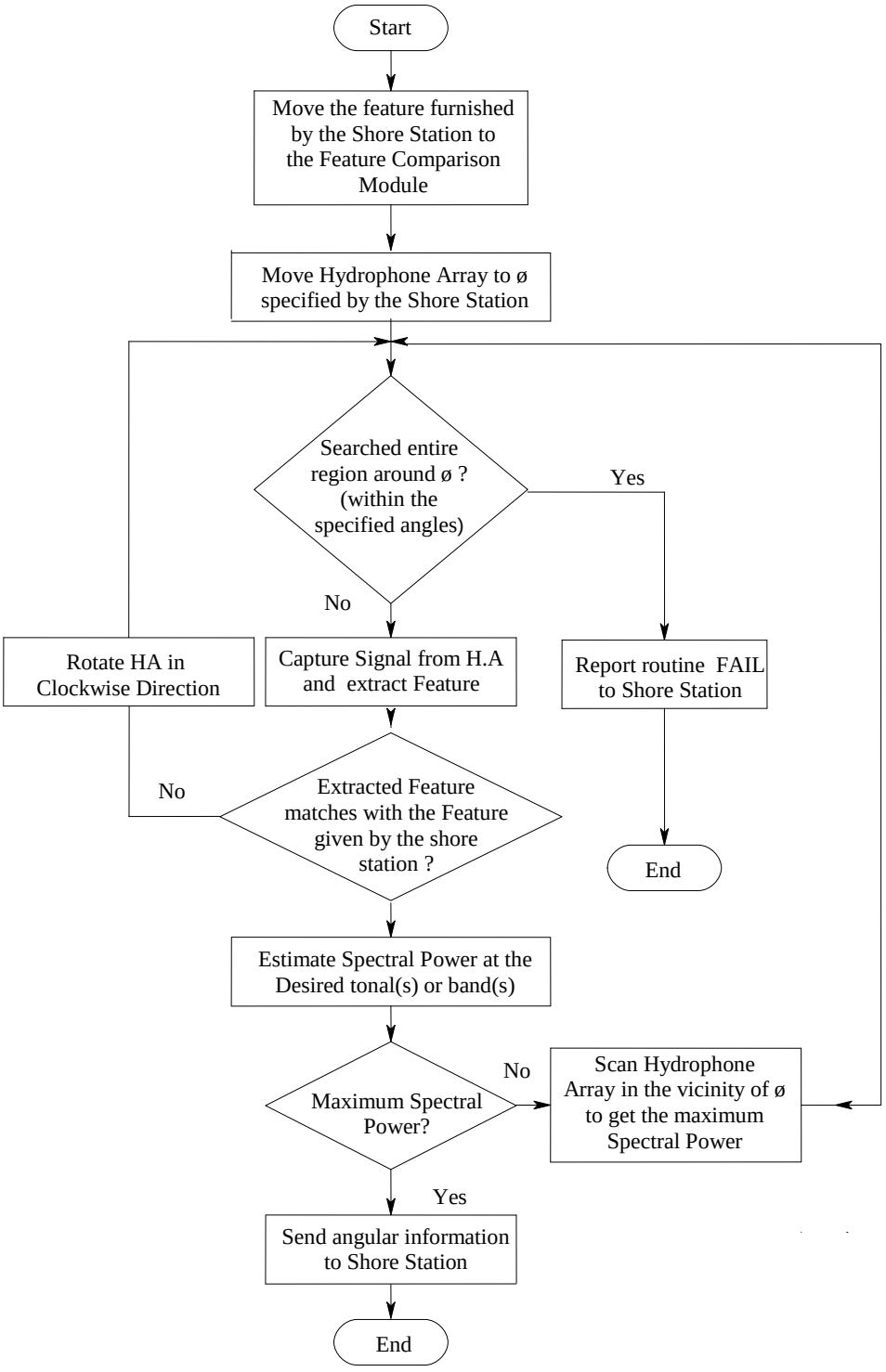

Fig. 5.30 Realignment Mode for handling Multi-target Scenario

CHAPTER 6

TARGET TRACKING

Target tracking pertains to the estimation of current state and prediction of the future states of a moving target, based on the outcome of measurements made by the observing sensor. Target tracking systems basically produce a stream of data related to the position of the target. This problem can be further divided into one dimensional motion of the target with inherent noises of different forms such as process noise and measurement noise. A study of one dimensional system is carried out and then extended to two dimensions, which can further be generalized to a multi-dimensional system depending on the nature of the problem. The observed errors in the case of a maneuvering target are more complex in nature than the one in the case of a target which is moving with constant velocity and hence need to be mitigated by using suitable estimation techniques. In the case of a highly maneuvering target, a chi-square based decision statistics can be applied for effecting necessary corrections to the Kalman filter algorithm, so that the system is capable of handling such abrupt maneuvers.

6.1 *Introduction*

Tracking of targets using various techniques in an underwater scenario is a problem of unfathomable extent, owing to the characteristics of the ambient environment. As the localization estimates may vary due to sensor and environmental errors, various techniques are applied to obtain reliably accurate estimates of localization. The results of tracked targets can

be mostly misleading, if enough measures for minimizing errors in every stage of the system are not employed. One of the major problems faced by underwater target tracking systems is the effects of noises of various forms, right from the ambient noises to system induced noises, which have to be dealt with, for reliable results.

The purpose of target tracking is to accurately estimate the target positions based on the observation data. The tracking performance depends on accurate description of the target state, and accurate tracking of the target can be obtained when the target state model matches with the target practical state. Among various techniques, Kalman filter tracking devices are getting more attention because of their practicality, as this method does not require the entire previous data to be stored and reprocessed every time a new measurement is taken.

Target tracking systems furnish a stream of data related to the target positions. This scenario is further segregated into one dimensional motion of the target with inherent noises of different forms such as process noise and measurement noise. A study of one dimensional system is carried out in the first section and then extended to two dimensions, which can further be generalized to a multi-dimensional system depending on the nature of the problem.

In the case of a maneuvering target, the observed errors are complex in nature than the one in the case of a target which is moving with constant velocity and hence appropriate correction measures need to be implemented. The main cause of such errors in tracking targets, is their abrupt change in velocity, which becomes difficult to be identified by the tracking device. This major issue is associated with tracking of maneuvering targets with highly adaptive generic filters like the Kalman

filters also, since these filters end up producing an output, erroneously considering the measured values in response to the maneuvering target, as noise. Hence optimizing the performance of the Kalman filter in a maneuvering target scenario warrants certain modifications, which are discussed in the final section of this chapter.

6.2 *Scenario Overview*

The key to successful target tracking lies in the effective extraction of useful information about the state of the target from the observations. A good model of the target facilitates the information extraction to a great extent. Tracking algorithms are mostly model based because some knowledge of target motion is available and a good model-based tracking algorithm will greatly outperform any model-free tracking algorithm.

Targets with single and two dimensional movements, measured in Cartesian co-ordinate system, are considered for the analysis in this chapter, with position and velocity as the quantities being tracked. Suitable transformations can be used, if the measurement data are in a format other than the Cartesian system. However the tracking system and design challenges are relatively insensitive to the choice of the co-ordinate system. The measurements expressed in Cartesian coordinates are not independent, but the effect of ignoring this fact is negligible in practice [57].

A target moving with nearly constant velocity is characterized by a state vector with position and velocity as elements. The observations made can be assumed as a linear combination of the target state corrupted by additive measurement noise. The Kalman gain is used to derive the estimates of the state vector which in turn is used to compute the estimates predicted for the next measurement state.

The difference between the measured or observed value and the predicted value is defined as the *residual* or *innovation.* The residual reflects the discrepancy between the predicted measurement and the actual measurement. In addition to being used for updating the filtered estimates, the residual values can be checked for consistency. This consistency check can be used to adjust the filter parameters when large residual values are interpreted as due to increased target dynamics or the detection of maneuvering of the target. The estimation accuracy provided by the Kalman filter through the covariance matrix is useful for detection of maneuver. Upon detecting such maneuver, the Kalman filter also provides an efficient way to adapt to a scenario of varying target dynamics [63].

6.2.1 Linear Systems Approximation for Kalman Filtering

The transition and observation matrices of the Kalman equations, (3.1) to (3.7) of Chapter 3, needed to be modified for tracking a target, according to the scenario under consideration. The Kalman filter is a tool that can estimate the variables of a wide range of processes. The Kalman filter theory is explained in the section 3.4. In mathematical terms, a Kalman filter estimates the states of a linear system. The Kalman filter not only works well in practice, but, it is theoretically attractive because it can be shown that, of all possible filters, it is the one that minimizes the variance of the estimation error. In order to use a Kalman filter to remove noise from a signal, the process under consideration for measurement must be able to be described by a linear system.

Many physical processes, like movement of a target, can be approximated as linear systems. A linear system is simply a process that can be described by the following two equations:

State equation:

$$x_{k+1} = Ax_k + Bu_k + w_k \tag{6.1}$$

Output equation:

$$y_k = Cx_k + z_k \tag{6.2}$$

In the above equations A, B and C are matrices, k is the time index, x is called the state of the system, u is a known input to the system, y is the measured output and w & z are the noises. The variable w is called the process noise and z is called the measurement noise. Each of these quantities is a vector and therefore contains more than one element. The vector x contains all of the information about the present state of the system. As x cannot be measured directly, y is measured as a function of x, which is corrupted by the noise z. y can be used to obtain an estimate of x, but cannot necessarily take the information from y at face value because it is also corrupted by noise.

6.3 *Tracking of a Moving Target*

An underwater target moving in two dimensions with nearly constant velocity is characterized by a state vector with position and velocity as elements. The observations made can be assumed as a linear combination of the state vector corrupted by additive measurement noise due to the wave action and other physical parameters of the ocean.

Hence the velocity υ for an arbitrary time step k+1, can be written as

$$\upsilon_{k+1} = \upsilon_k + Tu_k + \tilde{\upsilon}_k, \tag{6.3}$$

where u is the acceleration, T is the time interval and $\tilde{\upsilon}$ is the velocity

noise. A similar equation for position ***s*** can be expressed as,

$$s_{k+1}=s_k+ Tv_k +\frac{1}{2}\ T^2\ u_k+\tilde{s}_k \tag{6.4}$$

where $\tilde{s}$ is the position noise.

For an *n* dimensional system, the state vector at time step *k*, can be described as,

$$x_k=\begin{bmatrix} s_1 \\ s_2 \\ : \\ s_n \\ \\ v_1 \\ v_2 \\ : \\ v_n \end{bmatrix} \tag{6.5}$$

For a target moving in one dimension,

$$x_k=\begin{bmatrix} s_1 \\ v_1 \end{bmatrix} \tag{6.6}$$

Since the measurement vector contains only the position element, the linear system equations can be represented as,

$$x_{k+1}=\begin{bmatrix} 1 & T \\ 0 & 1 \end{bmatrix}x_k+\begin{bmatrix} T^2/2 \\ T \end{bmatrix}u_k+w_k \tag{6.7}$$

$$z_k=\begin{bmatrix} 1 & 0 \end{bmatrix}x_k+v_k \tag{6.8}$$

The process noise $\boldsymbol{w}_k$, represents the trajectory perturbations due to uncertainty in the target state whereas the measurement noise $\boldsymbol{v}_k$, represents the inability of the tracking device to precisely measure the position of the target due to unavoidable errors in the measurement system. Both these noises are assumed to be random Gaussian processes. The acceleration $\boldsymbol{u}$ can be assumed to be zero without disturbing the generality of the system for a target moving with a constant velocity.

The process noise is a Gaussian random process with zero mean and known covariance matrix *Q*. In general, the covariance of a vector of random variable, *X* is defined as $Cov(X)=E\{(X-E[X])(X-E[X])^T\}$,where *E[X]* is the mean of random variable *X*.

Because of the possible errors in the measuring device, measurement noise is added to the measurement vector. This represents the deviation between the positions that should be measured and the positions that are actually measured. This is also a Gaussian random process that follows a multivariate normal distribution with covariance matrix, *R*.

6.4 *Tracking of a Target Moving in Two Dimensions*

In this scenario, the target is moving in two dimensions with a constant velocity, and the measured data is represented in Cartesian coordinates. The state, prediction and correction equations of the model are the same as that of the one dimensional scenario, except that all the vectors are of dimension 2.

The true position of the target at the time $k+1$, given the position at time *k* is: $\boldsymbol{x}_{k+1} = \boldsymbol{A}\boldsymbol{x}_k + \boldsymbol{w}_k$ (6.9)

The state vector at time step k , when $n = 2$ is,

$$\boldsymbol{x}_k = \begin{bmatrix} s_1 \\ s_2 \\ \upsilon_1 \\ \upsilon_2 \end{bmatrix} \tag{6.10}$$

and the state transition model $\boldsymbol{A}$ is:

$$\boldsymbol{A} = \begin{bmatrix} I_2 & T.I_2 \\ \boldsymbol{0} & I_2 \end{bmatrix}, \tag{6.11}$$

where $\boldsymbol{I_2}$ is the identity matrix of order 2x2 and $\boldsymbol{0}$ is all zero matrix of 2x2.

The state vector keeps track of the positions of the target and velocities in different dimensions, which usually are the X and Y dimensions. The purpose of the Kalman filter is to estimate the true state vector given a series of discrete measurements. The state transition model updates the state vector in each time step by updating each position by adding the time interval between each measurement multiplied by the velocity in the same dimension.

Again, the measurement vector is a function of the state vector and a random noise process, expressed as,

$$\boldsymbol{z}_k = \boldsymbol{H}\boldsymbol{x}_k + \boldsymbol{v}_k \tag{6.12}$$

where the measurement vector is: $$\boldsymbol{z}_k = \begin{bmatrix} s_1 \\ s_2 \end{bmatrix} \tag{6.13}$$

and the observation model $\boldsymbol{H}$ is:

$$\boldsymbol{H} = \begin{bmatrix} I_2 & \boldsymbol{0} \end{bmatrix} \tag{6.14}$$

As the velocity is not measured directly, the observation model $\boldsymbol{H}$ is operated on the state vector in order to obtain the measurement vector.

6.5 *Tracking of a Maneuvering Target*

The primary objective of target tracking is to estimate the state trajectories of a moving target. Although a target is almost never really a point in space and the information about its orientation is valuable for tracking, a target is usually treated as a point object without a shape especially in target dynamic models. A target dynamic/motion model describes the evolution of the target state with respect to time. Almost all maneuvering target tracking methods are model based. They assume that the target motion and its observations can be represented by some known mathematical models sufficiently accurate. The most commonly used models are state-space models as given by the equations, (6.1) and (6.2).

One of the major challenges for target tracking arises from the target motion uncertainty. This uncertainty refers to the fact that an accurate dynamic model of the target being tracked is not available to the tracker. Specifically, although the general form of the state space model is usually adequate, a tracker lacks knowledge about the actual control input and the other parameters of the target or the statistical properties of the noise for the particular target being tracked. Target motion modeling is thus one of the first tasks for the tracking of maneuvering target. It aims at developing a tractable model that accounts well for the effect of target motion.

Target motions are normally classified into two classes viz., maneuver and nonmaneuver. A nonmaneuvering motion is the straight and level motion in a constant velocity system, sometimes also referred to as the uniform motion. Loosely speaking, all other motions belong to the maneuvering mode and tracking a maneuvering target assuming it is not maneuvering may have a serious consequences like the track loss, while

tracking a nonmaneuvering target assuming it is maneuvering usually only suffer minor performance degradation.

The standard Kalman filter cannot be applied while considering a maneuvering target that executes a turn or an evasive action to elude the detection, since the target movement appears as an extensive process noise on the target model, which cannot be circumvented by the process noise variance.

6.5.1 Maneuver Detection

Whether the target is maneuvering or not, is a decision problem and can be formulated as a hypothesis testing procedure, as under.

H_0: The target is maneuvering

H_1: The target is not maneuvering.

It is also important to infer the onset time and termination time of a maneuver. The determination of maneuver onset and termination times can be cast either as an estimation or decision problem. They both aim at inferring an unknown quantity using available information. Their basic difference is that, decision is the selection from a discrete finite set of candidates, while all possible outcomes of estimation form a continuum. In the continuous-time case, it would be more natural to formulate the determination of onset and termination times as an estimation problem, but a decision framework appears to be more appropriate for the discrete-time case [63, 66].

In maneuver detection, the focus is the detection of maneuver onset, rather than the maneuver termination. The two main reasons for this are, the level of difficulty and the consequences of an incorrect decision. In

general, it is more difficult to detect maneuver termination than maneuver onset because nonmaneuver is a well defined motion pattern, straight and level motion at a constant velocity, while maneuver essentially includes all other motion patterns. For instance, a maneuver model has a larger covariance of measurement residuals than a nonmaneuver model due to the fact that the latter has a larger state vector and assumes more motion uncertainty than the former. Fortunately, timely detection of maneuver termination is usually not as important as that of maneuver onset because tracking a nonmaneuvering target considering it is maneuvering usually may not have serious consequences.

In order to detect a maneuver, the difference between each measurement and its corresponding predicted value is computed, which is called residual or innovation. When the number of components in each measurement is more than one, a normalized distance function or total distance, d^2 is computed. This is done by squaring the differences in each of the component measurements, dividing by the respective error variances and then summed to form a total normalized distance [57].

A generalized form of normalized distance function can be formed with the application of Kalman filter by using the residual vector and the residual covariance matrix *S*,

$$d_k^2 = \tilde{\mathbf{z}}_k{}^T S^{-1} \tilde{\mathbf{z}}_k \tag{6.15}$$

where $\tilde{\boldsymbol{z}}_k = \boldsymbol{z}_k - \boldsymbol{H}\hat{x}_k^-$

$$S = S_k^- = HP_k^- H^T + R \tag{6.16}$$

The maximum allowable value for the residual is set using the accuracy statistics of the prediction and measurement values and is normally set to at least thrice the residual standard deviation assuming zero mean Gaussian statistics, for one dimensional movement of the target. The computed differences are compared with the above derived maximum allowable error value and if the difference exceeds the same, a target maneuver is considered as detected. When two dimensional systems are under consideration, simply comparing the distance between the predicted point and the measured point is insufficient due to state uncertainty.

In the subject case, the target has two dimensions of physical freedom. The normalized distance function, under the Gaussian assumptions, featuring a chi-square probability distribution with degrees of freedom equal to the number of the measurement dimensions, which in this case is 2. Based on this chi-square table for d^2, a threshold can be set to detect the target maneuver [57, 58].

Thus in order to detect the maneuvering of the target, the value of the distance function can be monitored in comparison to a threshold determined by the chi square probability distribution function. The validity of chi-square test relies on the assumption that the process is Gaussian and independent. Nevertheless, the chi-square tests are used in these situations, because of its simplicity even though it is not necessarily optimal.

6.5.2 Chi-Square Based Decision Test

Assume that ϵ is chi-square distributed with n degrees of freedom, then a chi-square test based maneuver detector will declare detection of a maneuver, if $\epsilon > \lambda = \chi_n^2(\alpha)$, where 1-$\alpha$ is the level of confidence, which should be set quite high, say 0.95 or 0.99. It is well known that the d^2

function is chi square distributed for any *n* dimensional Gaussian random vector. In this sense, chi-square test provides a check for the acceptability of fit to judge if the vector has the assumed distribution. The validity of a chi-square test relies on the assumption that individual terms are Gaussian and independent.

In maneuver detection, the two choices can be used in which one is based on the measurement residual and the other is based on input estimate. In the residual based case, *normalized residual squared* is used as the detection tool. On the other hand, in the input estimation method, the *control input* ***u***, which is acceleration in this case, can be used to detect the maneuver. When the target is not maneuvering, the control input is zero, which means acceleration is zero, assuming constant velocity. But while maneuvering, *u* changes and thus any estimate of this input, under the linear-Gaussian assumption, has a similar chi-square distribution, which can be used for maneuver detection.

6.5.3 Confidence Ellipsoid and Chi-square Distribution

Let X be a n-dimensional Gaussian random vector, with mean vector, m_x and covariance matrix, Σ_X. Consider a constant, $K_1 \in R$. The locus for which the pdf $f(x)$ is greater or equal a specified constant K_1, i.e.,

$$\left\{ x : \frac{1}{(2\pi)^{n/2}|\Sigma|^{1/2}} \exp\left[-\frac{1}{2}[x - m_X]^T \Sigma_X^{-1}[x - m_X] \right] \geq K_1 \right\} \qquad (6.17)$$

$$\text{which is equivalent to } \left\{ x : [x - m_X]^T \Sigma_X^{-1}[x - m_X] \leq K \right\} \qquad (6.18)$$

with $K = -2In((2\pi)^{n/2} K_1 |\Sigma| 1/2)$ is an n-dimensional ellipsoid centered at the mean m_X and whose axis are only aligned with the Cartesian frame if the covariance matrix Σ is diagonal. The ellipsoid is the region of

minimum volume that contains a given probability mass under the Gaussian assumption. In the equation there exits an equality, i.e.,

$$\left\{x:\left[x-m_X\right]^T \sum_X^{-1}\left[x-m_X\right]=K\right\}, \tag{6.19}$$

this locus may be interpreted as the contours of equal probability [72].

6.5.3.1 **Mahalanobis distance**

$\left[x-m_X\right]^T \sum_X^{-1}\left[x-m_X\right]=K$ is known as the *Mahalanobis distance* of the vector x to the mean m_X. The Mahalanobis distance, is a normalized distance where normalization is achieved through the covariance matrix. The surfaces on which K is constant are ellipsoids that are centered about the mean m_X. In the special case, where the random variables of X are uncorrelated and with the same variance, i.e., the covariance matrix Σ_X is a diagonal matrix with all its diagonal elements equal, these surfaces are spheres, and the Mahalanobis distance becomes equivalent to the Euclidean distance.

The contours of equal Mahalanobis and Euclidean distance around (m_X,m_Y) for a second order Gaussian random vector is represented in Fig. 6.1. Any point (x,y) in the ellipse is at the same Mahalanobis distance to the center of the ellipses and any point (x,y) in the circumference is at the same Euclidean distance to the center. This plot enhances the fact that the Mahalanobis distance is weighted by the covariance matrix.

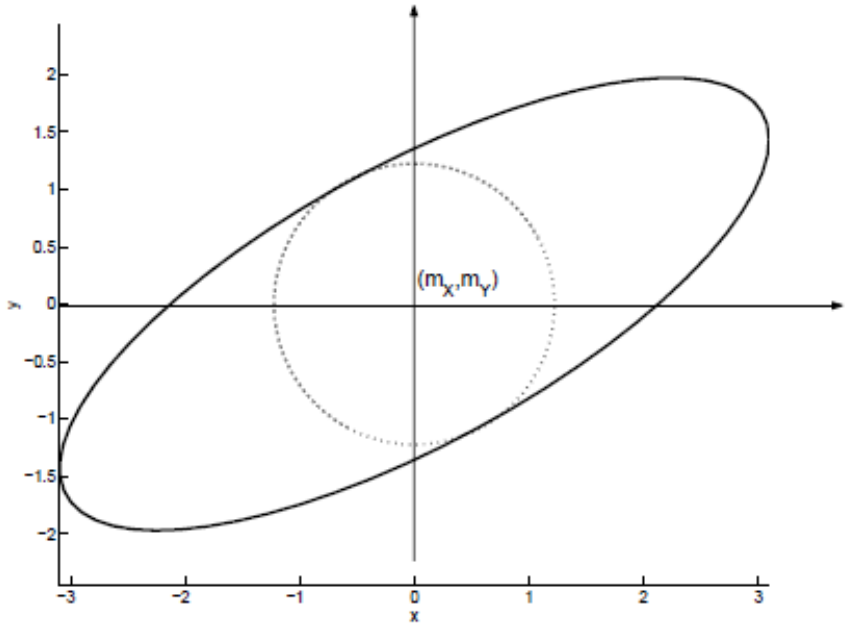

Fig. 6.1 Contours of equal Mahalanobis and Euclidean distance around (m_X,m_Y) for a second order Gaussian Random Vector

For decision making purposes, it is necessary to determine the probability that a given vector will lie within, say, the 90% confidence ellipse or ellipsoid. For a given K, the relationship between K and the probability of lying within the ellipsoid specified by K is,

$$n = 1;\ Pr\{x \text{ inside the ellipsoid}\} = -\frac{1}{\sqrt{2\pi}} + 2erf\left(\sqrt{K}\right) \qquad (6.20)$$

$$n = 2;\ Pr\{x \text{ inside the ellipsoid}\} = 1 - e^{-K/2} \qquad (6.21)$$

n =3; $Pr\{x$ inside the ellipsoid$\}$

$$= -\frac{1}{\sqrt{2\pi}} + 2erf\left(\sqrt{K}\right) - \sqrt{\frac{2}{\pi}}\sqrt{K}e^{-K/2} \qquad (6.22)$$

where n is the dimension of the random vector. The numeric values of probability for $n = 2$ for various values of K are depicted in Table 6.1.

Table 6.1 Numerical values of Probability for n = 2

K	**Probability**
1	**39.3%**
1.5	**52.76%**
2.0	**63.21%**
2.5	**71.35%**
3.0	**77.69%**
3.5	**82.62%**
4	**86.47%**

For a given *K*, the ellipsoid axes are fixed. The probability that a given value of the random vector *X* lies within the ellipsoid centered in the mean value, increases with the increase of *K*. In the case where a fixed probability value is specified, the value of *K* that yields an ellipsoid satisfying that probability can be found from analyzing the statistics of *K*, which has a known random distribution called Chi-Square distribution.

6.5.3.2 **Chi-Square distribution**

Given the *n*-dimensional Gaussian random vector *X*, the Mahalanobis distance *K* which is a random variable, has a Chi-Square probability distribution with *n* degrees of freedom.

The probability density function of *K*, i.e., the Chi-Square density with *n* degrees of freedom is,

$$f_K(k) = \frac{1}{2^{\frac{n}{2}}\Gamma\left(\frac{n}{2}\right)} k^{\frac{n-2}{2}} \exp^{\frac{-k}{2}} \tag{6.23}$$

and the Cumulative distribution function is

$$F_K(k) = \frac{\gamma(\frac{n}{2}, \frac{k}{2})}{\Gamma(\frac{n}{2})} \tag{6.24}$$

where the gamma function,

$$\Gamma = (n-1)!$$

$$\Gamma\left(\frac{1}{2}\right) = \sqrt{\pi}, \quad \Gamma(1) = 1, \quad \Gamma(n+1) = n\Gamma(n)$$

The probability that the scalar random variable, *K* is less than or equal to a given constant, χ_p^2 ,

$$\Pr\left\{K \le \chi_p^2\right\} = \Pr\left\{\left[x - m_X\right]^T \sum^{-1} \left[x - m_X\right] \le \chi_p^2\right\} = p \tag{6.25}$$

is given in the following chi-square distribution table, Table 6.2, where *n* is the number of degrees of freedom and the subscript *p* in χ_p^2 represents the corresponding probability under evaluation.

From this table, it can be seen that for a second third order Gaussian random vector, *n = 2*,

$$Pr\left\{K \le 4.61\right\} = Pr\left\{\left[x - m_X\right]^T \sum^{-1} \left[x - m_X\right] \le 4.61\right\} = 0.9$$

Table 6.2 Chi-Square distribution table

N	$\chi^2_{0.995}$	$\chi^2_{0.99}$	$\chi^2_{0.975}$	$\chi^2_{0.95}$	$\chi^2_{0.90}$	$\chi^2_{0.75}$	$\chi^2_{0.50}$	$\chi^2_{0.25}$	$\chi^2_{0.10}$	$\chi^2_{0.05}$
1	7.88	6.63	5.02	3.84	2.71	1.32	0.455	0.102	0.0158	0.0039
2	10.6	9.21	7.38	5.99	4.61	2.77	1.39	0.575	0.211	0.103
3	12.8	11.3	9.35	7.81	6.25	4.11	2.37	1.21	0.584	0.352
4	14.9	13.3	11.1	9.49	7.78	5.39	3.36	1.92	1.06	0.711

6.5.4 Threshold Setting and Correction Measures

A threshold for normalized distance function is set using the chi-square distribution table, beyond which the target is detected to be under maneuvering. From the table, it can be seen that for a second order Gaussian random vector, $n = 2$, $Pr\{K \leq 9.21\} = 0.99$. If the distance function exceeds the tolerance level during a set number of concurrent time steps, the maneuver detection is confirmed. Once the maneuver is detected, the Kalman filter parameters are reset and the filter is reinitialized using the last two measurements.

6.6 *Simulation*

The simulation of tracking underwater targets using Kalman filter has been implemented in MATLAB. It is assumed that the target is moving in a straight line. The measured values for tracking scenarios are simulated from the localizer output by adding appropriate random functions. The erroneous values are fed to the Kalman filter for refinement of the estimates. By iterating these values and minimizing the covariance, the Kalman filter eventually converges and generates the corrected values.

The flowchart for the tracking of a maneuvering target is illustrated in Fig. 6.2, which detects the maneuvering of the target and upon detection reinitializes the Kalman filter. The output figures vivify the effectiveness of the algorithm.

Using the chi-square distribution table, the value of the threshold is taken as 9.21 which is equal to the value of the chi-square corresponding to a probability of 0.99, beyond which the target is detected to be under maneuvering. The threshold crossing is checked for two more concurrent time steps in order to ensure the maneuver detection.

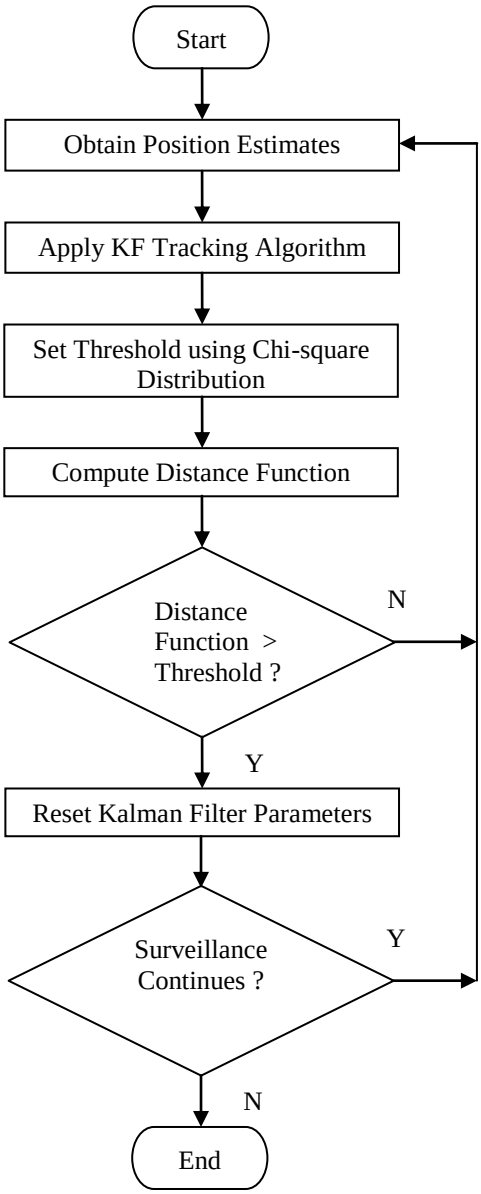

Fig. 6.2 Flowchart for tracking abruptly maneuvering target

6.7 *Results and Discussions*

6.7.1 Tracking of a Moving Target

In this scenario, it is assumed that the target is moving in one dimension and in a straight line with a constant velocity. The true position

of the target, the measured position and the estimated position are depicted in Fig. 6.3. The two curves are the true position and the estimated position and they are almost too close to be distinguished from one another while the '+' marks are the measured positions.

In order to compare the accuracy of the estimates generated by the Kalman filter, Fig. 6.4 depicts the error values between the true position and the measured position as well as between the true position and the estimated position as provided by the filter. It is clear from this plot that the positions that are estimated or predicted by the Kalman filter are much closer to the true positions almost at every data points. This plot also shows how the Kalman estimates improve over time.

The relative accuracy of the Kalman output is demonstrated in Fig. 6.5, which shows the target velocity estimate which is a part of the state variable x, along with the position estimates. Here the estimated velocity is plotted along with the velocity derived from the position measurements, as the system does not provide any velocity data measurements. As seen from the plot, the velocity estimates are remarkably more stable than the observed values.

The fact that Kalman filter reduces the residual errors with elapsed time is clearly proven in the plot shown in Fig. 6.6 which depicts the error between the true velocity and the estimated velocity. Though the initial predictions are not accurate, the filter adapts and gets tuned to the variations and limits the error range after a few iterations.

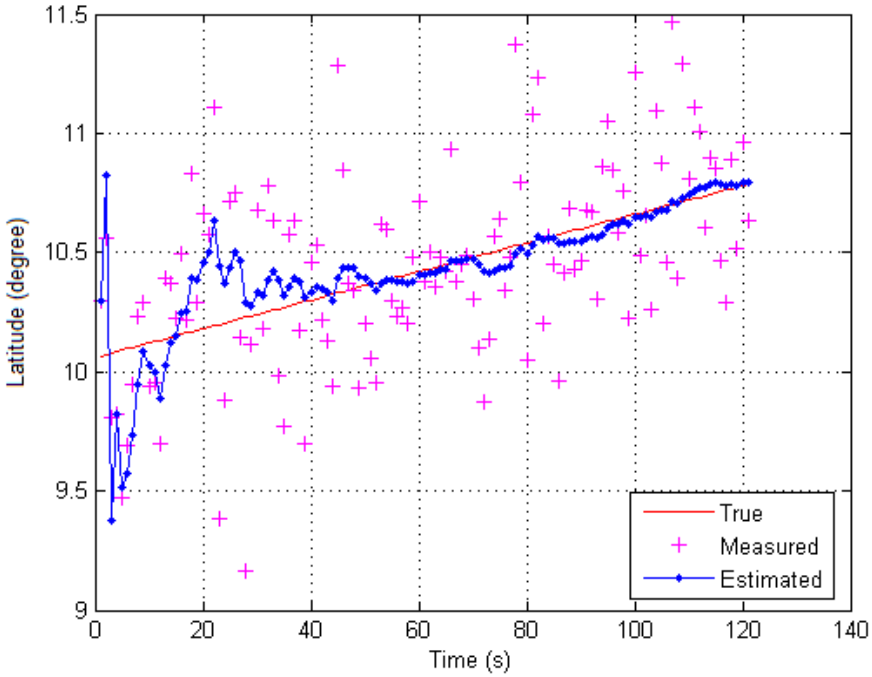

Fig. 6.3 True, measured and estimated positions plotted over time for one dimensional movement

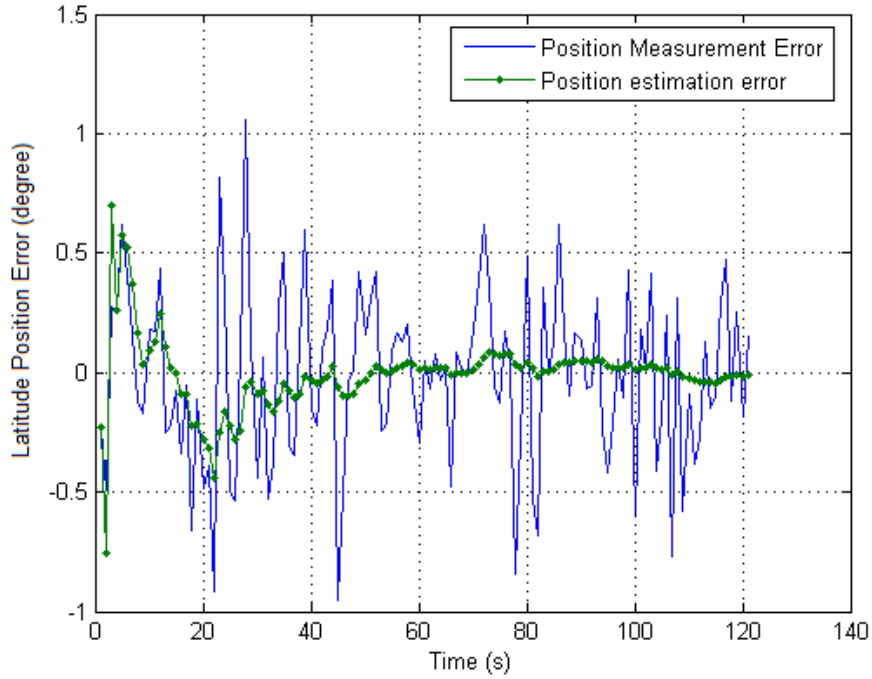

Fig. 6.4 The residual plot of measurement and estimation with respect to the true values

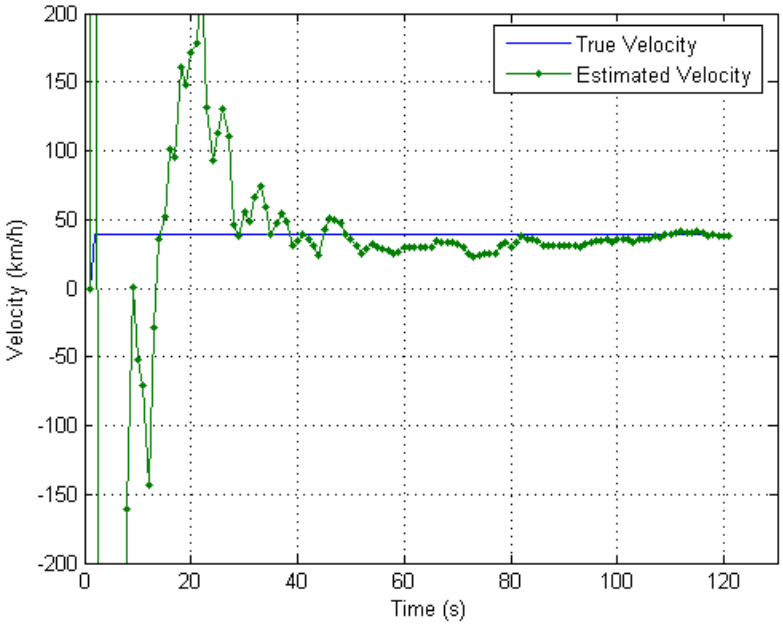

Fig. 6.5 Variation of estimated and true velocities with time

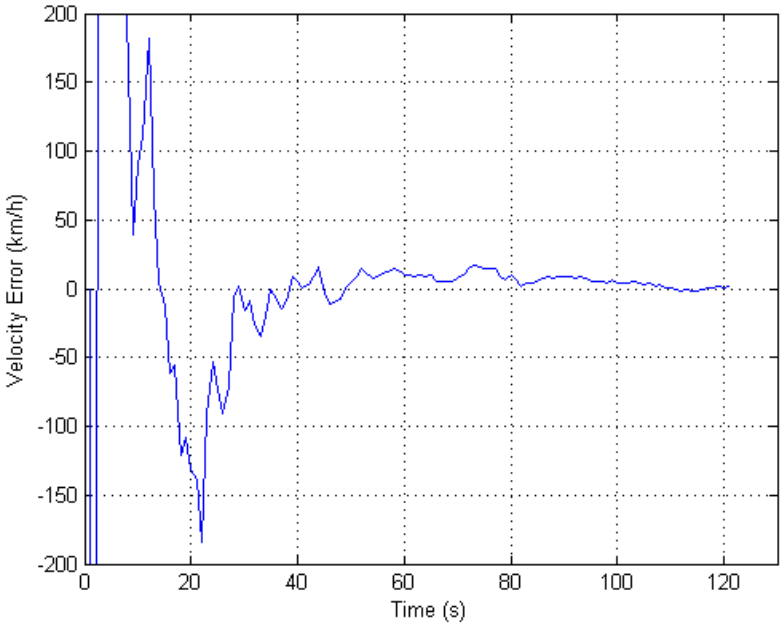

Fig. 6.6 Error variation between the true velocity and the Kalman filters estimated velocity

6.7.2 Tracking of a Target Moving in Two Dimensions

The analysis discussed clearly demonstrates that the Kalman filter is capable of making the predictions when the target moves in two dimensions, while other assumptions remain the same as that in the one dimensional scenario. The true, measured as well as the estimated positions of the target in x and y directions, together with the corresponding velocity variations are plotted in Fig. 6.7, Fig. 6.8, Fig. 6.9 and Fig. 6.10 respectively, typically depicting the features of Kalman filtering. The resultant readings reinforce the fact that the Kalman filter is a powerful approach and reduces the error considerably in both dimensions and also that the accuracy of the filter improves over time, as vivified in the 2D plot shown in Fig. 6.11.

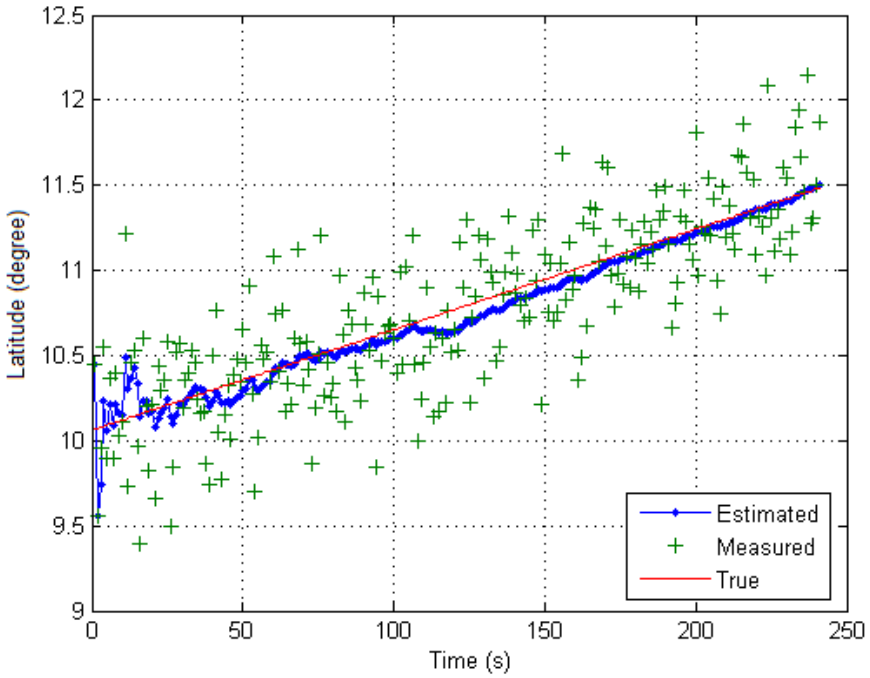

Fig. 6.7 True, measured and estimated positions of the target in x direction

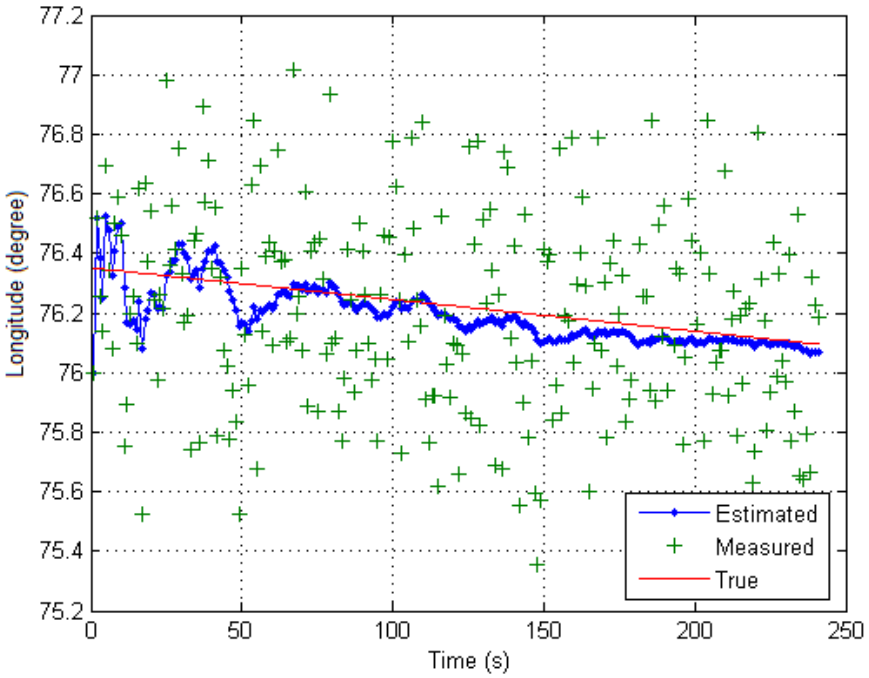

Fig. 6.8 True, measured and estimated positions of the target in y direction

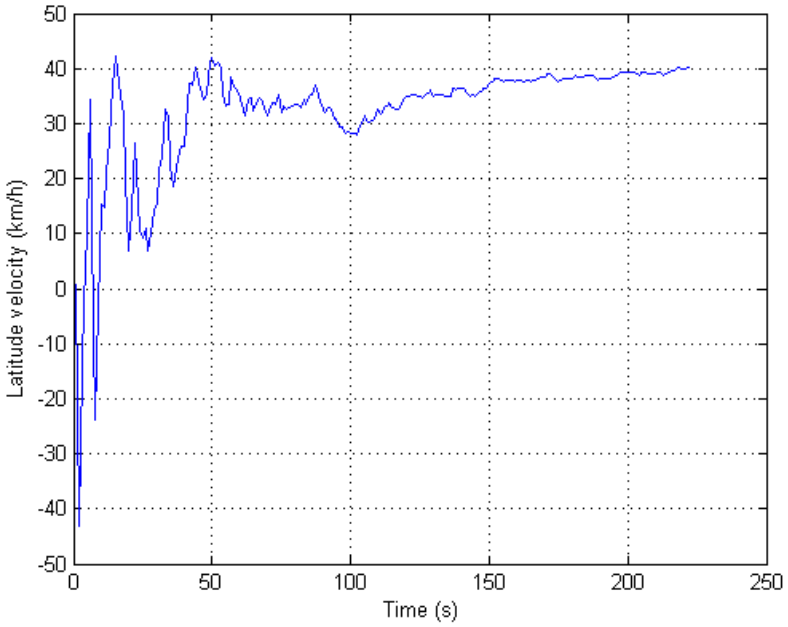

Fig. 6.9 Velocity variations in x direction

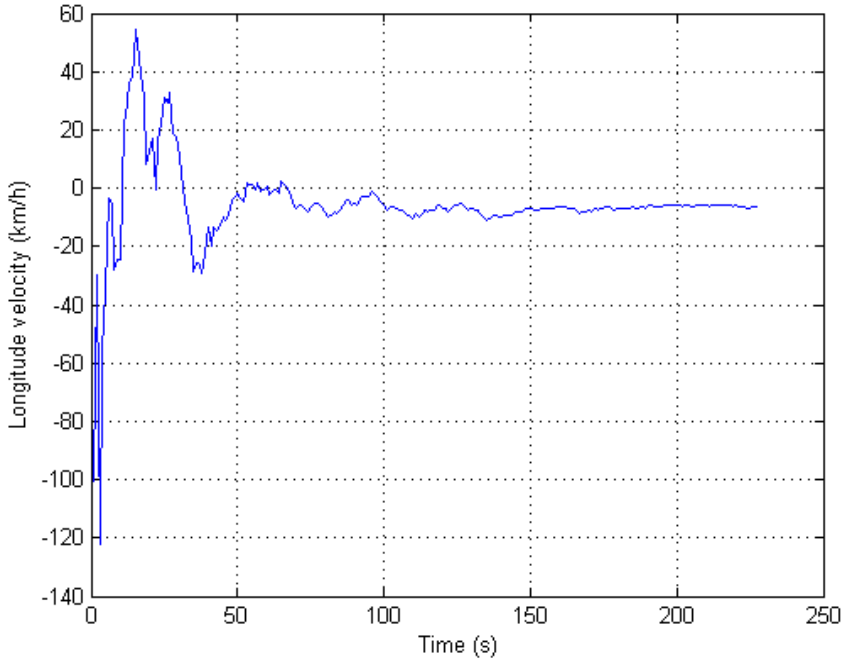

Fig. 6.10 Velocity variations in y direction

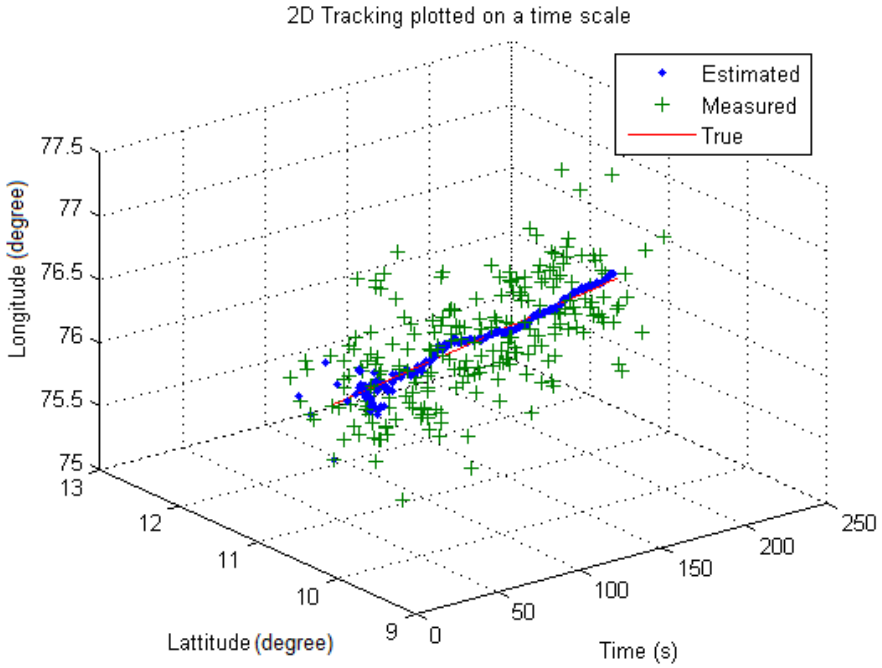

Fig. 6.11 Two dimensional tracking over time

6.7.3 Tracking of a Maneuvering Target

In this system model, the target is moving with nearly constant velocity in two dimensions and presumed to be abruptly changing its velocity or maneuvering twice. Maneuver of the target is detected by comparing the distance function with the threshold determined by the chi square probability distribution. Once the maneuver is detected, the Kalman filter parameters are reset and the filter is reinitialized using the previous measurements.

Algorithm for Tracking of a Maneuvering Target

START
LABEL : Obtain position measurements
Form state vector containing position and velocity
Implement KF tracking algorithm on the state vector
Compute the distance function
Select a threshold from the chi-distribution table
If threshold > distance, go to LABEL
Or else, Reset Kalman filter parameters
Reinitialize the filter from previous iterations
If surveillance active, go to LABEL
Or else, STOP

Fig. 6.12 shows the path of a Kalman tracker without using the corrective measures when it follows abrupt maneuvers. It can be seen that the Kalman filter is not able to track the target properly after the maneuver.

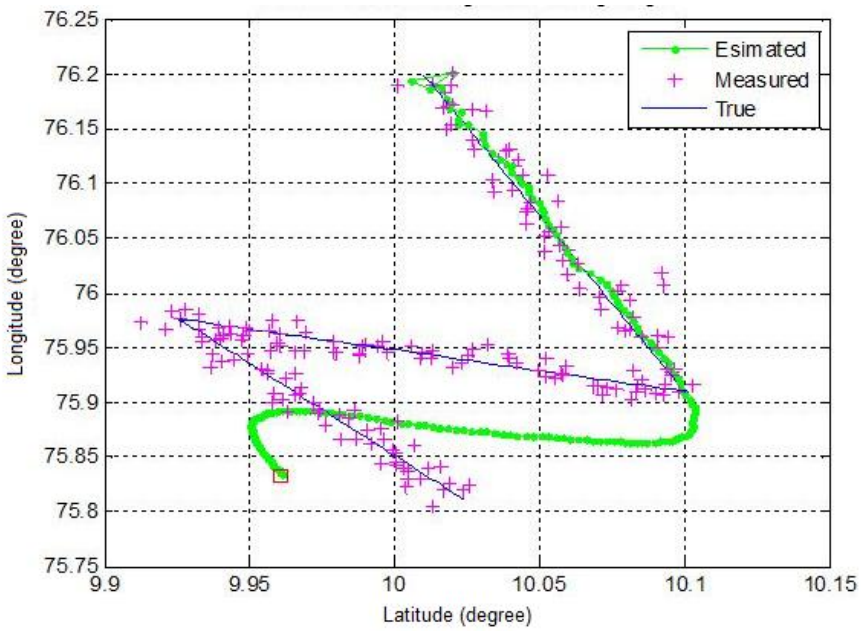

Fig. 6.12 Standard Kalman output without considering high maneuvering effects

As depicted in Fig. 6.13, the filter resets upon detecting a maneuver and thus it provides more accurate predictions over time. The position residual plot of the target maneuvering scenario depicted in Fig. 6.14 shows detection of the target maneuvers as graphical peaks at positions 62 and 123, which closely correlates with the simulated maneuvers at the positions 60 and 120 respectively.

The graphical user interface (GUI) developed for this target tracking scenario is shown in Fig. 6.15. While selecting one dimension or two dimension models, the corresponding measured values are loaded and the Kalman filter generates the corrected values.

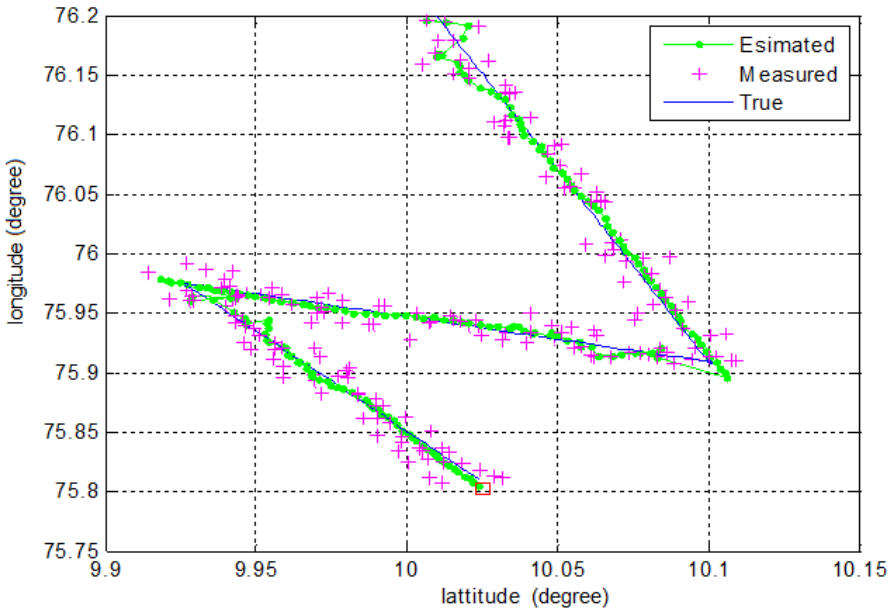

Fig. 6.13 True, measured and estimated positions of a maneuvering target

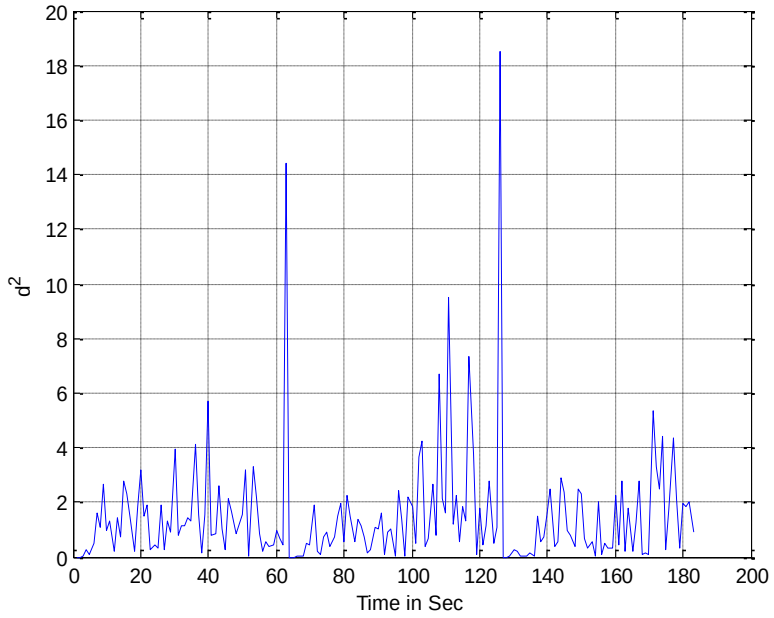

Fig. 6.14 Position residual graph showing the maneuvering points

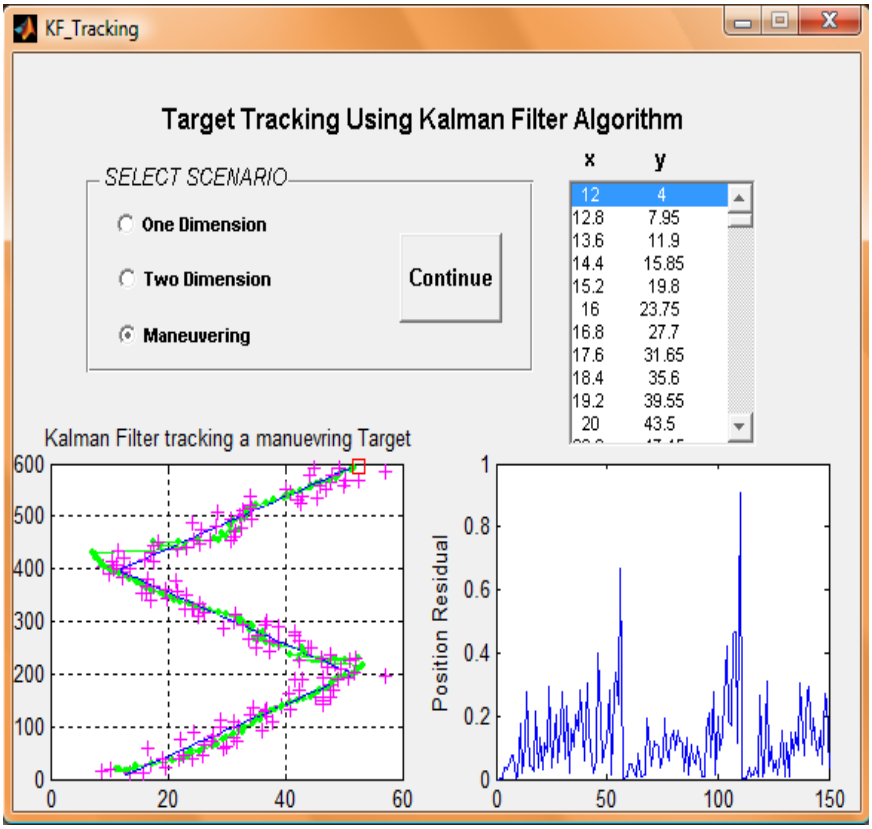

Fig. 6.15 Screen shot of the Graphic User Interface for Target Tracking

6.8 *Summary*

Kalman filter has been applied to the position estimates to improve the tracking results from the surveillance system. Various techniques that were implemented in the filter to circumvent the errors induced due to generic noises and the maneuvering of the target have been studied. Implementing Kalman filters to target tracking systems yield reliable results, given that the nature of the system can be modeled suitably. Applying such an adaptive filtering to a simulated one dimensional and two

dimensional system has yielded encouraging results, even when stochastic maneuvers were introduced on the target. Abrupt maneuver causes degradation in the performance of the results. The decision making approach based on measurement residuals using chi-square significance test is implemented and studied. This cure measure improves the tracking performance under highly maneuvering conditions [111, 112]. The system can be extended to three dimensions by appending desirable modifications in the system model.

CHAPTER 7

TARGET CLASSIFICATION

The proposed system, apart from performing the task of localization and tracking, also performs the task of target classification. The acoustic signals picked up by the buoy system may be of natural origin such as ice cracking, biological sources, thermal agitations, hydrodynamic sources, etc. or of manmade sources such as the ones from the ships, submarines, military operations, sonar, etc. The target specific features of the unknown target are compared with a set of archetypal features of a known pre-recorded data which have been previously generated and stored in a knowledge base, leading to the identification of the target. The various digital signal processing techniques used to extract the signature features, leading to the classification of the noise source are discussed in this Chapter. A Digital Signal processing module for the identification of noise sources in the ocean has also been implemented, with acceptable success rates. The system has been realized using a proprietary version of C language evolved for the digital signal processor TMS320C6713 development board. The feature vectors extracted for different sources were computed in MATLAB as well as in the DSP development board and the results were compared.

7.1 *Introduction*

Noise in the ocean is of utmost importance for ocean explorations, oceanographic as well as fisheries studies, sonar operations, etc. The wide range of systems for ocean research demands the need for characterizing the noise sources in the ocean. The ambient noise in the ocean is

composite in nature, comprising of components emanating from a variety of noise sources. The studies carried out on noise in the ocean reveal that its spectrum extends over the frequency range from a few Hz to about 100 kHz.

Ships, other surface crafts, submarines, torpedoes, etc. are excellent sources of underwater noise. They may have machineries of greater complexities, as they require numerous rotational and reciprocating machinery components for their propulsion, control and habitability. These machineries also generate vibrations, thus contributing their effect on to the underwater noise. Thus, the noise heard by a hydrophone operator contains a wide range of frequencies. These noises are very difficult to interpret into a pattern that will indicate the type of the vessel or its class, with the usual signal extraction methods. Moreover, some noises generated by a ship are intermittent in nature, typically the noise from the steering engine. Hence, in such situations, the tonal components present in the noise signals collected over a short period of time will be different from those taken for a long period. Scientists have been labouring hard for over five decades to develop electronic systems to understand and identify the noise sources in the ocean.

Spectral estimation techniques have been used as one of the vital signal processing tools for extracting valuable information about the signals as well as the noises, for many years. As the power spectrum is related to autocorrelation, it does not contain any information about the components higher than the second orders, whereas the higher order spectra contain certain information, not present in the power spectrum. Hence, power spectral estimation has limited applications in situations where the non-Gaussian noise has to be detected. Power spectral estimation techniques can be used for estimating the magnitude response of

the system. Estimates of bispectrum, which is the third order spectrum and bicoherence have been found useful in detecting nongaussianity and nonlinearity in system identification as well as detecting transient signals.

In order to interpret most effectively and efficiently the vast amount of data furnished by the signal processor, especially in situations where the detectable range of the system is very large, it is essential to have a fully automated and intelligent classifier, as most of the target information, in all probability, may not be of much interest to the user. Operator controlled classifier turns out to be inappropriate and highly inefficient in such situations. Automatic detection and classification algorithm attempts to alleviate this operability problem by taking over the operator's role of picking out targets from a background of noise and interferences.

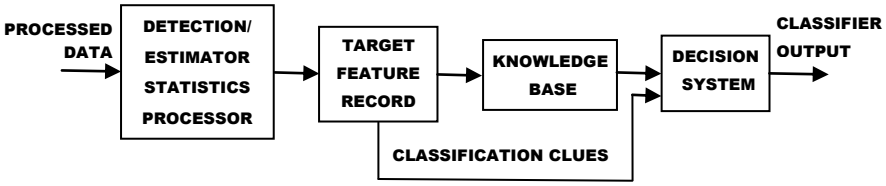

Fig. 7.1 Block Schematic of the Target Classifier

The generalized structure of the prototype target classifier is shown in Fig. 7.1. The output of the power spectral estimator is compared with the earlier detection/estimation decisions, which are stored in the target feature record and the relevant target feature are updated. In case, if a target feature is not updated over a significant period, the concerned feature will be dropped from the target feature record. In many situations, the system may have to backtrack or re-track through the stored features record to establish the links with the most recent features. As and when the required classification clues are available in the target feature record, the most

matching signature pattern is identified from the known target signatures in the knowledge base, depending on the allowable percentage of mismatch, chosen by the user.

In the signal processing module of the developed buoy system, the acoustic signals generated by target are captured by using a 20-element hydrophone array. The unique signature features of the target can be extracted from the captured acoustic signals using a 32-bit floating point DSP processor, TMS320C6713 [113, 114]. The features thus extracted can be used for comparing with those available in the knowledge base.

7.2 *Knowledge Base*

For the realisation of the target classifier, it is essential to have a powerful knowledge base comprising of the relevant parameters of different class and types of targets. The raw data collected has to be processed for gathering the relevant parameters for creating the knowledge base.

7.2.1 Noise Data

The noise data used for creating the knowledge base mainly comprises of the man made noises and noise that are of biological in nature. Some of the data sets used in developing the knowledge base were collected during scheduled cruises off Cochin and Mangalore.

7.2.1.1 **Man Made Noises**

Surfaced and submerged vessels create noise from their propellers, motors and gears. The noise generated by the motor is continuous and caused by the mini-explosions that occur, as the fuel burns rapidly inside the engine cylinders and by the rotating gears and shafts. Sound is also

generated due to the formation of bubbles during the rotation of propellers and, to a lesser extent, by the wake of waves produced due to the movement of the vessels. As the vessel moves and the propellers rotate, bubbles are formed in the water and the formation of these bubbles is known as cavitations**.** The breaking of these bubbles create a loud acoustic noise and is termed as cavitation noise which is directly related to the speed of the vessel. The faster the propeller rotates, the more will be the cavitation noise. The breaking bubbles produce noise over a range of frequencies, and at high speeds, these frequencies can be as high as 20,000 Hz. On the other extreme, a large ship with slowly turning propellers can generate very low frequencies to the extent of 10 Hz or even less. The rotation of the propellers creates bands of noise at more or less constant frequencies that are proportional to the rate of rotation of the propeller. The noise created by these rotations, called *blade-rate lines*, can help to distinguish between different sizes of ships and even a particular ship in certain cases. Low frequency noise generated by ships contributes significantly to the amount of low frequency ambient noise in the ocean, particularly in regions with heavy ship traffic. In fact, because of the increase in propeller-driven vessels, low frequency ambient noise has increased 10-15 dB during the past 50 years.

7.2.1.2 **Biological Noise Data**

A variety of biological noise data has been used for the purpose of creating the knowledge base. The beluga, a medium sized toothed whale, is amongst the loudest animals in the sea. They exhibit a wide range of vocalizations including clicks, squeaks, whistles and a bell-like clang. The sounds recorded are mostly in the range of 0.1 to 12 kHz. The humpback whale is best known for their vocalizations that are arranged in complex, repeating sequences with the characteristics of *song* and contain both tonal

and pulsed sounds. Some of the different types of the harbour seal calls are trill, chirp, multiple whistle, single whistle, growl, whoop, chug, and grunt. Sea robins are very noisy fishes and make sounds like grunting, growling and grumbling.

7.2.2 Data Analysis

For creating the knowledge base, the noise data waveforms of various targets are analysed following the procedures for extracting the spectral and bispectral features. The performance of the classifier depends on how extend and vast the knowledge base is. In the prototype system, all the available noise date waveforms were analyzed and a representative knowledge base has been developed. The knowledge base for the prototype classifier comprise of the spectral and bispectral features of different classes like ships, boats, marine mammals, environmental conditions, etc.

7.2.3 Updating of Knowledge Base

The knowledge base that has been developed for realizing the prototype target classifier is only representative and not complete in all respects. For making the system efficient, the knowledge base has to be updated with the signature patterns and the target dynamics for all the classes and types of targets.

7.3 *Extraction of Features*

The pre-processed noise data waveforms are analyzed in different ways in the Estimation Statistics Processor. The different techniques, like spectral analysis and bispectral estimation techniques, are used for extracting the various signatures of the targets are illustrated in Fig. 7.2.

The various features generated from this analysis are stored in a Target Feature Record (TFR), which is used for mapping the target signatures with the signatures available in the knowledge base. The generation of the target feature record as depicted in Fig. 7.3. plays an important role in the efficiency and success rate of the classifier.

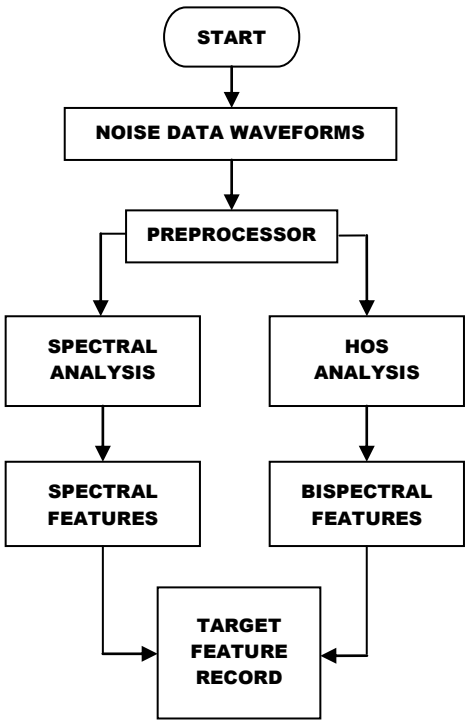

Fig. 7.2 Methods for extracting the target features

As such, when the noise data waveforms are made available to the classifier, it generates the target feature record by performing spectral estimation and bispectral estimation. The target feature records for various data records are generated. In case, if a TFR is not updated over a considerable period of time, the concerned feature record will be dropped and the system takes the average of all the TFRs which have close resemblances and thus generates the TFR.

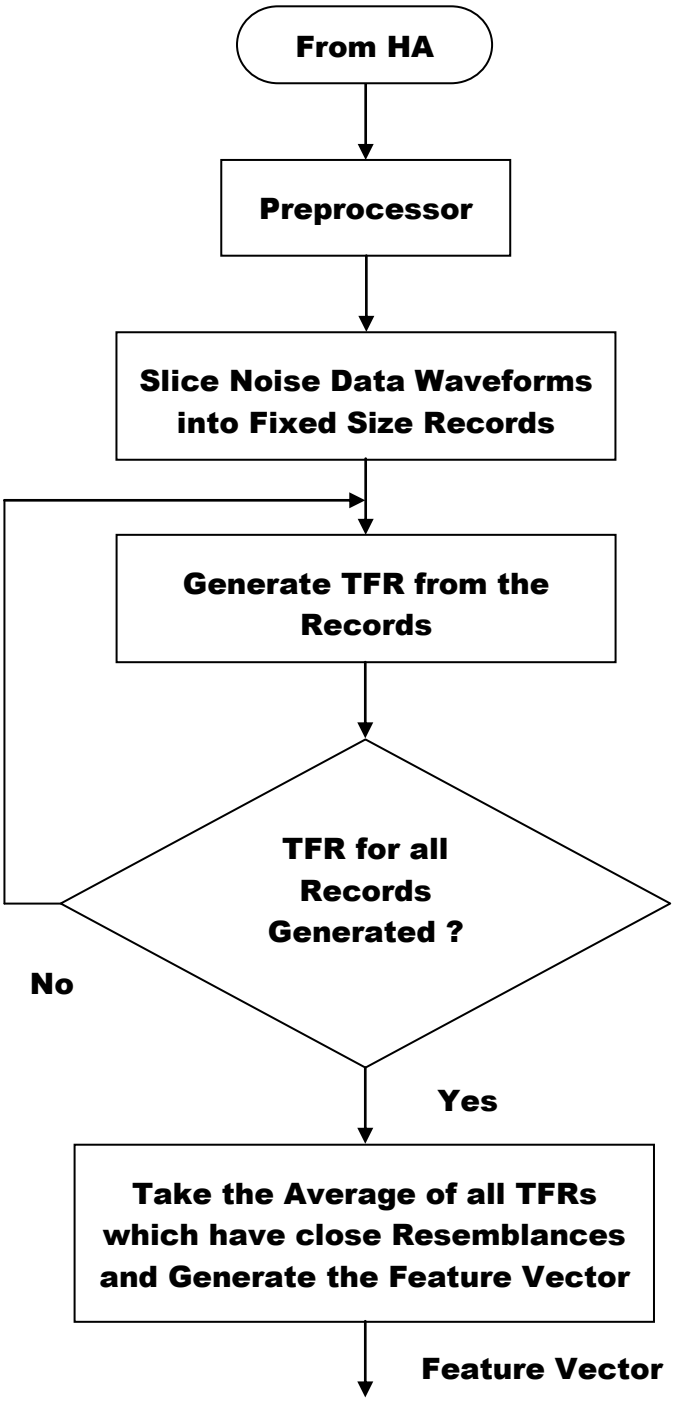

Fig. 7.3 Flowchart for generation of TFR

7.4 *Spectral Analysis*

Signal being analysed in frequency domain is known as spectral analysis. Spectral analysis methods can be classified as parametric and non-parametric methods based on the analysis of the signal in time domain. Non–parametric analysis require multiple periods for the particular spectral peak to appear whereas parametric analysis require the data segment to contain only single period to produce a pronounced peak. Non-parametric statistics have the advantage of being distribution independent as well as insensitive to extreme values or outliers. The disadvantages of non-parametric statistics are complexity, low power and time required for computation. Some of the non-parametric methods are Daniell Periodogram, Barlett Periodogram and Welch Periodogram. In contrast, parametric statistics are simple and easy to compute but rely upon the assumption of a "Gaussian" distribution. Parametric statistics are known to be generally robust even when the assumption of Gaussian distribution is violated. Widely used parametric approaches are Auto Regressive (AR) process, Moving Average process (MA) and ARMA process.

The major noise sources emanated from the targets are from propellers and propulsion or from other machinery of the targets, which can produce significant noise at low frequencies but little noise at high frequencies greater than 5 kHz, where wind and wave-generated noise dominates the spectrum of oceanic noise. In addition, higher frequency noise is strongly attenuated in seawater. Moreover, as the noise signals from the target are non-linear, intermittent and of short duration, parametric methods of spectral analysis are more appropriate and precise.

Though frequency analysis using Fourier methods, DFT or the computationally efficient FFT with periodogram methods are commonly

used, there are numerous disadvantages with these non – parametric methods as compared to parametric methods. Parametric methods give smoother spectrums than non-parametric methods although the latter using digital windowing techniques can smoothen the spectrum to some extent; they distort the true spectrum due to side lobe leakages. Parametric methods give better frequency resolution while avoiding picket fencing and scalloping loss faced by non – parametric methods. The latter consist of harmonic amplitude and phase components regularly spaced in frequency intervals. The spacing of the spectral lines depends on the number of data samples decreasing with number of data. Therefore, it is unable to estimate accurately the frequency component of the signal in between two adjacent harmonic frequency components. This problem is better known as picket fencing effects. This results in scalloping loss which attenuates the signal mid-way between the harmonically related frequency components.

Thus, more accurate power spectral density of the noise signal emanated from the target can be estimated using parametric spectral methods. Though several spectral estimation techniques have been evolved using parametric spectral methods, in an attempt to improve the spectral fidelity and resolutions, the power spectral density estimation using the autoregressive (AR) approach has been adopted here, for analyzing the spectral components in the noise waveforms, leading to the extraction of certain classification clues.

7.4.1 Spectral Features

Spectral features of an acoustic signal are unique in their characteristics and so they can be called as spectral signatures as they explicitly prove the identity of the signal. Therefore, the nature or class of the noise emanating from the target can be identified by extracting its

spectral features. The features are calculated after estimating the power spectral density of the signal using parametric spectral methods. Spectral features are extracted using power spectral statistics and higher order statistics [115-122].

7.4.2 Power Spectral Statistics

The power spectrum is the primary tool of signal processing and algorithms for estimating the power spectrum have found applications in areas such as radar, sonar, seismic, biomedical, communications and speech signal processing. The usefulness of the power spectrum arises from an important theorem known as Wold's decomposition theorem, which states that any discrete-time stationary random process can be expressed in the form,

$$x(n) = y(n) + z(n)$$

such that :

- Processes *y(n)* and *z(n)* are uncorrelated with one another
- Process *y(n)* has causal linear process representation,

$$y(n) = \sum_{k=0}^{\infty} h(k)u(n-k)$$

where, *h(0)=1*, $\sum_{k=0}^{\infty} h^2(k)$ <: and *u(n)* is a white–noise process; and

- *z(n)* is singular, that is, it can be predicted perfectly (with zero variance) from its past.

According to Wiener – Khintchine theorem, power spectrum, *Pxx(f)* of a stationary process, *x(n)* is defined as the Fourier transform of the autocorrelation sequence of the process.

$$P_{XX}(f) = \sum_{m=-\infty}^{\infty} R_{XX}(m) \exp(-j2\pi fm)$$

where, $Rxx(m) = E\,[x^*(m)\,x(n+m)]$ is the autocorrelation sequence of $x(n)$.

A sufficient, but not necessary, condition for the existence of the power spectrum is that the autocorrelation be absolutely summable. The power spectrum is real valued and non-negative, ie., $P_{xx}(f) >= 0$; if $x(n)$ is real valued, then the power spectrum is also symmetric, ie., $P_{xx}(f) = P_{xx}(-f)$.

7.4.3 Features using Power Spectral Statistics

Spectral features extracted using power spectral statistics are as follows:

- ❖ Spectral Centroid (Brightness)
- ❖ Spectral Range (Bandwidth)
- ❖ Spectral Roll off
- ❖ Spectral Slope
- ❖ Characteristic Frequencies
- ❖ Audio spectrum centroid
- ❖ Audio spectrum spread
- ❖ Spectral Flatness

7.4.3.1 **Brightness**

Brightness or spectral centroid is the amplitude-weighted average, or centroid, of the frequency spectrum, which can be related to a human perception of brightness. It is calculated by multiplying the value of each frequency by its magnitude in the spectrum and thereby summing them. The resultant is then normalised by dividing it by the sum of all the magnitudes [89, 115].

$$brightness = \left[\frac{(\sum mag\,[i] \times freq\,[i])}{\sum mag\,[i]}\right] \qquad (7.1)$$

i=0… frame size/2, where, *mag* = the magnitude spectrum.

freq = the frequency corresponding to each magnitude element.

e.g.: Brightness of engine.wav = 2824.5 Hz

7.4.3.2 **Bandwidth**

Bandwidth or spectral range is an amplitude weighted average of the differences between each frequency magnitude and the brightness, i.e. a representation of the range of frequencies that are present in a certain frame. It is computed by subtracting the mean value (in this case the brightness) from each data value:

$$bandwidth = \left[\frac{(\sum mag\ [i] \times freq\ [i] - brig\ htness\ )}{\sum mag\ [i]}\right] \qquad (7.2)$$

i = 0…..frame size/2.

where, *mag* = the magnitude spectrum.

freq = the frequency corresponding to each magnitude element.

e.g. Bandwidth of engine.wav = 1334 Hz

7.4.3.3 **Spectral Roll off**

Spectral Roll off is a measure of spectral shape, which could be used instead of bandwidth. It is defined as the frequency below which 85% of the magnitude distribution is concentrated. i.e.

MIN(R) such that,

$$\sum_{i=1}^{R} mag[i] \geq 0.85 \times \sum_{i=1}^{N} mag[i] \qquad (7.3)$$

where, *N* is the length of the signal.

e.g. Spectral Roll off of engine.wav = 4694 Hz

7.4.3.4 **Audio Spectrum Centroid (ASC)**

Audio spectrum centroid features a logarithmic frequency scaling centered at 1 kHz,

$$ASC_r = \frac{\sum_{K=1}^{N/2} log_2(f[k]/1000)P_r[k]}{\sum_{K=1}^{N/2} P_r[k]} \quad (7.4)$$

where, *Pr* is the power spectrum of the frame *r*.

e.g. Audio spectrum centroid of engine.wav = -5.02

7.4.3.5 **Audio Spectrum Spread (ASS)**

It describes concentration of the spectrum around the centroid and is defined as

$$ASS_r = \sqrt{\frac{\sum_{K=1}^{N/2}[log_2(f[k]/1000) - ASC_r]^2 P_r[k]}{\sum_{K=1}^{N/2} P_r[k]}} \quad (7.5)$$

Lower spread values would mean that the spectrum is highly concentrated near the centroid and higher values mean that it is distributed across a wider range at both sides of the centroid.

e.g. Audio spectrum spread of engine.wav = 0.737

7.4.3.6 **Audio Spectrum Flatness (ASF)**

It can be defined as the deviation of the spectral form from that of a flat spectrum. Flat spectra correspond to noise or impulse-like signals hence high flatness values indicate noisiness. Low flatness values generally indicate the presence of harmonic components. The flatness of a band is defined as the ratio of the geometric and the arithmetic means of the power spectrum coefficients within that band.

$$Flatness = \frac{\sqrt[N]{\prod_{n=0}^{N-1} x(n)}}{\left(\frac{\sum_{n=0}^{N-1} x(n)}{N}\right)} \quad (7.6)$$

e.g. Audio spectrum flatness of engine.wav = 0.21

7.4.3.7 **Spectral Slope**

It refers to the average slope of the power spectral density variation.

e.g. Spectral slope of engine.wav = -41.39.

7.4.3.8 **Peaking Frequencies**

Peaking frequencies will help in identifying the tonal as well as continuous frequency components.

e.g. One of the prominent peaking frequencies of engine.wav = 5117.3 Hz.

7.5 *Bispectral Statistics*

There is much more information in a stochastic non-Gaussian or deterministic signal than is conveyed by its autocorrelation or power spectrum. Higher order spectra which are defined in terms of higher order moments or cumulants of a signal contain this additional information [123-126].

In power spectrum estimation, the process under consideration is treated as a superposition of statistically uncorrelated harmonic components and the distribution of power among these frequency components is then estimated. As such, only linear mechanisms governing the process are investigated since phase relations between frequency components are suppressed. The information contained in the power spectrum is essentially that which is present in the autocorrelation sequence; this would suffice for the complete statistical description of a Gaussian process of known mean. However, there are practical situations

where we would have to look beyond the power spectrum (autocorrelation) to obtain information regarding deviations from Gaussianness and presence of nonlinearities. Higher order spectra (also known as polyspectra), defined in terms of higher order cumulants of the process, do contain such information. Particular cases of higher order spectra are the third order spectrum also called the bispectrum which is, by definition, the Fourier transform of the third order cumulant sequence and the trispectrum (fourth order spectrum) which is the Fourier transform of the fourth order cumulant sequence of a stationary random process. The power spectrum is, in fact, a member of the class of higher order spectra, i.e., it is a second order spectrum.

The general motivation behind the use of higher order spectra in signal processing is threefold:

(i) To extract information due to deviations from Gaussianness (normality)

(ii) To estimate the phase of non-Gaussian parametric signals, and

(iii)To detect and characterize the nonlinear properties of mechanisms which generate time series via phase relations of their harmonic components.

The first motivation is based on the property that for Gaussian processes, all polyspectra of order greater than two are identically zero. Thus, a non-zero higher order spectrum indicates deviation from normality. For a given zero-mean stationary real random process $\{Xn\}$; non-zero skewness, $E[X_n^3] \neq 0$ indicates the existence of its bispectrum where, E [.] is the expectation operation. Hence, in those signal processing settings where the signal is a non-Gaussian stationary process and the additive

noise process is stationary Gaussian, there might be certain advantages estimating signal parameters in higher order spectrum domains. The non-Gaussianess condition is satisfied in many practical applications, since any periodic or quasi-periodic signal can be regarded as a non-Gaussian signal and self emitting signals from complicated mechanical systems can also be considered as non-Gaussian signals.

The second motivation is based on the fact that higher order spectra preserve the phase information of non-Gaussian parametric signals. For modelling time series data in signal processing, least squares estimation is almost exclusively used because it yields maximum-likelihood estimates of the parameters of Gaussian processes and also because the equations obtained are usually in a linear form involving autocorrelation samples or their estimates. However, the autocorrelation domain suppresses phase information and therefore least squares techniques (or modelling autocorrelation methods) are incapable of representing non-minimum phase parametric processes. An accurate phase reconstruction in the autocorrelation (or power spectrum) domain can only be achieved if the parametric process is indeed minimum phase. Non-minimum phase estimation is of primary importance in deconvolution problems that arise in geophysics, telecommunications, etc., in which the wavelet shape must have the correct phase character.

One approach to the deconvolution problem that has emerged recently explores the use of higher order spectra to estimate the phase of the wavelet due to the ability of polyspectra to preserve non-minimum phase information. Assuming that the reflectivity series (input sequence) is non-Gaussian white with zero-mean, a mixed-phase wavelet can be reconstructed in the bispectrum domain if the input sequence has non-zero skewness, or in the trispectrum domain if the fourth-order cumulant

sequence is different from zero. Moreover, if the reflectivity series is Gaussian, no procedure can recover the actual shape of a non-minimum phase wavelet.

Finally, introduction of higher order spectra (HOS) is quite natural when we try to analyze the nonlinearity of a system operating under random input. General relations for arbitrary stationary random data passing through arbitrary linear systems have been studied quite extensively for many years. In principle, most of these relations are based on power spectrum (or autocorrelation) matching criteria. On the other hand, general relations are not available for arbitrary stationary random data passing through arbitrary nonlinear systems. Instead, each type of nonlinearity has to be investigated as a special case. HOS could play a key role in detecting and characterizing the type of nonlinearity in a system from its output data. Consider a linear time invariant (LTI) system as shown in Fig**.** 7.4 with input,

$$X_k = \sum_m A_m \exp j(\omega_m k + \phi_m),$$

where $\{\phi(m)\}$ are independent, identically distributed random variables.

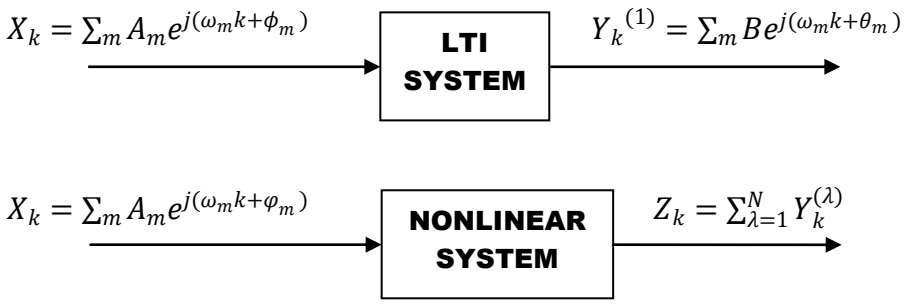

Fig. 7.4 Output of a Linear Time Invariant system and a nonlinear system to a sinusoidal input

Then the output of the LTI system, $Y_k^{(1)}$ is given by

$$Y_k^{(1)} = \sum_m B_m \, exp\, j(\omega_m k + \theta_m) \tag{7.7}$$

It can easily be verified that all higher order cumulants of $\{Y_k^{(1)}\}$of order greater than two are identically zero. Therefore, zero HOS of $\{Y_k^{(1)}\}$ will indicate that only linear mechanisms generate the output time series.

The output of the Nonlinear system is given by

$$Z_k = \sum_{\lambda=1}^{N} Y_k^{(\lambda)} \tag{7.8}$$

where $\{Y_k^{(1)}\}$ is given by (7.7) and

$$Y_k^{(2)} = \sum_m \sum_n C_m C_n exp\, j[(\omega_m + \omega_n)k + (\theta_m + \theta_n)] \tag{7.9}$$

A nonzero bispectrum, given by (7.9), will indicate the existence of the term, $\left\{Y_k^{(2)}\right\}$, and therefore, the presence of a quadratic nonlinearity in the system.

7.5.1 Cumulants and Higher Order Spectra

Higher order spectra are defined in terms of cumulants and therefore are called cumulant spectra. Given a set of n real random variables $\{x_1, x_2, \ldots, x_n\}$, their joint cumulants of order, $r = k_1 + k_2 + \ldots + k_n$ are defined as

$$c_{k_1 \ldots k_n} \triangleq (-j)^r \left. \frac{\partial^r ln\Phi(\omega_1, \omega_2, \ldots\ldots, \omega_n)}{\partial\omega^{k_1} \partial\omega^{k_2} \ldots\ldots\ldots \partial\omega^{k_n}} \right|_{\omega_1 = \omega_2 = \cdots = \omega_n = 0} \tag{7.10}$$

where, $\Phi(\omega_1, \omega_2, \ldots, \omega_n) = E[\exp\ j(\omega_1 x_1 + \ldots + \omega_n x_n)]$ is their joint characteristic function. The joint moments of order r of the same set of random variables are given by

$$m_{k_1 \ldots . k_n} \triangleq E\left[x_1^{k_1} x_2^{k_2} \ldots \ldots . x_n^{k_n}\right]$$

$$= (-j)^r \left. \frac{\partial^r \Phi(\omega_1, \omega_2, \ldots\ldots, \omega_n)}{\partial \omega^{k_1} \ldots\ldots\ldots \partial \omega^{k_n}} \right|_{\omega_1 = \ldots = \omega_n = 0} \qquad (7.11)$$

Hence, the joint cumulants can be expressed in terms of the joint moments of the random variables. For example, if $m_{1\ldots0} = E[X_1] = 0$, then

$$\begin{aligned} c_{1\ldots0} &= 0 \\ c_{2\ldots0} &= m_{2\ldots0} = E[X_1^2] \\ c_{3\ldots0} &= m_{3\ldots0} = E[X_1^3] \\ c_{4\ldots0} &= m_{4\ldots0} - 3c_{2\ldots0}^2 \\ &= E[X_1^4] - 3m_{2\ldots0}^2 \end{aligned} \qquad (7.12)$$

By taking $\{X(k)\}$, $k = 0, \pm1, \pm2, \ldots$ to be a real stationary random process with zero mean, $E[X(k)] = 0$**,** then the moment sequences of the process are related to its cumulants as follows:

$$\begin{aligned} &E[X(k)\, X(k+\tau_1)] = m_2(\tau_1) \\ &\quad = c_2(\tau_1) \qquad \text{(autocorrelation sequence)} \\ &E[X(k)\, X(k+\tau_1)\, X(k+\tau_2)] = m_3(\tau_1, \tau_2) \\ &\quad = c_3(\tau_1, \tau_2) \qquad \text{(third order moment or cumulant sequence)} \\ &E[X(k)\, X(k+\tau_1)\, X(k+\tau_2)\, X(k+\tau_3)] = m_4(\tau_1, \tau_2, \tau_3) \qquad (7.13) \\ &\quad = c_4(\tau_1, \tau_2, \tau_3) + c_2(\tau_1) \cdot c_2(\tau_3 - \tau_2) + c_2(\tau_2) \cdot c_2(\tau_3 - \tau_1) + c_2(\tau_3) \\ &\qquad \cdot c_2(\tau_2 - \tau_1) \text{ (fourth order moment sequence)} \end{aligned}$$

While the third order moments and third order cumulants are identical, this is not true for the fourth order statistics. In order to generate the fourth order cumulant sequence, we need knowledge of the fourth order moment and autocorrelation sequences.

7.5.2 Properties of Bispectrum

Let {*X(k)*} be a real, discrete, zero-mean stationary process with power spectrum *P(ω)*, defined as

$$P(\omega) = \sum_{\tau=-\infty}^{+\infty} r(\tau) exp\ -j(\omega\tau), \quad |\omega| < \pi \tag{7.14}$$

where,

$$r(\tau) = E[X(k)X(k+\tau)] \tag{7.15}$$

is its autocorrelation sequence. If *R(m, n)* denotes the third moment sequence of {*X(k)*}, i.e.;

$$R(m,n) = E[X(k)X(k+m)X(k+n)] \tag{7.16}$$

then its bispectrum is defined as

$$B(\omega_{1,}\omega_2) = \sum_{m=-\infty}^{+\infty} \sum_{n=-\infty}^{+\infty} R(m,n) \exp -j(\omega_1 m + \omega_2 n) \tag{7.17}$$

Since the third order moments and cumulants are identical, the bispectrum is a third order cumulant spectrum. From (7.16), it follows that the third order moments obey the symmetry properties such as,

R(m,n) = R(n,m) = R(-n,m-n) = R(n-m,-m) = R(m-n,-n) = R(-m,n-m)

As a consequence, knowing the third moments in any one of the six sectors, shown in Fig. 7.5 and Fig. 7.6, would enable us to find the entire third moment sequence.

❖ Gaussian Processes: If $\{X(k)\}$ is a stationary zero-mean Gaussian process, its third-moment sequence $R(m, n) = 0$ for all (m, n) and therefore its bispectrum $B(\omega_1, \omega_2)$ is identically zero.

❖ Linear Phase Shifts: Given $\{X(k)\}$with power spectrum $P_x(\omega)$ and bispectrum $B_x(\omega_1, \omega_2)$**,** the process, $Y(k) = X(k - N)$, where N is a constant integer, has power spectrum $P_y(\omega) = P_x(\omega)$ and bispectrum $B_y(\omega_1, \omega_2) = B_x(\omega_1, \omega_2)$ i.e., the second and third order moments suppress linear phase information. However, while the power spectrum (autocorrelation) suppresses all phase information, the bispectrum (third-moment sequence) does not.

❖ Non-Gaussian White Noise: If $\{W(k)\}$ is a stationary non-Gaussian process with $E[W(k)] = 0$, $E[W(k)\ W(k + \tau)] = Q.\delta(\tau)$ and $E[W(k)\ W(k + \tau)\ W(k + \rho)] = \beta.\delta(\tau, \rho)$**,** its power spectrum and bispectrum are both flat, i.e., $P(\omega) = Q$ and $B(\omega_1, \omega_2) = \beta$.

❖ Quadratic Phase Coupling: There are situations in practice where because of interaction between two harmonic components of a process, there is contribution to the power at their sum and/or difference frequencies. Such a phenomenon, which could be due to quadratic nonlinearities, gives rise to certain phase relations called quadratic phase coupling. In certain applications, it is necessary to find out, if peaks at harmonically related positions in the power spectrum are, in fact, coupled. The power spectrum suppresses all phase relations. The bispectrum, however, is capable of detecting and quantifying phase coupling.

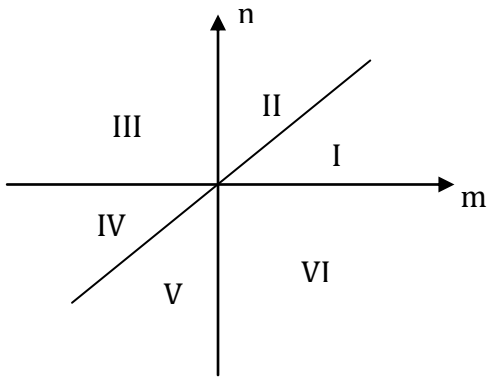

Fig. 7.5 Symmetry regions of third order moments

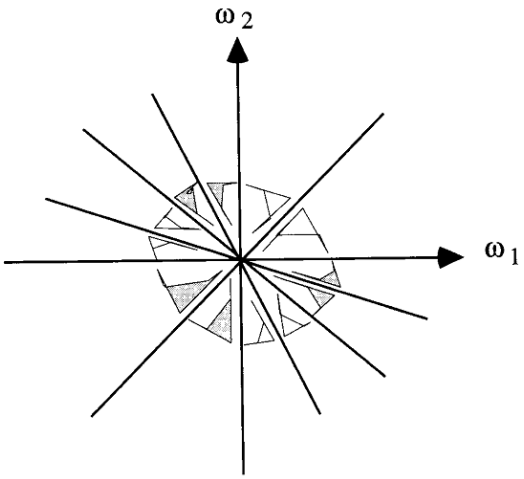

Fig. 7.6 Symmetry regions of the Bispectrum

With bispectral analysis, it has been evidenced that ship generated noise contain strong nonlinear components in its noise generating mechanisms, whereas the ambient noise does not. The bispectral analysis has the advantage that it is capable of distinguishing these nonlinear components in the noise generating mechanism. This leads us to some procedures for differentiating between shipping noise and ambient noise. Moreover, this procedure can also be used for differentiating various classes or types of ships.

Hence, the bispectral analysis can be used to extract the information for analyzing the ship radiated noise, on the existence of such noise sources that would normally be hidden in the ambient noise, when the spectral estimation approaches are carried out.

7.6 *DSP based Feature Extraction*

The omni-directional hydrophone element keeps monitoring for any acoustic disturbances near the deployed buoy system until the power of the captured acoustic signal reaches above a predefined threshold level. Once the threshold level is reached, the signal processing unit of the buoy electronics get triggered for extraction of features which can be used for identification of targets.

The signature features are extracted from the acoustic signals captured by the hydrophone array. The signal conditioning and feature extraction is performed using a 32 bit, DSP development board. The analog acoustic signals from the hydrophone array are fed into an AIC23 stereo CODEC for sampling and A/D conversion. The sampled digital output of the audio signals is stored as wave file for further signal analysis and processing. The acoustic signals from hydrophone array after preprocessing are analyzed in the Feature Extraction Unit which is implemented using a DSP development board manufactured by Texas Instruments. It consists of a higher end DSP Processor TMS320C6713 which is adequate for precision audio applications, Audio Codec, SDRAM, and FLASH memory. The board is compact, inexpensive, fast in operations, and works on 3.3 V supply.

The acoustic signal captured by the hydrophone array, after preliminary processing is sampled and digitized by the audio codec. The

digital signal is then read by the processor using one of the Multichannel Buffered Serial Ports (McBSPs). The data is then transferred to the internal L2 memory through the Enhanced Direct Memory Access (EDMA) channel. Double-Buffering is used to buffer the incoming data. When one of the buffers is full an interrupt is generated to process the data received. At the same time, the CODEC keeps sampling and saves data into the other buffer. So data sampling and processing can be done simultaneously and no incoming signals are missed even if the DSP is processing previously received data. Feature extraction and signal conditioning is done on the received signal. The digital signal is then send to RF Link for transmission through the serial port. The Flowchart depicting the algorithm for feature extraction is shown in Fig. 7.7.

7.6.1 Architecture of TMS320C6713

The TMS320C6713 DSP processor is a 32-bit floating point processor developed by Texas Instruments. Its key features are:

- Operating frequency is 225 MHz
- An AIC23 stereo codec for coding and decoding the audio signals
- 16 Mbytes of synchronous DRAM
- 512 Kbytes of non-volatile Flash memory
  (256 Kbytes usable in default configuration)
- 4 user accessible LEDs and DIP switches
- Software board configuration through registers implemented in CPLD
- Configurable boot options
- Standard expansion connectors for daughter card use
- JTAG emulation through onboard JTAG emulator with USB host interface or external emulator

❖ Single voltage power supply (+5V)

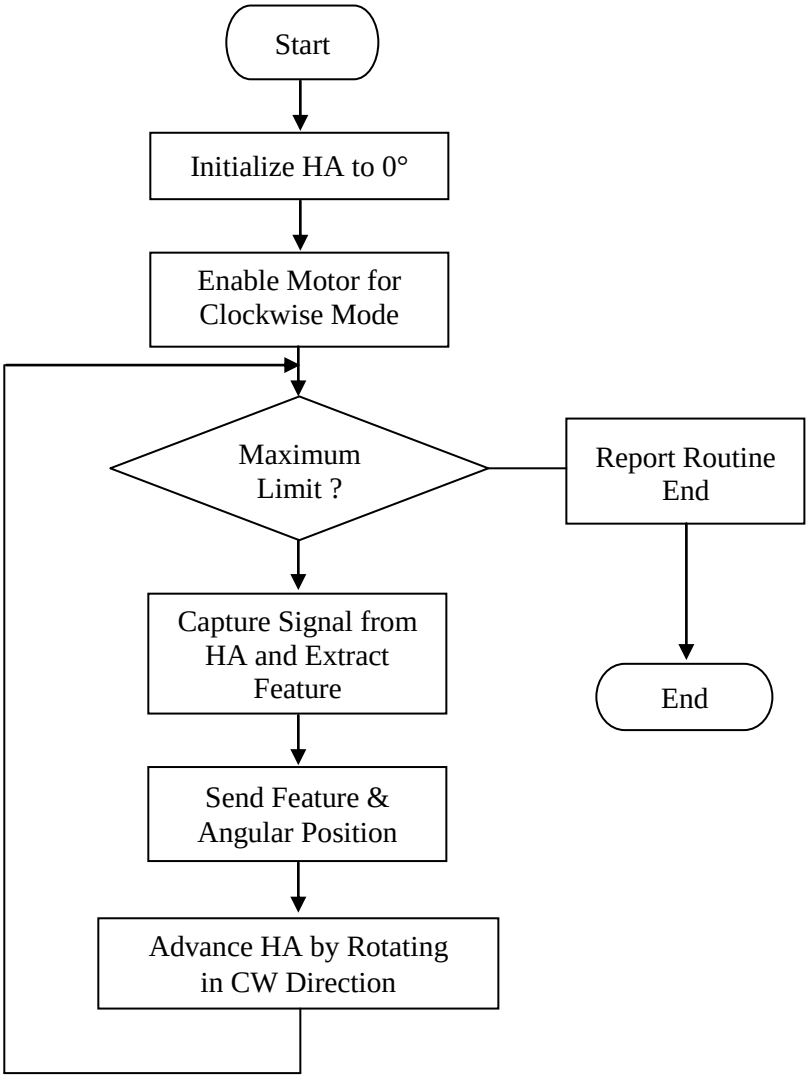

Fig. 7.7 Flowchart depicting the algorithm for feature extraction

The platform used for programming and communicating with the processor is Code Composer Studio (CCS) through an embedded JTAG emulator via USB interface or through an external emulator via JTAG connector. The block diagram of the DSK is shown in Fig. 7.8.

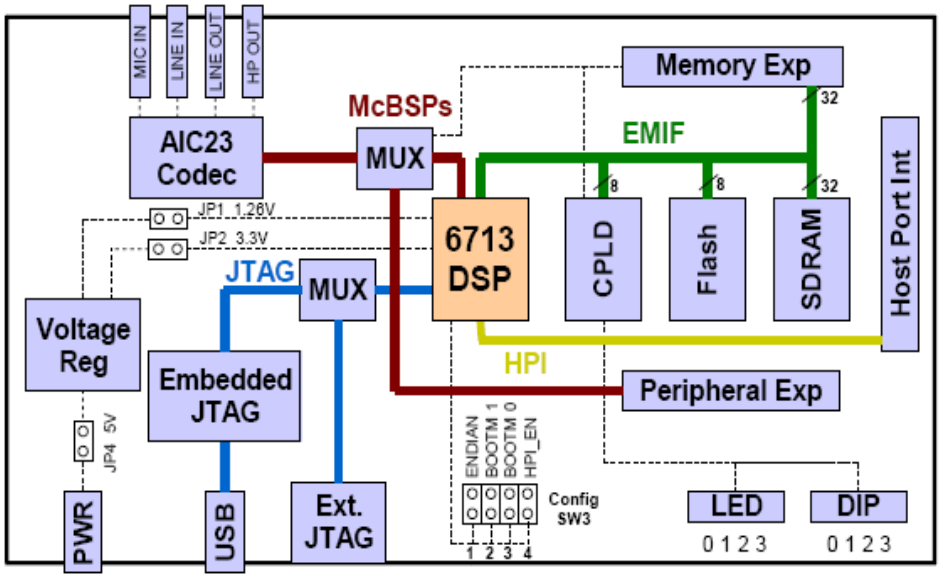

Fig. 7.8 Block Diagram of TI TMS320C6713 DSK

7.6.1.1 **Memory Map**

The C67xx family of DSPs has a large byte addressable address space. Program code and data can be placed anywhere in the unified address space. Addresses are always 32-bits wide. The memory map shows the address space of a generic 6713 processor on the left with specific details of how each region is used on the right. By default, the internal memory locates at the beginning of the address space. Portions of the internal memory can be reconfigured in software as L2 cache rather than fixed RAM. The EMIF has 4 separate addressable regions called chip enable spaces (CE0-CE3). The SDRAM occupies CE0 while the Flash and CPLD share CE1, CE2 and CE3 are generally reserved for daughter cards. The memory mapping is shown in Fig. 7.9.

7.6.1.2 **CPLD (Programmable Logic)**

The C6713 DSK uses an Altera EPM3128TC100-10 Complex Programmable Logic Device (CPLD) device to implement:

- 4 Memory-mapped control/status registers that allow software control of various board features.
- Control of the daughter card interface and signals.
- Assorted "glue" logic that ties the board components together.

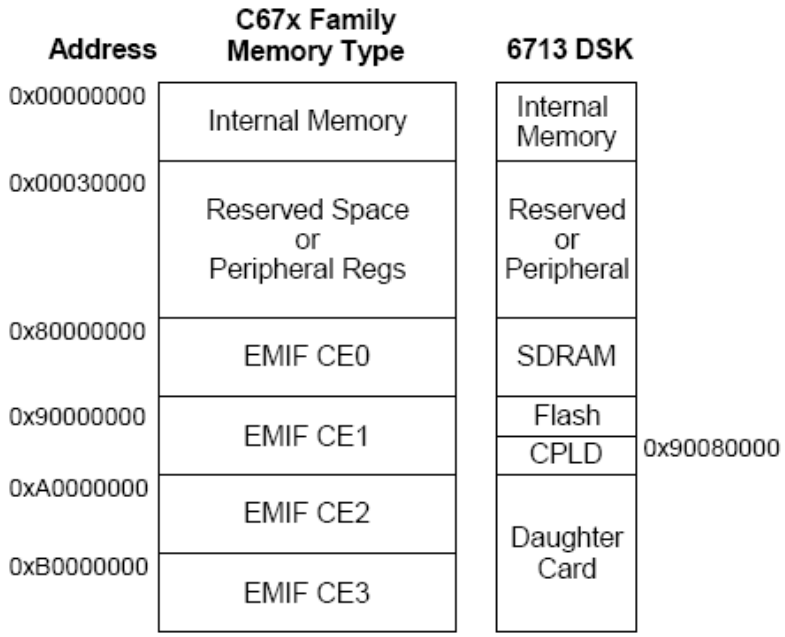

Fig. 7.9 Memory Mapping in TMS320C6713 DSK

7.6.1.3 **AIC23 Codec**

The DSK uses a Texas Instruments AIC23 (part #TLV320AIC23) stereo codec for input and output of audio signals. The codec samples analog signals on the microphone or line inputs and converts them into digital data so that it can be processed by the DSP. When the DSP is finished with the data it uses, the codec convert the samples back into analog signals on the line and the headphone outputs the signals so that the user can hear the output. The codec communicates using two serial channels, one to control the codec's internal configuration registers and one

to send and receive digital audio samples. The schematic of AIC23 codec is shown in Fig. 7.10.

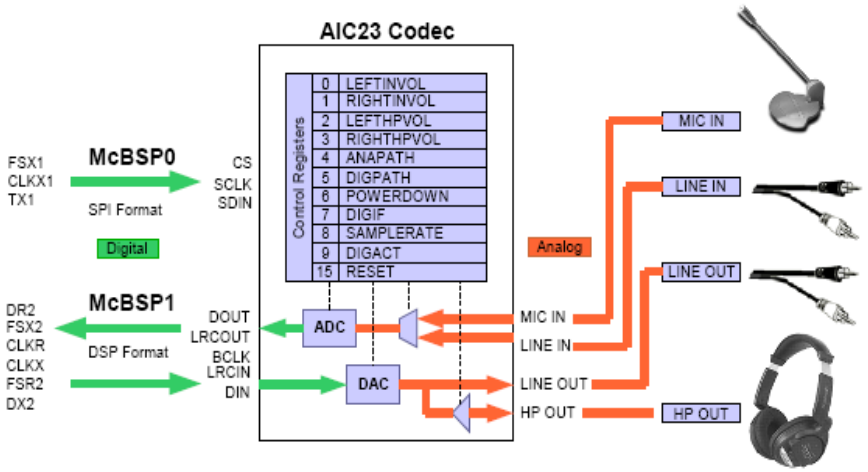

Fig. 7.10 Schematic of AIC23 CODEC

McBSP0 is used as the unidirectional control channel. It should be programmed to send a 16-bit control word to the AIC23 in SPI format. The top 7 bits of the control word should specify the register to be modified and the lower 9 should contain the register value. The control channel is only used when configuring the codec, it is generally idle when audio data is being transmitted, McBSP1 is used as the bi-directional data channel. All audio data flows through the data channel. Many data formats are supported based on the three variables, sample width, clock signal source and serial data format. The DSK examples generally use a 16-bit sample width with the codec in master mode, so it generates the frame sync and bit clocks at the correct sample rate without effort on the DSP side. The preferred serial format is DSP mode which is designed specifically to operate with the McBSP ports on TI DSPs. The codec has a 12MHz system clock. The 12MHz system clock corresponds to USB sample rate mode and can use the same clock for both the codec and USB controller.

7.6.1.4 **Synchronous DRAM**

The DSK uses a 128 megabit synchronous DRAM (SDRAM) on the 32-bit EMIF. The SDRAM is mapped at the beginning of CE0 (address 0x80000000) with a total available memory of 16 megabytes. The integrated SDRAM controller is a part of the EMIF and must be configured in software for proper operation. The EMIF clock is derived from the PLL settings and should be configured in software at 90MHz. This number is based on an internal PLL clock of 450MHz required to achieve 225 MHz operation with a divisor of 2 and a 90MHz EMIF clock with a divisor of 5. When using SDRAM, the controller must be set up to refresh one row of the memory array every 15.6 microseconds to maintain data integrity. With a 90MHz EMIF clock, the period is 1400 bus cycles.

7.6.1.5 **Flash Memory**

Flash is a type of memory which does not lose its contents when the power is turned off. When read, it looks like a simple asynchronous read only memory (ROM). Flash can be erased in large blocks commonly referred to as sectors or pages. Once a block has been erased each word can be programmed once through a special command sequence. After that, the entire block must be erased again to change the contents. The DSK uses a 512Kbyte external Flash as a boot option. It is visible at the beginning of CE1 (address 0x90000000). The Flash is wired as a 256K by 16 bit device to support the DSK's 16-bit boot option. However, the software that ships with the DSK treats the Flash as an 8-bit device (ignoring the top 8 bits) to match the 6713's default 8-bit boot mode. In this configuration, only 256Kbytes are readily usable without software changes.

7.6.1.6 **LEDs and DIP Switches**

The DSK includes 4 software accessible LEDs (D7-D10) and DIP switches (SW1) that provide the user a simple form of input/output. Both are accessed through the CPLD USER_REG register.

7.7 *Prototype Target Classifier*

The omni-directional hydrophone element keeps monitoring the acoustic disturbances near the deployed buoy system until the power of the captured noise signal reaches above a predefined threshold level. Once the threshold level is reached, the signal processing unit of the Buoy electronics gets triggered and generates the ALERT signal. The analog signals captured by the hydrophone array are coded to the required file format using the AIC23 CODEC of the TMS320C6713 DSK. This file can be used for further signal analysis and processing.

The classification function operates in a multidimensional space formed by the various components of the feature vector. For the purpose of target classification, one has to identify the characteristic features from the representation of an object. Upon generating the various features, those features that can indeed aid in the process of classification are selected. Though, such a selection will generally lead to loss of information, this will reduce the noise generated by the irrelevant features as well as the risk of over fitting the training data, thus making the classifier computationally efficient.

The signature features are used to generate the required classification clues towards the identification of the noise sources in the ocean. The function of classification is carried out by performing the template matching process, in which the various components of the feature

vector generated are mapped with the corresponding components of the feature vector available in the knowledge base.

7.7.1 Feature Vector based classifier

7.7.1.1 Euclidean Distance Model

Euclidean distance model is one of the simple yet efficient classifier algorithms and a properly weighted model, making use of the feature vector, could be used to find out the nearest match [127]. The weights for the various components of the feature vector have been selected based on heuristics, the knowledge gained from the training examples as well as trial and error procedures. For the purpose of feature vector based classification, the Euclidean distance between the feature vectors of the unknown target and that of the various targets in the knowledge base is computed. The vector components are normalized by standard deviation or the range of the features, across the whole knowledge base. Further to normalization, each feature is weighted in proportion to its significance in the similarity estimation.

The Euclidean distance D_E is computed as

$$D_E = \sqrt{\sum_{i=1}^{l}\left(\frac{(x_i - y_i)\times w_i}{v_i}\right)^2} \tag{7.18}$$

where x_i and y_i refers to the i^{th} feature component of the unknown target and that of the various targets in the knowledge base respectively, w_i is the weight assigned to the i^{th} feature component such that,

$$\sum_{i=1}^{l} w_i = 1,$$

v_i represents the normalization vector and l is the total number of features.

7.8 *Results and Discussions*

A feature extraction unit has been developed on the TMS320C6713 DSP development board, for extracting the characteristic features of the target. This hardware has been designed in such a way that it can handover the extracted features to the communications controller through the DSP interface provided in the Hydrophone Array Controller. The flowchart for the code for spectral feature extraction is shown in Fig. 7.11.

The signature features of the captured signals by the hydrophone arrays are extracted using MATLAB and TMS320C6713 DSK. Codes were written in 'C' language and were compiled and run on TMS320C6713 DSP processor using Code Composer Studio. The algorithms used in both the platforms were similar and the performance of the module for extracting the features and identifying the targets has been validated to a satisfactory level of repeatability and reproducibility.

The spectral features that are generated by the DSP module and MATLAB are compared with those available in the knowledge base. Features extracted for 3 targets using MATLAB and DSP processor are given in Table 7.1, Table 7.2 and Table 7.3.

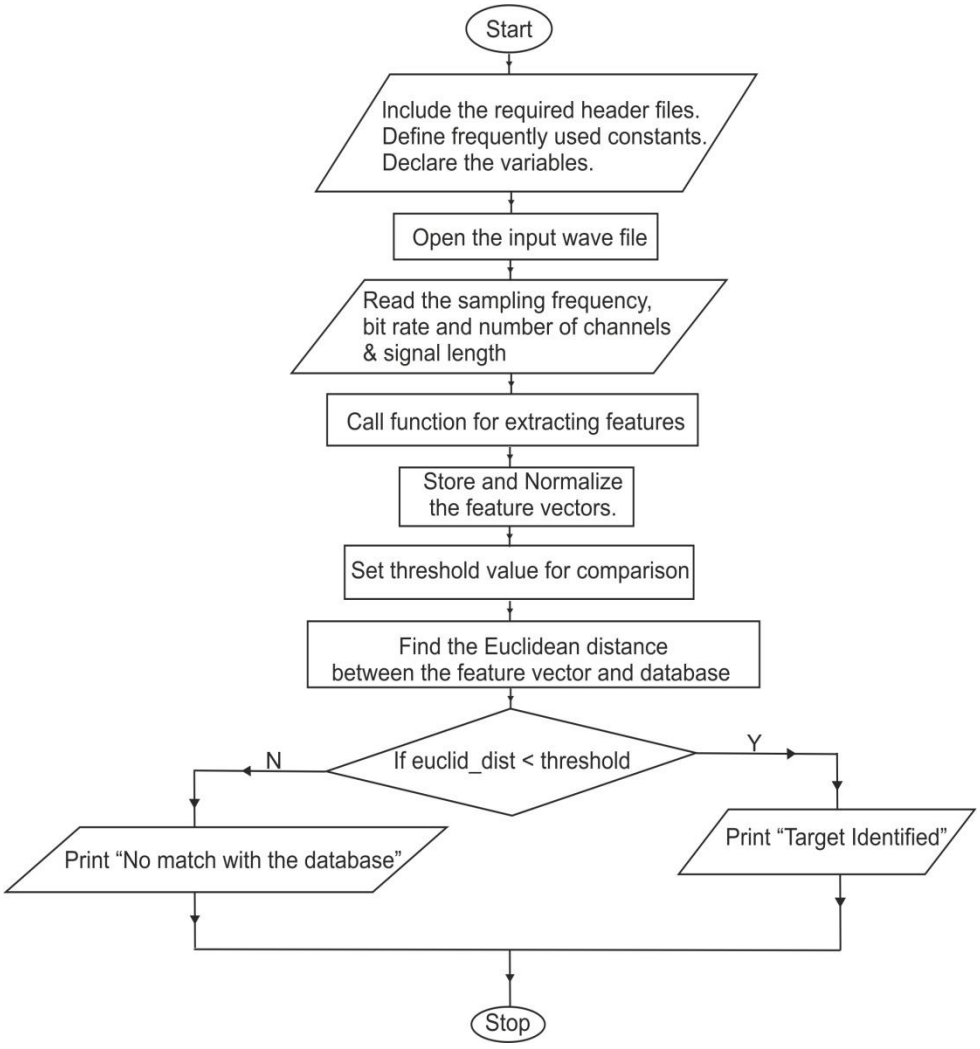

Fig. 7.11 Flowchart for extracting spectral features

Table 7.1 Spectral Features extracted using MATLAB and TMS320C6713 DSP Board for Engine noise

Spectral Features extracted using MATLAB and TMS320C6713 DSP processor			
Input (Wave File)	Feature	Output	
		MATLAB	TMS320C6713
Engine.wav	Sampling Frequency	11008	11008
	Spectral centroid	-5.02	-5.9
	Spectral Spread	0.737	1.9
	Bandwidth	1334	1355
	Brightness	2824.5	2830
	Spectral slope	-41.39	-45
	Spectral Roll off	4694	4700
	Spectral Flatness	0.21	0.5
	Prominent Peaking Frequencies	2913.1	2920.7
		3197.6	3200.3
		3448.1	3452.5
		3735.7	3738.4
		4035.1	4040.2
		4269.7	4270
		4549.2	4552
		4813.8	4815.7
		5117.3	5119
		5385.8	5385.8

Data Length = 110080

Table 7.2 Spectral Features extracted using MATLAB and TMS320C6713 DSP Board for Ship noise

Input (Wave File)	Feature	Output	
		MATLAB	TMS320C6713
Ship.wav	Sampling Frequency	22050	22050
	Spectral centroid	-4.19	-5.6
	Spectral Spread	0.39	0.6
	Bandwidth	2343	2343
	Brightness	7273	7252
	Spectral slope	-56.6	-59
	Spectral Roll off	10196	10200
	Spectral Flatness	0.13709	0.34
	Prominent Peaking Frequencies	2537.6	2542.5
		3339.5	3344.4
		4719.2	4722
		5401.1	5409
		6728.9	6732.8
		7502.7	7510
		8224.6	8234.6
		8784.5	8790
		9466.4	9472
		10234	10244

Data Length = 151806

Table 7.3 Spectral Features extracted using MATLAB and TMS320C6713 DSP Board for Boat noise

Input (Wave File)	Feature	Output	
		MATLAB	TMS320C6713
Boat.wav	Sampling Frequency	11025	11025
	Spectral centroid	-4.5	-5.1
	Spectral Spread	0.26	0.5
	Bandwidth	1103	1113
	Brightness	3693	3670
	Spectral slope	-160.5	-165
	Spectral Roll off	5027.2	5035
	Spectral Flatness	0.00016	0.00021
	Prominent Peaking Frequencies	224	230
		605	610.5
		1121	1127
		1709	1715.2
		3602	3610
		3963	3957
		4285	4277
		4269	4265
		4946	4950
		5237	5242

Data Length = 89856

7.9 *Summary*

A prototype underwater target classifier system based on the digital signal processor hardware has been developed for classifying the noise sources in the ocean using signature features extracted from the noise emanations. The various steps involved in the generation of feature vectors have been described in this chapter. The TMS320C6713 has been used for extracting the features and to handing over it to the communications controller through the DSP interface provided in the Hydrophone Array Controller. The performance of the module for extracting the features and identifying the targets has been validated to a satisfactory level of repeatability and reproducibility. The signal capturing, processing, feature extraction and target identification are subject to a real time constraint and these can be easily done using the DSP module. The knowledge base requires frequent updating for improving the success rates of the classifier.

CHAPTER 8

CONCLUSIONS

This chapter brings out the salient highlights of the activities undertaken for realizing the autonomous three buoy system for underwater target localization, tracking and classification along with an enlisting of the further scope and directions for future research in this area. The acoustic emanations from the noisy targets sampled by the hydrophone arrays at three spatially and non-collinearly distributed locations in the ocean are analyzed for position fixing and classification of the target. Kalman filter approach has been used for refining the estimates, leading to the precise localization and tracking. Corrective measures have been implemented in the algorithm for tackling the maneuvering target situations. The prototype buoy system for establishing the technique has been validated during the field trials in a Reservoir in Kulamavu, Idukki and the validation results were quite encouraging.

8.1 *Salient Highlights of the Work*

This thesis envisages the realization of an automated system, with the help of which underwater targets can be localized, tracked and classified using passive listening buoy systems and target classification techniques. The acoustic emanations from the noisy targets sampled by the hydrophone arrays at three spatially and non-collinearly distributed locations in the ocean are analyzed for decision making.

The following are the salient highlights of the activities carried out during the design, development and deployment of the prototype

underwater target localization, tracking and classification system.

8.1.1 Design and Fabrication of the Buoy

A new design making use of the concept of Small Water plane Area Buoy (SWAB) has been formulated. To facilitate the localization, tracking and classification of underwater targets, submerged hydrophone arrays should be deployed with suitable buoy systems. As the buoy needs specialized requirements for this application involving the steering of the submerged hydrophones supporting from the gear assembly, a specialized structural buoy design formulated, conforming to the concept of minimizing the water plane area, so that the disturbances of the buoy experience, is brought to the minimum.

8.1.2 Hydrophone Array Controller

For the purpose of establishing the technique proposed to be adopted in the thesis, the acoustic emanations from the noisy targets are to be sampled by the hydrophone arrays at three spatially and non-collinearly distributed locations in the ocean. The directions of arrival as sensed by the three hydrophone arrays are to be estimated by mechanically steering the arrays. An array steering mechanism centred on a hydrophone array controller has been designed and developed for estimating the direction of arrivals.

8.1.3 Preprocessing Module

A preprocessing module capable of sampling and converting the signals from the analog domain to the digital for further filtering and processing using a higher order IIR filter has been realized. The preprocessing module is capable of handling the noise waveforms captured from the real ocean scenario.

8.1.4 Communication Controller

The Communication controller of the buoy system, which is vital for establishing the communication between the shore station and the buoys as well as between the buoys have been developed. The communications controller transfers data using data packets in a predefined format under the control of the main system control. Since the whole system is powered by solar energy, power consumption of the communications controller should be minimal and power management is critical. The RF link has been realized using the XBee-Pro RF modules. These modules host various characteristics adaptable and compatible to the existing buoy design.

8.1.5 Simulation of Target Localization

Geometrical reconstruction procedures have been used for positioning and localizing the target with the known values of the position of the buoys furnished by the GPS modules integrated with the buoy electronics and the bearing of the target as sensed by the hydrophone arrays. Three different approaches, considering the mathematical technique and software used, have been adopted for simulating the localization of the targets. The first method adopted is an implementation of the Haversine formula for triangulation, carried out in AutoLISP. Localization using the Haversine formula for great circle distance and different triangulation techniques were also carried out in MATLAB. The equation considers the curvature of the earth and corrects the resulting positions accordingly. The Vincenty formula for ellipsoids is efficient for computation of values based on latitude and longitude, and hence for the proposed system, as GPS readings of the buoys can be directly applied to the equations. The equations can be solved for localization in direct and

inverse forms, which are implemented in the simulation after basic conversion of angles.

8.1.6 Power Management Controller

As the buoy system works entirely on solar power and for carefully planning the consumption of power through efficient power management techniques, a power management controller has been developed. The controlling part of the power management controller is a low power microcontroller, which drives two separate power supply sections and manages the charging of the batteries from the solar power. The low battery conditions are divided into two, depending on the criticality of the battery levels. The power manager cuts off the power for surveillance operations at the first critical battery level, while providing the power to continue communications, and cuts off the rest of the system from draining power, if the battery level is too low.

8.1.7 Field Trials for DOA Estimation

The buoy electronics was assembled on the shore and was tugged to the point of deployment by fastening it to a floating platform. The basic functionality of the buoy, like array rotation, RF communication link and mechanical setup were tested prior to its deployment. Pre-recorded waveforms and real noises of the barge and boat were used to verify the functioning of the direction of maximum signal arrival estimator. The array exhibited certain bearable back lobes.

8.1.8 Field Trials for Localization

The field trials leading to the localization were conducted by mooring three buoys in the reservoir at predetermined locations and by fixing the position of the noisy target. Trials were carried out by using pre-

recorded noise waveforms and also using the idling barge engine noise. The performance of the system was evaluated for localizing the target.

8.1.9 Improving Localization Estimates

A method for improving the accuracy of the localization and tracking estimates of an unknown target using Kalman filter approach has been attempted. As the hydrophone arrays are mechanically steerable, the recoiling effect, caused due to the movement of the array from one position to another, the instabilities of the buoy system caused by the surface waves, etc. will lead to unpredictable errors in the estimates of the direction of arrival of the noise waveforms in each of the hydrophone arrays. These inaccuracies are resolved, to a certain extent, by applying the concepts of Kalman filter, making use of which the refinement of the localization estimates are carried out by reducing the mean square error.

8.1.10 Target Tracking

Implementing Kalman filters to target tracking systems yield reliable results, given that the nature of the system can be modeled suitably. Applying such an adaptive filtering to a simulated one dimensional and two dimensional system has yielded encouraging results. Abrupt maneuver causes degradation in the performance of the tracking estimates. The decision based approach based on measurement residuals using chi-square significance test is implemented and studied. This rectification improves the tracking performance under highly maneuvering conditions.

8.1.11 Target Classifier

A prototype system for classifying the underwater targets using the signature features extracted from the noise emissions has been developed.

The process of feature extraction involves obtaining target specific characteristics through various signal processing techniques, so that they can be used for the purpose of classification. Though signal analysis can be carried out even in the time domain, most of the target specific signatures are extracted from the frequency domain representation and its variants. The system has been realized using a proprietary version of C language evolved for the digital signal processor TMS320C6713 development board. The feature vectors for different noise sources were computed in MATLAB as well as in the development board and the results were compared and summarised.

8.2 *Scope for Future Work*

The work presented in this thesis has a significant role to play in ocean surveillance applications. This work also has subsequent scope for further research for improving the overall performance of the system. Some of the possible areas of future work are enlisted below.

8.2.1 Refinement of the Buoy Electronics

The buoy electronics designed for the preliminary trials were developed mostly as individual modules for ease in testing and debugging. Integration of these subsystem modules is also proposed to be carried out in the future work. The layout of the design needs to be refined for consolidating the functions of the buoy electronics units.

8.2.2 The CDMA Link

The buoy system currently works on a Zigbee RF link, which is a single channel addressable link with a line of sight range of 1.5 km. This link is a good choice for an experimental setup, but impedimental in many

ways for the real scenario. Even during the trials, the RF link required a perfect line of sight positioning. The module also cannot communicate well when more than one device is used, unless the communication is well timed. Hence, a better RF link preferably, a CDMA link is proposed to be used in the future. The CDMA system can provide multiple independent channels to buoys for communication and is highly secure.

8.2.3 Improving Target Tracking

Target tracking schemes, considering one dimensional and two dimensional movements including maneuvering situations have been implemented which can be further extended to three dimensional movements by appending desirable modifications in the system model. The abrupt maneuvering of a target, which is supposed to be moving with a constant velocity is considered in this thesis. An effort for widening this work can be made in the future for getting more reliable results.

8.2.4 Collection of Noise Data

The shore station system is the nerve centre of this surveillance system. It should have a vast knowledge base containing the features of a variety of targets. This knowledge base needs to be augmented with more features as and when new noise data waveforms are encountered. For augmenting the knowledge base of the shore station, noise data needs to be collected and analyzed quite frequently.

8.2.5 Bispectral Features

For many signals, which are generated from nonlinear processes, second order statistical methods are not sufficient for analysis. Many of the naturally occurring signals deviate from Gaussianity and linearity. Hitherto, such signals were considered Gaussian or near Gaussian signals and the

analysis were carried out, which has resulted in loss of valuable information. For these reasons, higher order statistical methods have to be developed, which can handle non-Gaussian as well as non-linear signals. Phase information is not available in the second order measures such as the power spectrum and autocorrelation. Different types of nonlinearities results in different types of phase couplings. If a signal composed of two sinusoids is passed through a non linear system, then the output will contain components at the sum and difference frequencies as well. The procedures for generating the bispectrally extractable features have to be developed and integrated with the existing feature extracting techniques.

8.2.6 Interfacing of Classifier to HAC

The Buoy system and the technique of localization has been established successfully for identifying the noise sources in the ocean, making use of the features extracted from the target emanations. The feature extractor was implemented in a Texas Instruments' DSP board. This board needs to be interfaced with the Hydrophone Array Controller.

8.3 *Summary*

An attempt has been made in this chapter to bring out the salient highlights of the work carried out for developing an autonomous three buoy system for underwater target localization, tracking and classification. An effort has also been made to enlist the scope and directions for future work in this area.

Appendix I

A.1 *Design and Fabrication of the Buoy*

Detailed description on the design and fabrication of the Buoys are given here. The photograph of the Buoy is shown in Fig. A.1.

Fig. A.1 Photograph of the Buoy

A.1.1 Sizing of the Floats and Struts

The diameters of the floats and struts are initially estimated so as to provide the required buoyancy, which should equal the total weight of the buoy for equilibrium. The diameters and thicknesses of floats and struts are optimized to achieve the design objectives, subject

to the constraints of buoyancy and stability. A simple optimization process was adopted by programming an Excel spreadsheet, wherein for a given buoy configuration, different dimensions and scantlings can be checked out by trial and error and an optimum solution subject to the stability constraint can be arrived at. The final configuration and structural assembly are furnished in the sectional elevation bottom plan and top plan shown in Fig. A.2, Fig. A.3 and Fig. A.4. The top plan view of the electronics and payload chamber made of GRP with the reinforcements for housing the batteries, solar panels, shaft, motor and gearbox assembly is shown in Fig. A.5.

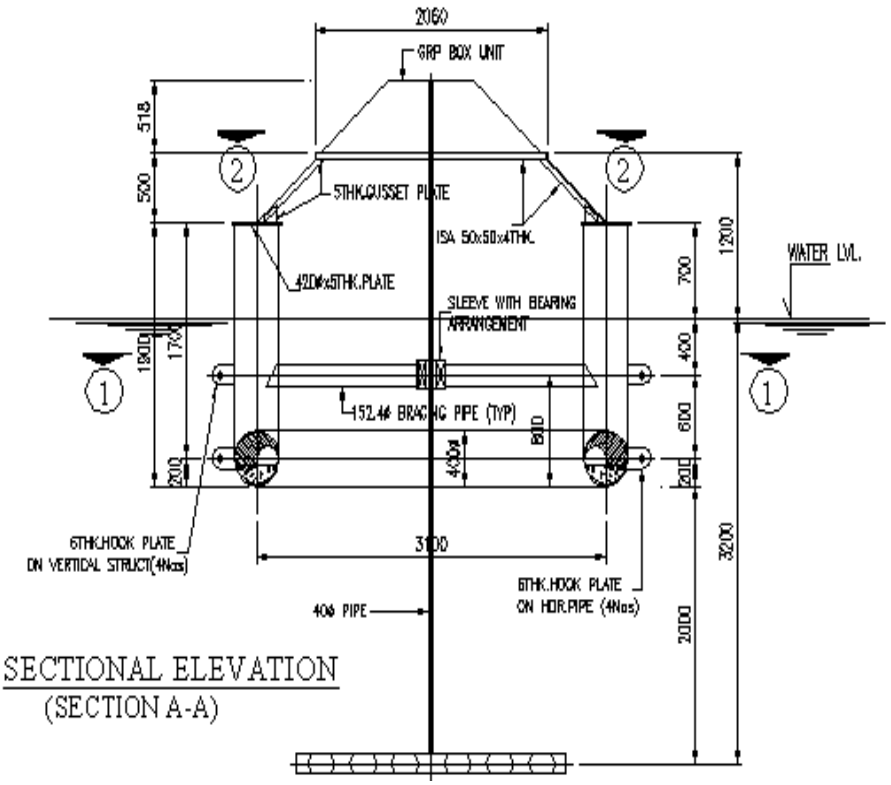

Fig. A.2 The Sectional Elevation of Buoy, B1

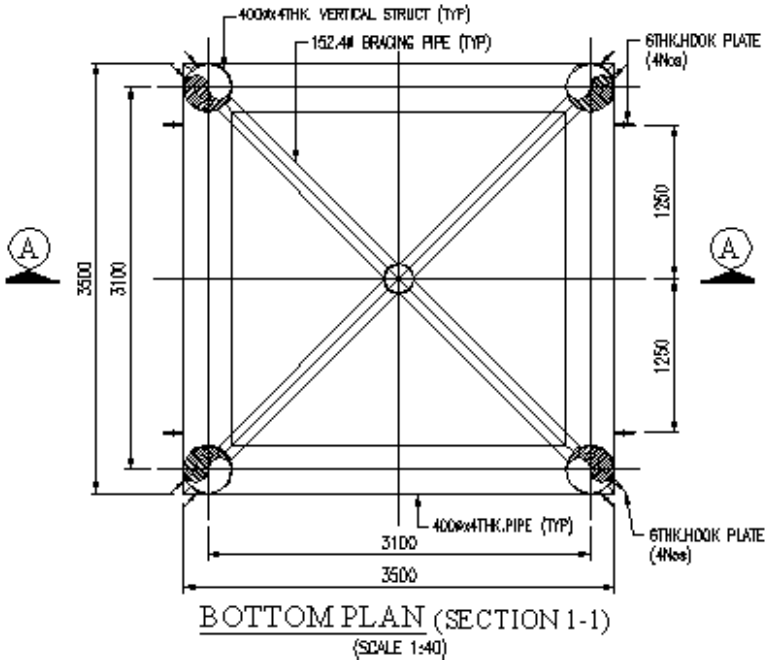

Fig. A.3 The Bottom Plan View of the Buoy, B_1

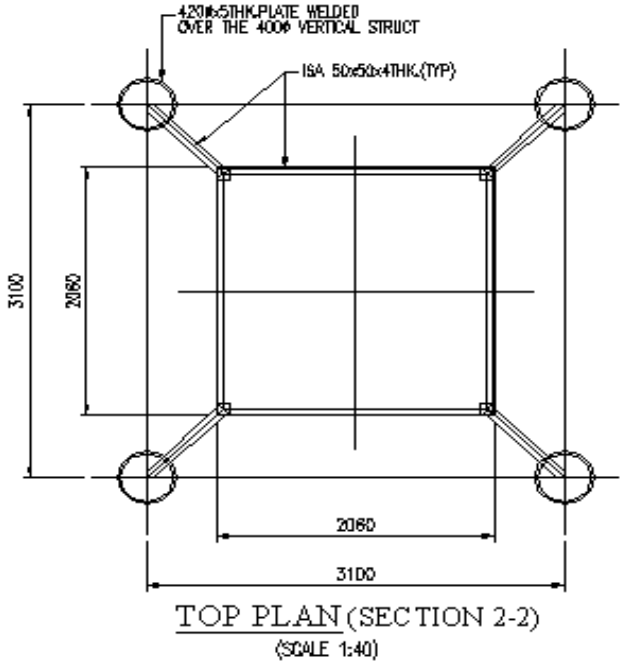

Fig. A.4 The Top Plan View of the Buoy, B_1

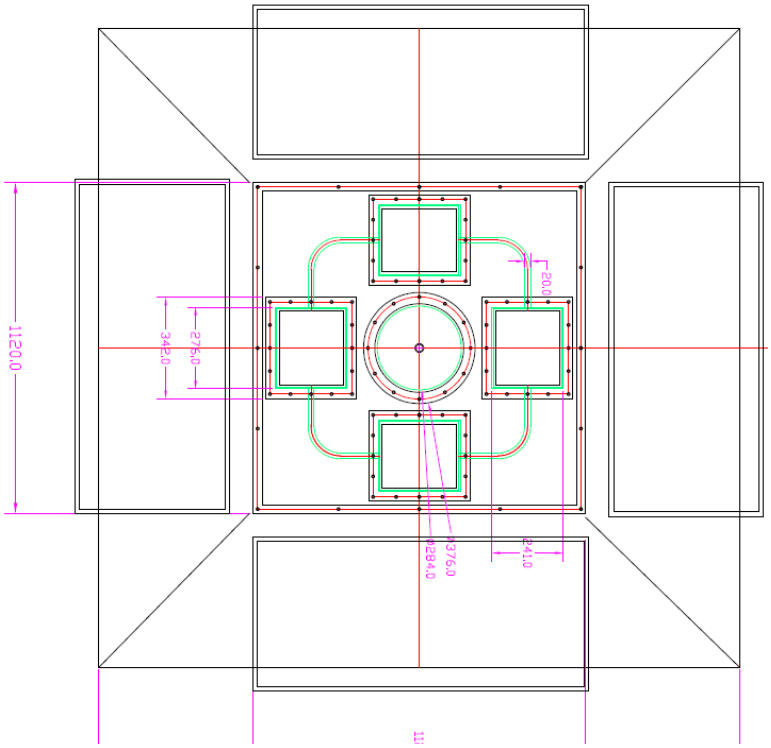

Fig. A.5 The Top Plan of the Electronics and Payload Chamber

A.2 *Small Water Plane Area Buoy (SWAB)*

As the Buoy needs specialized requirements for the proposed application involving the steering of the submerged hydrophones supporting from the gear assembly, the experts formulated a specialized structural design conforming to the concept of minimizing the water plane area, so that the disturbances the buoy experience, is brought to the minimum. The dimensions of the various structural segments of the two types of buoys and B_2/B_3 are given in Table A.1. The actual/estimated weights of various components of the buoy and accessories are listed in Table A.2.

Table A.1 Dimensions of the Structural Buoys B_1 and B_2/B_3

DIMENSIONS(in mm)	SWAB I (B_1)	SWAB II & III (B_2 and B_3)	MATERIAL
Length Overall	3500	3500	Mild Steel
Breadth Overall	3500	3500	IS2062
Height Overall from Base	2918	2918	IS2062
Float dia.	406.4	406.4	IS2062
Float thickness	4	5.2	IS2062
Strut dia	406.4	406.4	IS2062
Strut thickness	4	5.2	IS2062
Cross structure dia.	152.4	152.4	IS2062
Cross Structure thickness	4	4	IS2062

Table A.2 Actual Estimated Weights of the Constituent Components of Buoys B1 and B2/B3

SL. NO.	ITEM	WEIGHT (kg)	
		SWAB I	SWAB II & III
1	Float	589.49	686.37
2	Strut	285.24	332.11
3	Cross tie	247.89	247.89
4	Platform	150.00	150.00
5	Box	60.00	60.00
6	Float brackets	10.00	10.00
7	Strut bottom brackets	10.00	10.00
8	Strut top closing plate	16.29	16.29
9	Lugs for anchor cable	16.00	16.00
10	Batteries	60.00	60.00
11	Solar panels	60.00	60.00
12	Motor & gear	25.00	25.00
13	Electronics	10.00	10.00
14	Shaft	12.60	12.60
15	Hydrophone array	30.00	30.00
17	Resin coating	40.00	40.00
18	Concrete Ballast	350.00	400.00
19	Steel Ballast	360.00	200.00

A.2.1 Design of the Cabin

The payload and the electronics chamber was designed with a view to minimizing its size, weight and surface area leading to minimization of wind loads, lowering of the overall centre of gravity of the buoy and a consequent improvement in stability. The floor area of the cabin should be sufficient to accommodate the electronic equipment, motor and battery. The height of the cabin should be sufficient to accommodate the solar panels mounted on its sidewalls. Adequate access to install and maintain the Buoy Electronics in the chamber has been provided at the top.

It was decided to adopt the shape of a frustum of a pyramid, as this was the best shape to achieve the functions stated above. The material selected was GRP, due to its light weight and good corrosion resistance. Steel framing of 50x50x4 M.S. angles supports the chamber.

A.3 *Stability of the Buoy in Free-Floating Condition*

The motions of a floating body in waves, described above are proportional to the water plane area of the body. The lesser the water plane area, the smaller will be the motions of the body in heave, roll and pitch. In this design, the water plane area is made as minimum as possible while maintaining the required buoyancy and stability by means of the immersed buoyancy chambers.

A.3.1 Initial Stability

The indicator for initial stability is the metacentric height ***GM***, defined as the height of the metacentre above the centre of gravity of the floating body.

$$GM = KB + BM - KG$$

where *KB* is the height of Centre of Buoyancy above Base Line, *KG* is the height of Centre of Gravity above Base Line and *BM* is the metacentric Radius given by

$$BM = I/V$$

where the Moment of Inertia of the waterplane area and *V* is the Volume of Displacement of the floating Body.

A.3.2 Waterplane Area

For the semi-submersible buoy, the waterplane area is provided by the 4 cylindrical struts and is given by

$$A_W = 4\pi D_S^2/4 = \pi D_S^2$$

where D_S is the diameter of the strut

The moment of inertia of waterplane area is computed by finding the own moment of inertia of waterplane area of a strut about its own axis and transferring it to the centre line axis of the buoy using parallel axis theorem. The total moment of inertia is then 4 times the value obtained above, due to the four struts. The moment of inertia can be increased by increasing the diameter of struts or by increasing the distance between struts or both. The above parameters are iterated during the optimization process to satisfy the stability constraints.

A.3.3 Volume of Displacement

The buoyancy force is directly proportional to the volume of displacement provided by

- Horizontal floats
- Vertical Struts

- ❖ Cross-tie
- ❖ Immersed part of shaft
- ❖ Immersed hydrophone array

For drafts below crosstie, the volume of displacement is given by

$$V = \pi D_F^2/4L_F + 4(\pi D_S^2/4)\ (T-D_F)$$

For drafts above the crosstie, the volume of displacement is given by

$$V = \pi D_F^2/4L_F + \pi D_C^2/4L_C + 4\ (\pi D_S^2/4)\ (T-D_F)$$

Where D_F is the diameter of float, L_F is the total length of floats, D_C is the diameter of the crosstie, L_C is the total length of crosstie members and T is the draft from Base Line.

A.3.4 Vertical Centre of Gravity above Base Line

The Vertical Centre of Gravity (VCG) above base line is given by

KG = Total moment of mass about base line/total mass

= $\Sigma(m_i\ z_i)/\ \Sigma m_i$

where m_i is the mass of the i^{th} item and z_i is the vertical lever centre of gravity from base line of the i^{th} item.

A.3.5 Vertical Centre of Buoyancy above Base Line

The Vertical Centre of Buoyancy (VCB) above base line is given by

KB = Total moment of mass about base line/total mass

= $\Sigma(v_i\ z_i)/\ \Sigma v_i$

where v_i is the volume of the i^{th} item and z_i is the vertical lever of centre of buoyancy from base line of the i^{th} item. Clearly only items that are submerged and contributed to the buoyancy of the buoy will be included.

Initial stability of the buoy was calculated for different buoy configurations by changing the dimensions of the floats, struts and crosstie,

the thicknesses of these members and the solid ballast inside the floats and outside. The design aimed at an initial metacentric height of at least 20 cm against the IMO criteria of 15 cm for sea-going vessels. The final stability calculations for Buoys B_1, B_2 and B_3 are furnished in Tables A.3 through A.10.

Table A.3 Parameters of the Structural Components of the Buoys

WEIGHT/UNIT LENGTH AND BUOYANCY/UNIT LENGTH OF PIPES						
Sl. No.	Item	OD (m)	ID (m)	Wt/m (kg/m)	Buo/m (kg/m)	Total Length (m)
1	Float	0.4064	0.3968	47.53960	129.71742	12.400
2	Strut	0.4064	0.3968	47.53960	129.71742	6.000
3	Cross tie	0.1524	0.1444	14.63910	18.24151	16.934
	Draft	0.99	m			

Table A.4 Weights and Centre of Gravity of Buoy B_1

WEIGHTS AND CENTRE OF GRAVITY						
SL. NO.	ITEM	WEIGHT	LCG FROM AFT END	MOMENT ABOUTAFT END	VCG FROMBASE	MOMENT ABOUT BASE
		kg	m	kg.m	m	kg.m
1	FLOAT	589.49	1.750	1031.609	0.200	117.898
2	STRUT	285.24	1.750	499.166	1.050	299.499
3	CROSS TIE	247.89	1.750	433.812	0.800	198.314
4	PLATFORM	150.00	1.750	262.500	2.345	351.750
5	BOX	60.00	1.750	105.000	2.600	156.000
6	FLOAT BRACKETS	10.00	1.750	17.500	0.203	2.030
7	STRUT BOTTOM	10.00	1.750	17.500	0.470	4.700
8	STRUT TOP	16.29	1.750	28.512	1.900	30.956
9	LUGS FOR	16.00	1.750	28.000	0.200	3.200
10	BATTERIES	60.00	1.750	105.000	2.276	136.560
11	SOLAR PANELS	60.00	1.750	105.000	2.660	159.600
12	MOTOR & GEAR	25.00	1.750	43.750	2.500	62.500
13	ELECTRONICS	10.00	1.750	17.500	2.500	25.000
14	SHAFT	12.60	1.750	22.050	1.100	13.860
15	HYDROPHONE	30.00	1.750	52.500	-1.200	-36.000
16	CONCRETE	450.00	1.750	787.500	0.100	45.000
17	STEEL BALLAST	150.00	1.750	262.500	0.253	37.950
18	RESIN COATING	40.00	1.750	70.000	0.800	32.000
	Total	**2222.51**	**1.750**	**3889.399**	**0.738**	**1640.818**

Table A.5 Buoyancy and Center of Buoyancy of Buoy B_1

SL. NO.	ITEM	BUOYANCY	LCB FROM AFT END	MOMENT ABOUT AFT END	VCB FROM BASE	MOMENT ABOUT BASE
		kg	m	kg.m	m	tonne.m
1	Float	1608.50	1.750	2814.868	0.200	321.699
2	Cross tie	308.89	1.750	540.565	0.800	247.116
3	strut	308.44	1.750	539.777	0.697	215.056
	Total	**2225.83**	**1.750**	**3895.210**	**0.352**	**783.870**

Table A.6 Water plane Moment of Inertia of Buoy B_1

I_{own}	0.005027	m^4
d	1.550	m
Ad^2	1.208	m^4
$I_{centroid}$	1.21266	m^4
BM_T	0.54562	m
GMT	**0.16**	**M**

Table A.7 Parameters of the Structural Components of Buoys B_2 and B_3

WEIGHT/UNIT LENGTH AND BUOYANCY/UNIT LENGTH OF PIPES						
Sl.No.	Item	OD	ID	Wt/m	Buo/m	Total Length
		(m)	(m)	(kg/m)	(kg/m)	(m)
1	Float	0.4064	0.3952	55.35238	129.71742	12.400
2	Strut	0.4064	0.3952	55.35238	129.71742	6.000
3	Cross tie	0.1524	0.1444	14.63910	18.24151	16.934

Table A.8 Water plane Moment of Inertia of Buoys B2 and B3

I own	0.005027	m^4
D	1.550	m
Ad^2	1.208	m^4
I centroid	1.21266	m^4
BM_T	0.53148	m
GMT	0.16	m

Table A.9 Weights and Centre of Gravity of Buoys B_2 and B_3

SL. NO.	ITEM	WEIGHT	LCG FROM AFT END	MOMENT ABOUT AFT END	VCG FROM BASE	MOMENT ABOUT BASE
		kg	m	kg.m	m	kg.m
1	FLOAT	686.37	1.750	1201.147	0.203	139.470
2	STRUT	332.11	1.750	581.200	1.050	348.720
3	CROSS TIE	247.89	1.750	433.812	0.800	198.314
4	PLATFORM	150.00	1.750	262.500	2.345	351.750
5	BOX	60.00	1.750	105.000	2.600	156.000
6	FLOAT BRACKETS	10.00	1.750	17.500	0.203	2.030
7	STRUT BOTTOM BRACKETS	10.00	1.750	17.500	0.470	4.700
8	STRUT TOP CLOSING PLATE	16.29	1.750	28.512	1.900	30.956
9	LUGS FOR ANCHOR CABLE	16.00	1.750	28.000	0.200	3.200
10	BATTERIES	60.00	1.750	105.000	2.276	136.560
11	SOLAR PANELS	60.00	1.750	105.000	2.660	159.600
12	MOTOR & GEAR	25.00	1.750	43.750	2.500	62.500
13	ELECTRONICS	10.00	1.750	17.500	2.500	25.000
14	SHAFT	12.60	1.750	22.050	1.100	13.860
15	HYDROPHONE ARRAY	30.00	1.750	52.500	-1.200	-36.000
16	CONCRETE BALLAST IN FLOAT	400.00	1.750	700.000	0.100	40.000
	Total	2281.68	1.750	3992.933	0.744	1697.091

Draft 1.11 m

Table A.4 Buoyancy and Center of Buoyancy of Buoys B2 and B3

SL. NO.	ITEM	BUOYA-NCY	LCB FROM AFT END	MOMENT ABOUT AFT END	VCB FROM BASE	MOMENT ABOUT BASE
		kg	m	kg.m	m	tonne.m
1	float	1608.50	1.750	2814.868	0.203	326.846
2	Cross tie	308.89	1.750	540.565	0.800	247.116
3	strut	367.61	1.750	643.311	0.754	277.262
	Total	2285.00	1.750	3998.744	0.373	851.224

A.4 *Mooring / Anchoring*

The buoy will be anchored to the sea floor by four anchor chains or SS wire ropes with suitable anchors at the bottom. The anchoring will ensure that the buoy is held in position and will also restrict the roll, sway, pitch, yaw and heave motions of the buoy. The buoys are shacked from the four corners of the buoyancy structure and anchored to the sea bed with concrete cubical blocks (45^3cm). Small floats made of GRP/FRP can be attached along the wire rope or chain for making it neutrally buoyant as shown in Fig. A.6. The buoy proposed to be used for the prototype system is a miniaturized version of the field deployable system described above.

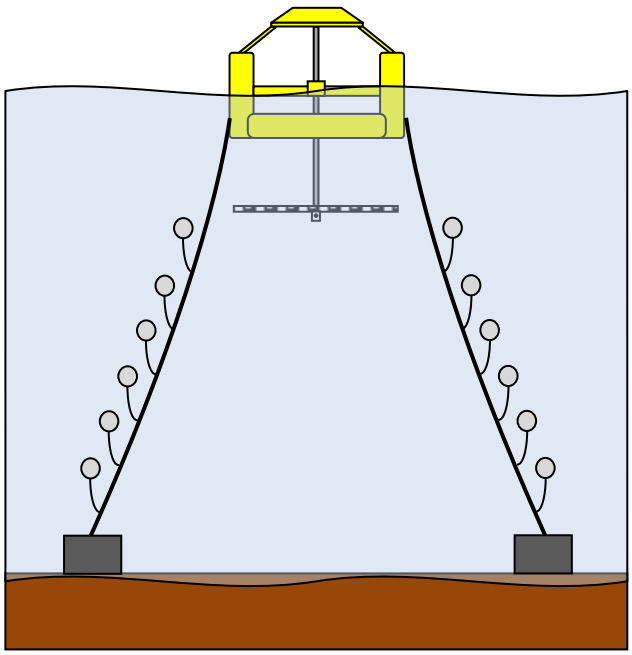

Fig. A.6 Mooring Scenario of the Buoy

References

[1]. Robert J. Urick, *Principles of Underwater Sound*, McGraw Hill, 1975

[2]. John G. Proakis, *Digital Communications*, McGraw Hill, 2000, pp. 6-11

[3]. Richard O. Nielsen, *Sonar Signal Processing*, Artech House, 1991

[4]. Simon Haykin, *Array Signal Processing*, Prentice Hall, 1990

[5]. William C. Knight, Rogar G. Pridham and Steven M. Ray, *Digital Signal Processing for Sonar*, Proceedings of IEEE, vol. 69, 1981, pp. 1451-1505

[6]. Monson H. Hayes, *Statistical Digital Signal Processing and Modeling*, New York, John Wiley & Sons Inc., 2003

[7]. Somanathan Nair B., *Digital Signal processing Theory*, *Analysis and digital filter design*, Prentice Hall, India, 2006

[8]. The Vessel Monitoring System, Fisheries and Oceans, Canada, Available : http://www.glf.dfo-mpo.gc.ca/ Gulf/FAM/CP/VMS

[9]. Australian Fisheries Monitoring Authority (AFMA), Available : http:// www.afma.gov.au/services-for-industry/vessel-monitoring-systems/

[10]. Northwest Atlantic fisheries Organization (NAFO), Monitoring, Control and Surveillance (MCS), Available : http:// www.nafo.int /fisheries/ frames/mcs.html

[11]. The Complete Guide to Automatic Identification Systems, Leica Geosystems Inc., 2001, Available: www.siitech.com/ files/ ais/ ais_ guide.pdf

[12]. http://www.ledwoodtechnology.co.uk/media/1509/lps_vts_flyer.pdf

[13]. Vessel Monitoring System Program, Gulf of Mexico Commercial Reef Fish, 2007, Available: http://sero.nmfs.noaa.gov/ vms/ VMS FAQs 041707_2.pdf

[14]. Marine Exchange of Alaska, Pactracs, Vessel Tracking System, User's Manual, Available: www.mxak.org

[15]. Shipborne Automatic Identification System (AIS), Australian Maritime Safety Authority Canberra, ACT Australia December 2003, Available : http:// www.fargisinfo.com/ AIS2010/ Linked Documents/ Fact _Sheet.pdf

[16]. Martin Redoutey, Eric Scotti, Christian Jen, Cyril Ray and Christophe Claramunt, *Efficient Vessel Tracking with Accuracy Guarantees*, W2GIS, LNCS 5373, pp. 140–151

[17]. RFID Based Tracking System, *Effectively Tracking Large volumes of Small Boats in a Given Area*, Available: http:// www.rolta.com/ product4_MP_RFID_based_vehicle_track_system.html

[18]. Applied Weather Technology (AWT), CA, USA, Available : http:// www.awtworldwide.com/assets/pdf/AWT_Tracking_Polling_A4_0 51313.pdf

[19]. Anna Dzvonkovskaya, Klaus-Werner Gurgel, Hermann Rohling and Thomas Schlick, *HF Radar WERA Application for Ship Detection and Tracking,* European Journal of Navigation, Vol. 7, No. 3, December 2009, pp. 18-25

[20]. Anna Dzvonkovskaya & Hermann Rohling, *Monitoring ship traffic using oceanographic WERA high-frequency radar*, port technology International, Available: http://www.porttechnology.org/

[21]. Steen Weber, *Ship Tracking Service using Google Earth*, Real Time Ship Tracking Service, SHIPPOS, http://www.shippos.dk/

[22]. Internet- Based Vessel Tracking System (I-Vet), 2005 Computer world Honors Case Study, Available: http:// www. cwheroes.org/ laureates/ transportation/maritime.pdf

[23]. Marek Dziewicki, Maritime Office Gdynia, *The role of AIS for small ships monitoring,* Department of ATON Technique and Radio navigation Systems, Report, 2007, Available: http:// www. balticmaster.org/ media/files/general_files_704.pdf

[24]. ORCA, Multi-sensor Maritime surveillance System, PEGASE Systems, Available : http:// www. pegase-systems. com/Brochures

[25]. Blue Tracker Vessel Monitoring System, eiiia wireless data solutions, Available : www.bluetracker.com

[26]. Vessel tracking Systems, 3iTechnologies, Available : www. 3i technologies.com

[27]. Long Range Identification and Tracking of Vessels, Fulcrum maritime systems, Available : fulcrum-maritime.com

[28]. How real – time ship tracking works, Available : Real-time_ SF_ bay_ Ship_tracking/ships

[29]. Vessel and Voyage Optimization Solution, Jeppesen, Available : jeppesen.com/marine

[30]. AgroNET to track all Panama flag fishing vessels, ArgoNET newsletter, Available : www.cls.fr

[31]. Rom Vessel monitoring system, Available : http:// www. romcomm. com/ VesselMonitoringSystem.html

[32]. MetTrac Vessel Monitoring System, Available: https:// www. mettrac. com/ daysatsea/includes/mettrac.pdf

[33]. THEMIS : Maritime Surveillance Software Suite, Available : Themis@cls.fr

[34]. Kevin Gregory, *Latest technological developments in vessel tracking and monitoring*, port technology international, pp. 50-52, Available : www.porttechnology.org

[35]. G.G. Lemoine, H. Greidanus, I. M. Shepherd and N. Kourti, *Developments in satellite fisheries Monitoring and Control*, Int. Conf. Remote Sensing for Marine and Coastal Environments, Canada, 2005, pp. 17-19

[36]. T. Samad and A. M. Annaswami, *Dynamic Positioning System for Marine Vessels*, The Impact of Control Technology, 2011, Available : www.ieeecss.org

[37]. ACSA, *Underwater GPS applications*, Available : http:// www. underwater-gps.com/uk/technology-GIB-concept.php

[38]. Alcocer P. Oliveira and Pascoal, A., *Underwater Acoustic Positioning System based on Buoys with GPS*, Proceedings of 8th European Conference on Underwater Acoustics, Portugal, 2006

[39]. Alcocer P. Oliveira and Pascoal, A., *Study and implementation of an EKF GIB-based underwater positioning system*, 2004, Available : welcome.isr.ist/img/pdfs/1504_cep07_ONLINE.pdf

[40]. Hubert G. Thomas, *GIB Buoys: An Interface Between Space and Depths of the Oceans*, Available: 0-7803-5 190-8/98/$10.00 01998 IEEE, http://ieeexplore.ieee.org/stamp/stamp.jsp?arnumber=00744453

[41]. Vemco VRAP hardware manual, [online], http:// www.vemco.com/ pdf/ vrap_hw_manual.pdf, Accessed on 9th December 2011

[42]. Lock Robert Philip, Cockings, Grenville Roderick Dillon, European Patent, Dec. 05, 1991

[43]. Clarence J. Funk, *Acoustic Device*, US patent, Sep.12 , 1978

[44]. Charles Bertolino, *Method of screening acoustic signals transmitted by a moving target*, US patent, March 27 , 2001

[45]. Edward P. Harvey Jr. and Jack McGlnn, *System and method for determining the location of an acoustic event*, US patent, Jun. 19, 2007

[46]. Altan Turgut, *Method and apparatus for passive acoustic ranging*, US patent, Dec. 30, 2008

[47]. A. Peter Klimley, Burney J. Le Boeuf, Kelly M. Cantara, John E. Richert, Scott F. Davis and S. Van Sommeran, *Radio-acoustic positioning as a tool for studying site-specific behavior of the white shark and other large marine species*, Marine Biology, Vol. 138, Issue 2, pp. 429-446, 2001

[48]. Kalman R. E., *A new approach to linear filtering and prediction*, Journal of Basic Engineering (ASME), vol. 82D, 1960, pp. 35-45,

[49]. Greg Welch and Gary Bishop, *An Introduction to the Kalman Filter*, Department of Computer Science, University of North Carolina, 2006

[50]. www.cs.unc.edu/~welch/KalmanLinks

[51]. Dan Simon and T. Chia, *Kalman Filter with state equality constraints*, IEEE Transactions on Aerospace and Electronic Systems, vol.38, no.1, 2002, pp. 128-136

[52]. Dan Simon, *Kalman Filtering*, Embedded Systems Programming, 14 (6), pp. 72-79, 2001

[53]. P. S. Maybeck, *Stochastic Models, Estimation and Control*, Academic Press, Inc. New York, 1979

[54]. Chiman M. Kwan, and Frank, L. Lewis, *A Note on Kalman Filtering*, IEEE Transactions on Education, vol. 42, no. 3, 1999, pp. 225-228

[55]. Y. T. Chan, J. R. T. Bottomley, *A Kalman Tracker with a Simple input Estimator*, IEEE Transactions on Aerospace and Electronic Systems,18:235-241, 1982

[56]. Y. T. Chan, Hu and Plant, *A Kalman Filter Based Tracking Scheme With Input Estimation*, IEEE Transactions on Aerospace and Electronic Systems, Vol.15, No.2 :237-243, 1979

[57]. Samuel S. Blackman, *Multiple-Target Tracking with Radar Applications*, Norwood: Artech House, 1986

[58]. Yaakov Bar-Shalom and X. Rong Li, *Estimation and Tracking : Principles, Techniques and Software*, Artech House, Boston, London, pp. 432-437, 2001

[59]. Y. Bar-Shalom, K. C. Chang and H. A. P. Blom, *Tracking A Maneuvering Target Using Input Estimation Versus The Interacting Multiple Model Algorithm*, IEEE Transactions on Aerospace and Electronic Systems, Vol.25, No.2 :237-243, 1989

[60]. Radhakisan S. Baheti, *Efficient Approximation o f Kalman Filter for Target Tracking*, IEEE Transactions on Aerospace and Electronic Systems, 22:8-14, 1986

[61]. K. Takaba, Y. Iiguni and H. Tokumaru, *An Improved Tracking Kalman Filter Using A Multilayered Neural Network*, Mathl. Comput. Modelling, Vol. 23, No.1/2, pp. 119-128, 1996

[62]. B. J. Lee, J. B. Park, Y. H. Joo and S. H. Jin, *Intelligent Kalman filter for Tracking a Manoeuvring Target*, IEEE Proc. Radar and Sonar Navigation, Vol. 151, No.6, Dec 2004

[63]. X. Rong Li and Vesselin P. Jilkov, *Survey of Maneuvering Target Tracking. Part I: Dynamic Models*, IEEE Transactions on Aerospace and Electronic systems,Vol.39, No.4, pp. 1333-1364, 2003

[64]. X. Rong Li and Vesselin P. Jilkov, *Survey of Maneuvering Target Tracking. Part II: Motion models of Ballistic and Space Targets*, IEEE Transactions on Aerospace and Electronic systems, Vol. 46, No. 1, pp.96-116, 2010

[65]. X. Rong Li and Vesselin P. Jilkov, *A Survey of maneuvering target tracking: III. Measurement models*, Proc. SPIE4473, Signal and Data Processing of Small Targets, 423, 2001

[66]. X. Rong Li and Vesselin P. Jilkov, *A Survey of Maneuvering Target Tracking—Part IV: Decision-Based Methods*, SPIE Conf. Signal and Data Processing of Small Targets, 2002

[67]. X. Rong Li and Vesselin P. Jilkov, A s*urvey of maneuvering target tracking. Part V: Multiple-model methods*, IEEE Trans. Aerospace and Electronic Systems, Vol. 41, No. 4, pp. 1255–1321, 2005

[68]. X. Rong Li and Vesselin P. Jilkov, *A survey of maneuvering target tracking-Part VIa: Density-based exact nonlinear filtering*, Proc. SPIE 7698, Signal and Data Processing of Small Targets, 76981D, 2010, DOI: 10.1117/12.851393

[69]. X. Rong Li and Vesselin P. Jilkov, *A survey of maneuvering target tracking-part VIb: approximate nonlinear density filtering in mixed time*, Proc. SPIE 7698, Signal and Data Processing of Small Targets 2010, 76981E, 2010, DOI:10.1117/12.851394

[70]. X. Rong Li and Vesselin P. Jilkov, *A survey of maneuvering target tracking, part VIc: approximate nonlinear density filtering in discrete time*, Proc. SPIE 8393, Signal and Data Processing of Small Targets 2012, 83930V, 2012, DOI: 10.1117/12.921508

[71]. X. Rong Li and Vesselin P. Jilkov, *A survey of maneuvering target tracking: approximation techniques for nonlinear filtering*, Proc. SPIE 5428, Signal and Data Processing of Small Targets, 2004, DOI: 10.1117/12.553357

[72]. M. Isabel Ribeiro, *Gaussian Probability Density Functions : Properties and Error Characterization*, 2004

[73]. M. H. Bahari, F. Netaji Moharrami, M. A. Ebrahimi Ganjeh and A. Karsaz, *Tracking a High Maneuver Target Based on Intellegent Matrix Covariance Resetting*, Proc. International Symposium on image and Signal Processing and Analysis, pp. 35-40, 2007

[74]. M.H. Bahari, A. Karsaz and M. B. Naghibi-S, *Intelligent Error Covariance Matrix Resetting for Maneuver Target Tracking*, Journal of Applied Sciences, 8: 2279-2285, 2008

[75]. Mohamad Hasan Bahari, Mohammad Bagher Naghibi Sistani and Naser Pariz, *Intelligent fading memory for high maneuvering target tracking*, International Journal of Physical Sciences Vol. 4 (10), pp. 548-554, 2009

[76]. Mohamad Hasan Bahari, Ali Karsaz and Naser Pariz, *High Maneuvering Target Tracking Using A Novel Hybrid Kalman Filter-Fuzzy Logic Architecture*, International Journal of Innovative Computing, Information and Control, Vol. 7, No. 2, pp. 1349-4198, 2011

[77]. Shi Jianfang, Wang Minghui and Zhang Xueying, *Improve the Tracking Performance of Maneuvering Target Based on Wavelet Neural Network*, Global Congress on Intelligent Systems, IEEE Computer Society, pp.107-111, 2009, DOI 10.1109/GCIS.2009.327

[78]. Steven M. Kay, Stanley Lawrence, Marple, Jr., *Spectrum Analysis-A modern perspective*, Proceedings of IEEE, Vol. 69, N0. 11, 1981

[79]. Marple, S.L., Jr.; *A tutorial overview of modern spectral estimation***,** International Conference on Acoustics, Speech, and Signal Processing, 4, 1989, pp:2152 - 2157

[80]. Ricardo S. Zebulum, Marley Vellascot, Guy Perelmuter and Marco Aurelio, *A Comparison of Different Spectral Analysis Models For Speech Recognition Using Neural Networks*, Proceedings of the

IEEE 39th Midwest symposium on Circuits and Systems, 3, 1996 pp:1428-1431

[81]. Chun Ru Wan, Joo Thiam Goh and Hong Tat Chee, *Optimal tonal detectors based on the power spectrum* IEEE Journal of Oceanic Engineering, 25(4), 2000, pp: 540 - 552

[82]. Igor Luzin, Maxim Dubinsky, and Magistrant; *High Resolution Spectrum Estimating Algorithm*, Proceedings of the IEEE OCEANS Conference, 3, 1998, pp:1409 - 1412

[83]. Christopher Bingham, Michael D. Godfrey, and John W. Tukey; *Modern Techniques of Power Spectrum Estimation*, IEEE Transactions on Audio and Electroacoustics, 2, 1967, pp:56 - 66

[84]. Massimo Aiello, Antonio Cataliotti, and Salvatore Nuccio; *A Comparison of Spectrum Estimation Techniques for Nonstationary Signals in Induction Motor Drive Measurements*, IEEE Transactions on Instrumentation and Measurement, 54(6), 2005, pp:2264 – 2271

[85]. Eftestol T. and Vatland *E., A method for detection of signal harmonics in the spectrum*, Computers in Cardiology, 1999, pp: 547 – 550

[86]. Lorenzo Peretto, Gaetano Pasini and Carlo Muscas, *Signal Spectrum Analysis and Period Estimation by Using Delayed Signal Sampling*, Proceedings of the IEEE International Conference on Acoustics, Speech and Signal Processing, 2, 1994, pp:1035 – 1040.

[87]. Supriya M. H., Shaheer, K., Mahendran, M.G. and P. R. Saseendran Pillai, (2007), *Towards Improving the Target Recognition Using a Hierarchical Target Trimming Approach*, WSEAS Transactions on Signal Processing, Vol 3(5), pp. 340- 345.

[88]. Supriya M. H. and P. R. Saseendran Pillai, *Towards Improving the Target Recognition Using Spectral and Cepstral Features*, Journal of Acoustical Society of America. 121 (5, Pt. 2), 2007, pp. 3046.

[89]. Supriya M. H., *Realisation of A Target Classifier for Noise Sources in the Ocean*, Chapt.3, 2007, pp. 70-74

[90]. Supriya M. H. and P. R. Saseendran Pillai, *An optimised autoregressive spectral estimator for vessel generated noise, Journal of Acoustical Society of India*. vol. 33, 2007, pp. 584-590

[91]. Supriya M.H. and P.R. Saseendran Pillai, *Implementation of Algorithms for Extracting Tonal Components in Underwater Noise*, J. Acoust. Soc.Am.115 (5, Pt. 2), 2004, p. 2613.

[92]. R. Rodney W. Johnson and John E. Shore, *Minimum Cross-Entropy Spectral Analysis of Multiple Signals*, IEEE Transactions On Acoustics, Speech and Signal Processing, 31(3), 1983, pp:574 - 582

[93]. G-Mouse GPS User Manual, GPS GGM309R, Version 1.01, 2006 Available : http://www.coxmate.nl/handleidingen/ GPS _ manual (GGM 309R_ Manual_V1.01).pdf

[94]. NMEA data, Available : http:// www. gpsinformation. org/ dale/ nmea.htm

[95]. www.movable-type.co.uk/scripts/latlong.html

[96]. T. Vincenty, *Survey Review*, Vol. XXIII, No.176, April, 1975, Ministry of overseas development, Surrey

[97]. *www.movable-type.co.uk/scripts/latlong-vincenty.html*

[98]. C. M. Thomas and W. E. Featherstone, *Validation of Vincenty's Formulas for the Geodesic Using a New Fourth-Order Extension of Kivioja's Formula*, Journal of Surveying Engineering, Vol. 131, No. 1, 2005, pp. 20-26

[99]. http://www.irf.com/product_info/datasheets/data/ir2110.pdf, high voltage, high speed power datasheet MOSFET drivers with independent high and low side referenced output channels.

[100]. http://www.datasheetcatalog.com/datasheets_pdf/I/R/F/Z/IRF48.shtml 60V Single N-Channel HEXFET Power MOSFET in a TO-220AB package.

[101]. http://ww1.microchip.com/downloads/en/DeviceDoc/70143C.pdf-Microchip dsPIC30F6014A datasheet

[102]. http://ww1.microchip.com/downloads/en/DeviceDoc/70143G.pdf-Microchip dsPIC30F6010A datasheet

[103]. http://local. wasp. uwa.edu.au/~pbourke /miscellaneous/ dft/ Fast Fourier Transform by Paul Bourke, June 1993

[104]. http://www.datasheetcatalog.com/datasheets_pdf/P/I/C/1/

PIC16F88.shtml

[105]. http://www.national.com/an/AN/AN-31.pdf - Application Note 31 Op Amp Circuit Collection

[106]. http://focus.ti. com/ docs/ prod/ folders/ print /tl084.html TL084 Datasheet

[107]. Prabha C., Ananthakrishnan V., Supriya, M. H., P. R. Saseendran Pillai, *Localization of underwater targets using sensor networks*,

International journal of sensor networks(IJSNet), Vol. 13 , No. 3 , 2013, pp. 185-196

[108]. V. Ananthakrishnan, C. Prabha, Supriya. M. Hariharan and Saseendran pillai, *Development of an ocean surveillance system*, J. Acoustical Soc. Am. 123(5), Pt.2, 2008, P.3895

[109]. Prabha C., Supriya, M. H., P. R. Saseendran Pillai, *Improving the Localization Estimates using Kalman filters*, Proceedings of International Symposium on Ocean Electronics, Kochi, India, pp. 190-195, 2009 and published in IEEE Xplore

[110]. Prabha C., Supriya, M. H., P. R. Saseendran Pillai, *Model Studies on the Localization of Underwater Targets using Sensor Networks*, Proceedings of International Symposium on Ocean Electronics, Allied Publishers, New Delhi, Vol .1, pp. 257-263. 2007

[111]. Prabha C., Supriya, M. H., P. R. Saseendran Pillai, *Refining Underwater Target Localization and Tracking Estimates*, Signal Processing: An International Journal (SPIJ), Vol. (5): Issue (5), pp. 203-214, 2011

[112]. Prabha C., Supriya, M. H., P. R. Saseendran Pillai, *Tracking of a Maneuvering Underwater Target*, Proceedings of International Symposium on Ocean Electronics, Kochi, India, pp. 93-100, 2011 and published in IEEE Xplore

[113]. TMS320C6713 Datasheet from Texas Instruments SPRS2948 October 2005, Revised June 2006

[114]. Practical Guidelines and Examples for TMS320C6713 DSK, November 2008, ISSN 2070-3740

[115]. George Tzanetakis and Perry Cook, *Musical Genre Classification of Audio Signals*, IEEE Transactions On Speech And Audio processing, 10(5), 2002, pp: 293-302.

[116]. Sujay Phadke, Rhishikesh Limaye, Siddharth Verma and Kavitha Subramanian, *On Design and Implementation of an Embedded Automatic Speech Recognition System*, Proceedings of the 17th IEEE International Conference on VLSI Design, 2004, pp: 127-132.

[117]. Vaishali Nandedkar, *Audio retrieval using multiple feature vectors*, IJEEE, Vol. 1, Issue.1, 2011

[118]. M. Casey, *General sound classification and similarity inmpeg-7*, Organized Sound, Vol. 6(2), 2001, pp. 153-164

[119]. J.J. Burred and A. Lerch, *Hierarchical Automatic Audio Signal Classification*, J. Audio Eng. soc., Vol. 52, pp. 724-739, 2004

[120]. Ki-man kim, Se-Young Kim, Jae-Kuk Jeon and Kyu-sik park, *Quick Audio Retrieval Using Multiple feature Vectors*, IEEE transactions on Consumer Electronics, Vol. 52, No.1, 2006, pp. 200-206

[121]. Ahmed M. Abdelatty Ali, Jan Van der Spiegel and Paul Mueller, *Acoustic–Phonetic Features for the Automatic Classification of Stop Consonants*, IEEE Transactions on Speech and Audio Processing, Vol. 9, No. 8, 2001, pp. 833-841

[122]. Power Spectral Estimation, National Semiconductor Application Note, 255, November 1980

[123]. Nikias C.L. and Raghuveer, M.; *Bispectrum Estimation : A digital Signal processing frame work*, Proceedings of the IEEE, 75(7), 1987, pp. 869-891

[124]. Chrysostomos L. Nikias and Jerry M. Mendel, *Signal Processing with Higher Order Spectra*, IEEE Signal Processing Magazine, July, 1993, pp. 10-36

[125]. T. Subba Rao and M. M. Gabr, *The Estimation of the Bispectral Density Function and the Detection of Periodicities in a Signal*, Journal of Multivariate analysis 27, 1988, pp. 457-477

[126]. Ananthram Swami, Jerry M. Mendel, Chrysostomos L. (Max) Nikias, *Higher-Order Spectral Analysis Toolbox For Use with MATLAB*, Users Guide, Ver. 2, 1998

[127]. Perfecto Herrera, Xavier Amatriain, Eloi Battle and Xavier Serra, Towards Instrument *Segmentation for Music Content Description: A Critical Review of Instrument Classification Techniques*, Proceedings of the International Symposium on Music Information Retrieval, 2000

Publications Brought out in the Field of Research

[1]. Prabha C., Ananthakrishnan V., Supriya, M. H., P. R. Saseendran Pillai, *Localization of underwater targets using sensor networks*, International journal of sensor networks(IJSNet), Vol. 13 , No. 3, pp. 185-196, 2013

[2]. Prabha C., Supriya, M. H., P. R. Saseendran Pillai, *Refining Underwater Target Localization and Tracking Estimates,* Signal Processing: An International Journal (SPIJ), Vol. (5): Issue (5), pp. 203-214, 2011

[3]. Prabha C., Supriya, M. H., P. R. Saseendran Pillai, *Tracking of a Maneuvering Underwater Target*, Proceedings of International Symposium on Ocean Electronics, Kochi, India, pp. 93-100, 2011 and published in IEEE Xplore

[4]. Prabha C., Supriya, M. H., P. R. Saseendran Pillai, *Improving the Localization Estimates using Kalman filters*, Proceedings of International Symposium on Ocean Electronics, Kochi, India, pp. 190-195, 2009 and published in IEEE Xplore

[5]. V. Ananthakrishnan, C. Prabha, Supriya. M. Hariharan and Saseendran Pillai, *Development of an ocean surveillance system*, J. Acoustical Soc. Am. 123(5), Pt.2, P.3895, 2008

[6]. Prabha C., Supriya, M. H., P. R. Saseendran Pillai, *Model Studies on the Localization of Underwater Targets using Sensor Networks*, Proceedings of International Symposium on Ocean Electronics, Allied Publishers, New Delhi, Vol .1, pp. 257-263. 2007

Other Publications

[1]. Prabha C., *A novel data dissemination in wireless sensor networks*, National Conference On Recent Trends In Computer Networking And Communications, Bannari Amman Institute of Technology, Erode, (RTCNC-2006)

Subject Index

L

M

N

P

Q

R

S

T

V